THE APPLICATION OF LINEAR FILTER THEORY TO THE DIRECT INTERPRETATION OF GEOELECTRICAL RESISTIVITY MEASUREMENTS

PROEFSCHRIFT

TER VERKRIJGING VAN DE GRAAD VAN DOCTOR IN DE TECHNISCHE WETENSCHAPPEN AAN DE TECHNISCHE HOGESCHOOL DELFT, OP GEZAG VAN DE RECTOR MAGNIFICUS DR. IR. C. J. D. M. VERHAGEN, HOOGLERAAR IN DE AFDELING DER TECHNISCHE NATUURKUNDE, VOOR EEN COMMISSIE UIT DE SENAAT TE VERDEDIGEN OP WOENSDAG 22 APRIL 1970 TE 16.00 UUR

DOOR

DEVA PRASAD GHOSH

Master of Science

geboren te Allahabad (India)

1970

PRINTED IN THE NETHERLANDS BY

DRUKKERIJ J. H. PASMANS - 's-GRAVENHAGE

Dit proefschrift is goedgekeurd door de promotor

Prof. O. Koefoed.

Aan mijn ouders

Aan Ellen en Sheila

Acknowledgements

I am grateful to Mr. E. van der Veldèn, Mr. A.F.G. Faessen and Miss P. van der Hout for helping me in various ways in the preparation of the manuscript. Mr. J.J. Bruinsma deserves also mention for kindly helping me with the Dutch scientific terminology. Finally the author records his sincere thanks to the various organizations, mentioned in the text, whose standard and field resistivity curves have been utilized for the purpose of demonstration of the working of the method.

Table of Contents

List of Illustrations

List of Tables

"Throughout ages man has improved his lot steadily through the acquisition of better tools. Indeed, it is the technological status of a society that determines the limits of its wealth, the acquisition of its social goals, the achievement of its aspirations. ..... The central point is that no civilization can realize its goals beyond the capability of its technology."

L. V. BERKNER

Geophysics - Challenge and Change,
GE, vol. 31

CHAPTER 1

INTRODUCTION

Geoelectrical depth sounding resistivity measurements have found wide application in diversified fields. In Civil Engineering it is used to determine the depth and nature to the bed rocks, in the quest of solid foundations for dam, bridge, tunnel and road constructions (4)[1]. It is being used to study the crustal electrical properties involving great depths (22, 23, 24, 62, 77). However, by far the greatest application is in the field of hydrogeology where it is used as a tool for exploration and exploitation of ground water resources (15, 78). This mostly involves shallow depths to within about 300 metres, although very recently a deep sounding for ground water has been reported (76).

Although drinking water is of vital importance, a step-mother attitude has been given to this problem by persons involved in geoexploration. As such many countries, specially those in arid regions, are in acute shortage of water, arising mostly out of insufficient effort diverted towards exploration of their own ground water resources. There is thus immediate and urgent need for concentrated intensive exploration, that calls for fast improved techniques of acquiring and interpreting the data.

Principle and field variations employed

The main purpose of a geoelectrical measurement is to delineate the subsurface structure by basing its study on the electrical condition of the earth. The property studied is resistivity $\rho(z)$, which is the inverse of conductivity $\sigma(z)$. The situation commonly encountered is horizontal layering. Permeable formations are known to carry in their pore spaces ionic fluid that permits the flow of electricity. A four

----

[1] The numbers in brackets refer to the References page 119-125.

point electrode system, with the electrodes placed symmetrically in a straight line, is employed. The ground is energized galvanically by the help of two external electrodes and the response of the ground, in the form of potential difference, is measured between the inner pair of electrodes. Two variations in field techniques, named after the pioneers in this field, are commonly employed. In the SCHLUMBERGER method used widely in Europe, the potential electrodes are close to each other and kept stationary for long periods during which the current electrodes are moved outwards progressively at a ratio of about 1.4.

In the WENNER's arrangement used mostly in North America and other English speaking countries, all the four electrodes are expanded outwards with respect to the centre of the system, always maintaing equal spacing among the electrodes. The relative merits of these two techniques have been debated in literature (9, 34). It suffices here to remark that field procedure is easier with the SCHLUMBERGER method and that the surface inhomogeneities affect the measurements also to a lesser degree than with the WENNER arrangement. The procedure of expanding outwards the electrodes simply implies that progressively deeper and deeper horizons are reached by the current. Thus this form of resistivity measurements is aptly known in geophysics as electrical drilling (HEDSTRÖM) or vertical electrical sounding (V.E.S.) or simply as depth sounding. The potential difference and the current are observed at each electrode-layout and the multiplication of their ratio i.e. the resistance with a suitable geometrical factor, defined by the electrode layout, determine a function called *apparent resistivity*. The unit is ohm-metre and the dimension is resistance multiplied by length. The fieldwork is completed by plotting this function on bilogarithmic paper against one half the current electrode distance in SCHLUMBERGER and one third the current electrode distance in WENNER arrangement.

Concept of apparent resistivity

The meaning of the term apparent resistivity is quite vital towards proper understanding of interpretational methods. It is the true resistivity that a homogeneous half space earth should have, if it had to record the same potential difference as observed on a stratified earth, thinking for a moment that the same measurement was being repeated (the layout and current are kept exactly the same). It is an artificial concept and as has rightly been pointed out by PARASNIS (51) does not represent an average resistivity of a certain volume, as certain writers have erroneously mentioned, because it is also a function of the electrode arrangement used. The desired information about the subsurface is concealed in the apparent resistivity curve in such an intriguing fashion that simple depth rules are dangerous and not recommended.

Theoretical assumptions

The situation is alarming which requires a complete analysis based on solid theoretical foundations. The mathematical treatment is simplified by idealizing the geological situation. The layers are treated as homogeneous and isotropic while the boundaries are taken as plane parallel. It cannot, however, be said with surety that this condition is always met in practice, but it is not possible to incorporate these deviations as it makes the mathematics too complicated. The practice is to complete the interpretation on the above assumption and to alter the interpretation if necessary, mostly in a qualitative or semi-qualitative fashion to include deviations that come to our knowledge from geology and drill hole information. It may be said for a passing remark, that the effect of dip is less severe than anisotropy in depth determination based on a consideration assuming ideal conditions stated above (25). For further details on anisotropy reference is made to the work of MAILLET (38) and SCHLUMBERGER (63). Extensive treatment about the effect of dip has been given by NOSTRAND and COOK (47). Surface inhomogeneities also influence resistivity measurements (1).

Equivalence Problem

Further difficulties arise due to limitations in the physical nature of the problem. This is introduced by the fact that quite different horizontal layer distributions may produce almost the same pattern of apparent resistivity curves. This ambiguity is known as the *equivalence* problem (39) and although methods are known to solve this problem (19) the best is to rely on external control as a check on our interpretation.

Interpreting the field observations

The interpretation of the field data is done in two stages. In the first stage the data is interpreted purely on theoretical considerations. Then in the latter stage, the interpreted result is correlated with available geological knowledge to arrive at a realistic picture of the subsurface. The success of geoelectrical methods depends much on this geological interpretation. FLATHE, 1955 (15), gives a critical review of the applicability and limitations of the geoelectrical method specially towards hydrogeological problems.

In this thesis we shall be concerned only with the first stage i.e. physical interpretation. This is based on an expression by STEFANESCO, 1930 (67), for the potential due to a point source of current on a stratified earth. He expressed the potential in the form of an HANKEL integral, the integrand of which is a product of a BESSEL function of zero order and of a function dependent on the layer parameters called the *kernel function*. The technique applied in interpreting the data has been mostly indirect, in that the field curve is matched with standard graphs prepared from the STEFANESCO expression for known earth models. This procedure of trial and error costs time and in many instances the possible cases outnumber the small number of cases for which standard graphs can be prepared.

Direct derivations of layer parameters

The idea of obtaining the layer parameters directly from field measurements is due to SLICHTER, 1933 (64), who showed that it could be obtained in two steps. In the first step, the kernel function in the STEFANESCO integral was determined from field measurement and in the second step the layer distribution was deduced from the kernel function. However, SLICHTER's procedure was laborious and thus unsuitable. PEKERIS, 1940 (54), gave an extremely useful method for carrying out SLICHTER's second step. These suggestions, however, found very little application because there was no means of determining the kernel suitable to field parties. So KOEFOED's method, 1968 (32), was of great practical significance, because he gave a procedure to obtain the kernel from the apparent resistivity curve, that was not only accurate but simple in application. To carry out the second step of SLICHTER's proposal, two methods were suggested by him, one of which was similar to that of PEKERIS. However, KOEFOED (33), subsequently modified his second method by introducing a new function called the *resistivity transform*, related to the kernel function. The speed of obtaining the parameters from the transform was accelerated by the introduction of a standard curve.

The need of a new technique for calculating the resistivity transform

KOEFOED's method as such was complete. The modification mentioned above for obtaining the parameters from the transform gave considerable gain of working speed. On the other hand the first step was relatively lengthy. It was thus desired to devise a method for carrying the first step, which should give considerable speed to the application of direct methods and yet retain the accuracy of KOEFOED's method of obtaining the kernel from the field data. The knowledge of sampling and filter theory in the field of communication theory was applied to obtain the resistivity transform from the apparent resistivity curve. For the deduction of the layer parameters from the transform, KOEFOED's method cited above is recommended. It is hoped that these two procedures should give a new meaning to the application of the direct method in resistivity interpretation.

CHAPTER 2

THE FUNDAMENTAL RELATION BETWEEN POTENTIAL, APPARENT RESISTIVITY, RESISTIVITY TRANSFORM AND THE LAYER DISTRIBUTION OF A STRATIFIED EARTH

2.1 Potential distribution about a point electrode

It is required to determine the potential at an arbitrary point on the surface due to a point electrode emanating a current I, also placed on the surface of the n-layered horizontal earth. The layers have resistivities ρ_1, ρ_2, ρ_3, ..., ρ_m, ...ρ_{n-1}, ρ_n and thicknesses d_1, d_2, d_3, ..., d_m, ...d_{n-1}. The n^{th} layer is the substratum, and the air with infinite resistivity is not taken as a section but is of importance in governing the boundary conditions. These details are shown in fig. 2.1.1

The potential V has to satisfy LAPLACE's equation $\nabla^2 V = 0$, everywhere except at the electrode. Such a solution can be obtained by considering LAPLACE's equation in cylindrical coordinates. There exists circular symmetry of the field about a vertical line through the electrode. The electrode is taken as the origin of the polar coordinate system with the vertical line as the z-axis positive downwards and the r-axis ~~along~~ (in a plain // to) the surface of the earth. In view of the above mentioned symmetry, LAPLACE's equation in cylindrical coordinates degenerates to

$$\nabla^2 V = \frac{\delta^2 V}{\delta r^2} + \frac{1}{r}\frac{\delta V}{\delta r} + \frac{\delta^2 V}{\delta z^2} = 0 \qquad (2.1.1)$$

This differential equation can be solved by FOURIER's method by assuming a solution of the form

$$V = X(r).Y(z) \qquad (2.1.2)$$

where X(r) is a function of r only and Y(z) of z only, each solution being independent of the other. The solution in the process has to meet the following boundary and continuity conditions:

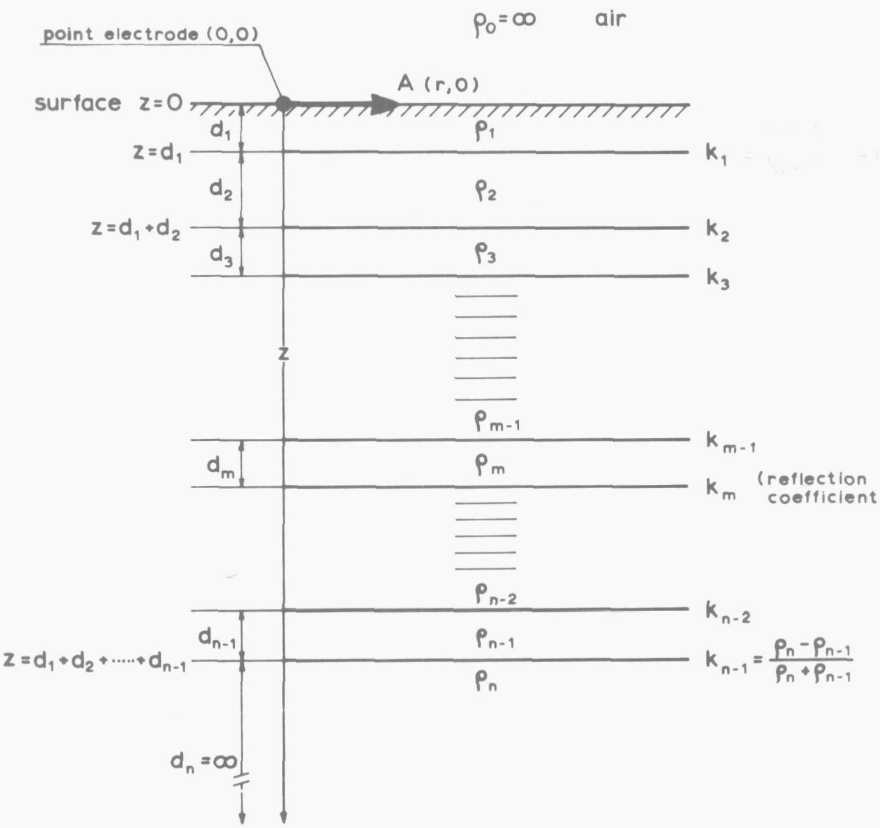

fig. 2.1.1 Layering notations

1) potential is finite and continuous across the interfaces
2) normal component of current density is also continuous across the interfaces
3) at the surface, $\frac{\delta V}{\delta z} = 0$, as the air has infinite resistivity
4) potential vanishes at great distances from the electrode.

STEFANESCO et al, 1930 (67), gave a solution to eq (2.1.1) by the method enumerated by eq (2.1.2), on the basis of the above conditions. They expressed the potential as

Kern functie

$$V = \frac{\rho_1 I}{2\pi} \{ \frac{1}{r} + 2 \int_0^\infty \underbrace{B_1(\lambda,k,d).J_0(\lambda r).d\lambda \}}_{\text{Stefanesco functie}} \qquad (2.1.3)$$

where

$J_0(\lambda r)$ = BESSEL function of zero order and first kind

$B_1(\lambda,k,d)$ = *Kernel function*, determined by thicknesses and resistivities of enclosed layers of the subsurface under consideration. It is a quotient in which both the numerator and denominator are polynomials in $v = e^{-2\lambda}$. The kernel function can have all possible values ranging from $-\frac{1}{2}$ to infinity.

λ = Integration variable, a real number and in the present problem can assume values from zero to infinity. It has the dimensions of inverse length.

The expression under the integral is known as the STEFANESCO function and is of fundamental importance in resistivity interpretation. STEFANESCO solved the problem for three and four layers and indicated it for others. FLATHE, 1955 (14), gave mathematical expressions of the kernel function, in terms of depths and resistivities of the subsurface layers, for up to six layers. A recurrence formula was included by which the kernel for any number of layers could be determined from its preceding one.

He dropped the suffix 1 from the expression of the kernel function and instead preferred to use a suffix that referred not to the fact that the measurement was made at the surface but instead indicated the number of layers involved. There is apparently no real advantage gained in using a suffix in the kernel so long as the meaning is maintained. As such none will be used here further on.

KOEFOED, 1968 (32, p. 14), showed that errors in the apparent resistivity curve did not show up to the same degree in the corresponding kernel curve, such that any method based on the transformation of the apparent resistivity to the kernel is bound to lead to inaccurate representation. With this aim he introduced a new function called the *raised kernel* function defined by

$$H(\lambda) = B(\lambda) + \frac{1}{2} \tag{2.1.4}$$

He showed that there the changes in the kernel were of the same magnitude as the changes in apparent resistivity, such that all the information was retained in the conversion process.

2.2 The concept of Resistivity Transform

Critical examination of apparent resistivity curves and their corresponding raised kernel curves, specially Fig. 10.1.1 of KOEFOED's book (32, p. 82), revealed an interesting feature that if the $H(\lambda)$ curve was raised by a factor $2\rho_1$ on the logarithmic scale, then the resulting curve followed the apparent resistivity curve much more faithfully than any of the kernels mentioned earlier. Moreover, as it was directly proportional to the H-curve, it retained its important property of no loss of accuracy during conversion. So it was decided to use this function as an intermeditary step, to obtain the layer distribution from the apparent resistivity, instead of the kernel functions used in previous work. We shall introduce the concept of this new function, which is called the *resistivity transform* $T(\lambda)$ (33), in the expression of the potential (eq (2.1.3)).

Taking the help of the knowledge in BESSEL functions (72) we can rewrite eq (2.1.3) as

$$V = \frac{\rho_1 I}{2\pi} \{ \int_0^\infty J_0(\lambda r).d\lambda + \int_0^\infty 2B(\lambda).J_0(\lambda r).d\lambda \}$$

or

$$V = \frac{\rho_1 I}{2\pi} \int_0^\infty \{1 + 2B(\lambda)\}.J_0(\lambda r).d\lambda$$

or

$$V = \frac{I}{2\pi} \int_0^\infty T(\lambda).J_0(\lambda r).d\lambda \tag{2.2.1}$$

where

$$T(\lambda) = \rho_1\{1+2B(\lambda)\} \tag{2.2.2}$$

The Resistivity Transform $T(\lambda)$ has the property that for small values of $1/\lambda$ it approaches ρ_1 and for large values of $1/\lambda$ asymptotically approaches the resistivity of the substratum (see fig. 7.3.1). In other words it is a very good reflector of the apparent resistivity curve. Thus if we are able to determine $T(\lambda)$ from the apparent resistivity by some process, then the layer parameter could immediately be obtained from it by methods already known (33). For this purpose an explicit expression is necessary relating the resistivity transform to the apparent resistivity. This will be given in section 2.5 of this chapter.

The relation of the resistivity transform to the various kernels used in literature can be deduced from eq (2.2.2). The following relations have been given here to avoid confusion

$$\left.\begin{aligned}
&\text{SLICHTER's kernel} = T(\lambda)/\rho_1 \\
&\text{Kernel function, } B(\lambda) = \frac{T(\lambda)-\rho_1}{2\rho_1} \\
&\text{Raised kernel, } H(\lambda) = T(\lambda)/2\rho_1 \\
&\text{Modified kernel, } G(\lambda) = \frac{T(\lambda)-\rho_1}{T(\lambda)+\rho_1} \\
&\text{PEKERIS function, } f_1(\lambda) = \frac{T(\lambda)+\rho_1}{T(\lambda)-\rho_1}
\end{aligned}\right] \qquad (2.2.3)$$

2.3 The Resistivity Transform for two and three layers

Like the kernel function, the resistivity transform is also related to the thicknesses and resistivities of the subsurface layers. These expressions can be deduced from the corresponding expression of the kernel function in terms of the layer parameters that arise in the solution of eq (2.1.1) (see 14, 32). However, these expressions are not of direct interest in the working of the method proposed. Nevertheless expressions for two and three layers are given, as they have been used extensively in the development of the method.

Two layer case

$$T(\lambda) = \rho_1 . \frac{1+k_1.e^{-2\lambda d_1}}{1-k_1.e^{-2\lambda d_1}} \tag{2.3.1}$$

Three layer case

$$T(\lambda) = \rho_1 . \frac{(1+k_1.k_2.e^{-2\lambda d_2}) + (k_1.e^{-2\lambda d_1} + k_2.e^{-2\lambda(d_1+d_2)})}{(1+k_1.k_2.e^{-2\lambda d_2}) - (k_1.e^{-2\lambda d_1} + k_2.e^{-2\lambda(d_1+d_2)})} \tag{2.3.2}$$

The resistivity transform for any number of layers can be found by taking the help of FLATHE's recurrence formula (14).

2.4 Apparent Resistivity

Expressions for apparent resistivity can be found from the expression for the potential due to a point electrode.

SCHLUMBERGER arrangement: If the distance between the current electrodes is taken as 2s, then the apparent resistivity is given by

$$\rho_{aS} = -\frac{2\pi}{I}.r^2.\left(\frac{dv}{dr}\right)_{r=s} \tag{2.4.1}$$

Taking the help of eq (2.2.1), we have

$$\rho_{aS} = s^2\int_0^\infty T(\lambda).J_1(\lambda s).\lambda.d\lambda \tag{2.4.2}$$

WENNER arrangement: Calling the spacing between consecutive electrodes a, the WENNER potential difference becomes

$$\Delta V_W = V_a - V_{2a} = \frac{I}{2\pi}\int_0^\infty T(\lambda).\{J_0(\lambda a)-J_0(\lambda 2a)\}.d\lambda \tag{2.4.3}$$

The apparent resistivity is given by

$$\rho_{aW} = \frac{2\pi a}{I}.\Delta V_W$$

or

$$\rho_{aW} = a\int_0^\infty T(\lambda).\{J_0(\lambda a)-J_0(\lambda .2a)\}.d\lambda \tag{2.4.4}$$

The suffix S and W in the apparent resistivity in eqs (2.4.2) and (2.4.4) simply signify the type of arrangement used.

2.5 Explicit Expression for the Resistivity Transform

As stated in section 2.2 an explicit expression for the resistivity transform function $T(\lambda)$ is of fundamental importance to a method that uses to determine this function as an intermediatary step in the interpretation of field data. Applying HANKEL's inversion theorem of the FOURIER-BESSEL integral (72) to eq (2.4.2) we obtain

$$T(\lambda) = \int_0^{\infty} \rho_{aS} . J_1(\lambda s) . \frac{ds}{s} \qquad (2.5.1)$$

For the WENNER's arrangement, a different procedure will be followed as no simple and direct relation of the form of eq (2.5.1) is obtainable for it.

2.6 Image approach

HUMMEL, 1929 (20), prior to STEFANESCO's solution solved the identical problem for a two layer case. However, this method was different as he took the help of *image theory* of optics. The stratified ground was replaced by a fictitious homogeneous medium with an infinite series of image poles, placed one above the other at a spacing determined by the thickness of the bed in question. The potential at a point was thought to be as the sum of the contributions of the source and its infinite images.

LASFARGUES (36), and others have demonstrated the correspondence between HUMMEL's and STEFANESCO's expression for a two layer case (also see chapter 3, section 3.2a). HUMMEL also obtained an expression for the potential for a three layer problem on similar reasoning.

A different set of image configuration applicable to any layer distribution was obtained by EHRENBURG and WATSON, 1932, and independently by WATSON, 1934 (12). Detailed comparison of these methods and their relation to a similar method based on STEFANESCO's expression has been dealt with by VAN DAM, 1964 (7).

CHAPTER 3

AN OUTLINE OF EXISTING RESISTIVITY INTERPRETATIONAL TECHNIQUES

3.1 General Considerations

The interpretation of field observations in terms of depths and resistivities is the basic task of a geoelectrical survey. The problem is not so simple as several complexities are known, some of them inherent to the physical nature of the problem as discussed in chapter 1. As such several attempts have been made in the past to interpret the data correctly. Most of these methods are far from being perfect, anyway they have contributed to a better understanding of the problem and need to be discussed, because they are the foundations of future methods.

The techniques commonly used either start of from STEFANESCO's expression for the potential or HUMMEL's equation. The image method had been used by several workers (12, 20, 27, 59, 60, 69) to solve 2 or 3 layer problems. The obvious limitations in the application to a multilayer problem was soon recognized (60), as such now it is seldom used and will not thus be discussed.

Methods can be classified as *direct* or *indirect* depending on the manner in which the parameters of the subsurface are deduced from the field observations. An attempt will be made to state the principles involved in the development of the methods, according to this classification, with special emphasis to direct methods only for the method suggested in this thesis is a part of it.

INDIRECT METHODS

3.2 Evaluation of the STEFANESCO function

The basic problem involved in the computation of standard curves used in indirect interpretation, is the evaluation of the integral in eq. (2.1.3), which does not render itself to integration analytically.

Various procedures attempted to evaluate it, have been dealt with by KUNETZ (34).

The infinite integral is often replaced by finite intervals and integrated numerically. The advent of digital computers have made this feasable, although several difficulties are known (43). The tables of MOONEY and WETZEL, 1956 (42), were obtained by SIMPSON's method of numerical integration.

An attempt to simplify the integrand by expanding the BESSEL function in series (45) was not very successful. The most accepted procedure is to resolve the kernel function into an infinite series or into a series of partial fractions; other processes like expansion into a series of LEGENDRE orthogonal polynomials (49) or into a series of powers of half the relative difference of resistivity of adjacent beds, have been attempted (17).

(a) *Expansion into an infinite series*

This is rendered possible by the fact that the kernel being a ratio in which both the numerator and denominator are polynomials in $v = e^{-2\lambda}$, could be expressed as an infinite sum of terms $Q_i . e^{-\lambda D_i}$, such that the integral in eq (2.1.3) becomes

$$V_i = \sum_{n=-\infty}^{\infty} Q_i . e^{-\lambda D_i} . J_0(\lambda r) . d\lambda \qquad (3.2.1)$$

Taking the help of Lipschitz integral (72) we have

$$V_i = \sum_{n=-\infty}^{\infty} \frac{Q_i}{(r^2 + D_i^2)^{1/2}} \qquad (3.2.2)$$

Each term can be regarded as the contribution to the potential due to an image at depth D_i and strength determined by Q_i. This is the similarity with image methods mentioned in section 2.6. The choice of the number of terms depends on the convergence of the series. The methods of VAN DAM, 1964 (7) and MOONEY et al. 1966 (43), are based on this principle of expansion. The method of "finite forward differences" has been employed by NABHIGHIAN, 1966 (46), for improved convergence of the infinite series.

(b) *Expansion into a series of partial fractions*

FLATHE, 1955 (14), showed that the kernel function of a multilayered earth, in cases of infinitely resistive or conductive substratum could be replaced by a series of partial fractions called *prime elements*. Each element referred to a three layer case with a conductive substratum and varying ρ_2. The apparent resistivity curve could then be constructed as a linear combination of a finite number of such elements multiplied by suitable weighting factor. C.G.G., 1955 (6), obtained a major part of their master curves on a similar method of decomposition of the kernel with a slightly different system of the prime elements.

For the rapid convergence of the series, considered in both group (a) and (b) methods, the restriction is laid down that the layer thicknesses be integral multiple of some common thickness which can be taken small (14).

3.3 Practical procedures followed in Indirect Interpretations

(a) *Curve matching*

This employs bilogarithmic curve matching, the advantages of which are well recognized (25). The field curve is superposed on a set of standard curves, prepared by methods cited in 3.2. In case of perfect match the parameters of the standard curve determine the unknown layer distribution.

(b) *Computing your own curve*

In case of failure of obtaining a fit, the interpreter can obtain his own curve by any of the methods of 3.2. When the computers are not available, the methods of VAN DAM or FLATHE could be used. A theoretical curve could also be constructed graphically (4, 34) taking the help of the principle of equivalence. Everything said the computation of field curves is decidedly a burden to field parties.

(c) *Method using asymptotic curves*

When the interpreter is not inclined to compute his curve, he has the option to use approximate methods to interpret the data. A multi-layer problem could be reduced to simple cases by using asymptotic two layer curves and the parameters of the subsurface determined from these two layer curves, taking the help of auxiliary charts. HUMMEL, 1932 (20), expressed the relation between parameters of the subsurface and those of asymptotic curves mathematically, while CAGNIARD (36), and later KOEFOED, 1960 (28), expressed them graphically.

HUMMEL gave rules of combining layers by treating them as resistances in parallel, which must be understood as applicable only to the specific case of a resistive substratum (26). For other resistivity distributions empirical rules and graphs have been worked out by EBERT, 1943 (11), and can be found in SOROKIN's book (66). For a proper understanding a knowledge of *Dar-Zarrouk* parameters (39) is necessary. An article by ZOHDY, 1965 (75) is very useful in this respect.

As parts of the curve are matched by the asymptotic curves, these methods are also known as *partial curve matching* or also as *auxiliary point method*. Although these semi-empirical methods can accommodate a large number of cases, they are inaccurate and the greatest objection is that large significant parts of field information remain unused.

DIRECT METHODS

3.4 Introduction

In this section methods will be discussed in which attempts have been made to determine the layer distribution directly from field measurements, by taking the help of certain mathematical processes.

In any problem of mathematical physics a direct solution is preferred, as a trial and error process is in its very nature not only time consuming but at times unreliable. Yet surprisingly enough resistivity interpretation has been mostly indirect, although the foundations of direct methods were laid down at least three decades before. This leaves to our mind the question about the possible shortcoming of these methods that prevented them to widespread application. A more detailed investigation will be made into this question.

LANGER's theorem, 1933 (35), that the knowledge of potential about a point electrode uniquely determined the unknown conductivity function, gave the necessary impetus to workers to devise methods to determine directly the layer parameters.

3.5 Techniques based on potential measurements about a single electrode

(a) In accordance with LANGER's suggestion, SLICHTER, 1933 (64), solved the relevant differential equation, arising out of zero divergence for the electrical field, due to a point electrode on the surface of an earth in which the *conductivity was a continuous function of depth.*

However, the most significant part of SLICHTER's analysis was the step in which he obtained an expression for the SLICHTER's kernel by applying HANKEL's FOURIER-BESSEL theorem (72) to the equation of the potential, that was obtained earlier by solving the differential equation mentioned above. His expression in the finite interval (o,ℓ) of measurement took the form

$$T(\lambda).b.\frac{\text{Sin } \lambda a}{\lambda a} = \int_0^{\ell} V(r).J_0(\lambda r).r.dr. \qquad (3.4.1)$$

A knowledge of the measured potentials about the electrode determined SLICHTER's kernel, which could be obtained by numerical or mechanical integration of eq (3.4.1).

The determination of the unknown conductivity function from the kernel was the next problem. For this SLICHTER expressed both the kernel function and the conductivity function $\sigma(z)$ as power series and comparing the coefficients of the two sets of series could arrive at the conductivity distribution.

The original symbol of the authors relating to the kernel function has been replaced by $T(\lambda)$ taking ρ_1 as unity and maintaining the relationship defined by eq. (2.2.3).

The latter step could also be done in an indirect fashion, by establishing standard relations of coefficients between $\sigma(z)$ and their associated kernels for known earth models and then comparing them with the relations obtained for the field data.

(b) SLICHTER's power series could only handle problems concerning uniform half space as such, LANGER, 1936, extended it to handle a two layer problem and STEVENSON to a three layer problem.

(c) PEKERIS, 1940 (54), suggested a more straightforward approach to the second step of SLICHTER's proposal. He gave an extremely practical method of deducing the layer distribution after the SLICHTER's kernel was determined by numerical or mechanical integration of field potential observations.

He obtained a function $f_1(\lambda)$ (eq 2.2.3) from the kernel and plotted it on a semilog. scale against λ, which was plotted on the linear scale. According to this theory, for large values of λ the points fall on a straight line the slope of which is $2d_1$ and the intercept $1/k_1$.

(d) NOSTRAND and COOK, 1966 (47), describe a procedure which is very similar to that of PEKERIS.

(e) VOZOFF, 1958 (71), based on SLICHTER's analysis, proposed a method in which he assumed the initial values of the parameters of the layer distribution and then slowly changed the variables in such wise that the theoretical kernel approximated to the field kernel obtained by mechanical or numerical integration of field potential data. The least square statement of the problem was

$$\Sigma_{j=1}^{\infty}\left[T_t(\lambda) - T_f(\lambda)\right]^2 = \text{minimum} \tag{3.4.2}$$

where T_t = theoretical and T_f = field transform.

The method needed the use of computer and was suitable only for up to three layers. There was also considerable ambiguity in the solution as there was no way of checking whether the solution obtained was the correct one.

(f) Other important contribution to the direct method is due to BELLUIGI, 1957 (3).

3.6 Conclusions on methods discussed in section 3.5

(1) Although the idea of obtaining the kernel from the field data is a unique one, there is, however, no simple procedure to compute it. Either mechanical or numerical integration requires a lot of computational time and computers are not accessable to field parties.

(2) SLICHTER's solution was of academic interest as it deviates from our geological knowledge, that resistivity is constant in discrete layers.

(3) The field procedure commonly followed is to measure potential difference and not potential alone. It could be argued, that we could remove the second electrode far away and only measure the potential about one elctrode, to suit our interpretational procedure. However, this too has practical disadvantages in that potentials cannot be measured accurately in the vicinity of an electrode and particularly serious are errors in measurements at distances farther from the electrode specially when the effect of deeper beds are sought (47).

(4) The method of PEKERIS is simple to carry out but it requires considerable computational time. The transformation of the kernel to the function $f_1(\lambda)$ involves loss of accuracy (32).

(5) Although LANGER's theorem does suggest uniqueness in solution, it should not be misinterpreted into the fact that changes in potential are directly related to corresponding changes in resistivity (18), because of the equivalence limitation. Thus direct interpretation may lead to erroneous results if the above limitation is overlooked. It will be shown in section 3.7 that there is enough scope to check the results even in direct interpretation.

3.7 Techniques based on apparent resistivity field measurements

KOEFOED, 1968 (32), attempted to remove the shortcomings stated in section 3.6 by giving an extremely useful method of carrying out SLICHTER's first step and two procedures to determine the layer distribution from the kernel function. His method was acceptable in the sense that it was commensurate with the field procedure commonly followed, easy in application and hence adaptable to field parties as the whole process could be carried out graphically for which standard curves were supplied.

It was also in line with geologic considerations as the resistivity was considered as a step-function of depth i.e. on STEFANESCO's expression.

The splitting of the interpretation into two steps was of great utility hitherto unrealized by previous workers but pointed out by KOEFOED, 1965 (30). He showed that the relation between the kernel and the apparent resistivity was a 'one to one' relation such that ambiguity if any resides only in the step between obtaining the layer distribution from the kernel. So the kernel may be determined from field observations once for all, and as external information becomes available, only the second step of interpretation could be changed. This is a big advantage to all direct methods, utilizing the determination of the kernel function as an intermediate step.

He introduced a new function the *raised kernel* function, for reasons already discussed in section 2.1. The apparent resistivity curve was decomposed into a series of partial resistivity functions and their associated raised kernel functions were defined by

$$\Delta_i H(\lambda) = \int_0^\infty \frac{\Delta_i \rho_{aS}}{2\rho_1 . s} . J_1(\lambda s).ds \qquad (3.7.1)$$

where

$\Delta_i \rho_{aS}$ = are the partial resistivity functions

$\Delta_i H(\lambda)$= are their corresponding raised kernel functions

A set of standard curves were given for the partial resistivity function and their corresponding kernels. The apparent resistivity field curve was approximated stepwise by these resistivity functions graphically, until the whole curve was accounted for. The corresponding kernel curves were drawn and added up to yield the total raised kernel curve.

The next task was to determine the layer distribution. This is carried out best by a modified method suggested by KOEFOED, 1969 (33), in which he used the resistivity transform to determine the layer distribution instead of the raised kernel or modified kernel used before (32). A standard curve was also added to speed up the process.

The basic principles of the above method involved the reduction of the transform to a lower boundary plane, namely the successive derivation of the T_{n-1} curve from the T_n curve yielding d_i and ρ_i of the *removed* top layer in question.

KOEFOED gave separate standard curves for SCHLUMBERGER and WENNER arrangement. For the latter arrangement, he preferred to assume a relation of the form of eq. (3.7.1). PAUL, 1968 (53), indicated that expressions of the from of eq.(3.7.1) could also be deduced for the WENNER arrangement from eq. (2.4.4), taking the help of FOURIER-BESSEL integral (72). There are, however, unfortunate crossovers in some of his equations.

CHAPTER 4

THE APPLICATION OF LINEAR FILTER THEORY

4.1 Fourier Transform

Fourier transform is a powerful tool to solve problems in diversified fields by transferring a function from its *function* domain to the *frequency* domain. Salient features, hitherto unrealized become conspicious in the frequency behavior of the function.

Let g(x) be an aperiodic function of the space variable x. Then its transform G(f) is given by

$$G(f) = \int_{-\infty}^{\infty} g(x).e^{-i2\pi fx}.dx \tag{4.1.1}$$

G(f) is in general a complex quantity and can be split as

$$G(f) = A(f)+iB(f) \tag{4.1.2}$$

where A(f) and B(f) are its real and imaginary components respectively. The spectrum G(f) is described completely by

$$\left.\begin{aligned} &\text{amplitude density spectrum, } |G(f)| = \sqrt{A^2(f)+B^2(f)} \\ &\text{phase density spectrum, } \phi(f) = \{B(f)/A(f)\} \end{aligned}\right\} \tag{4.1.3}$$

For the validity of eq (4.1.1), two conditions are often imposed. They are

1) that g(x) has finite number of discontinuities
2) that g(x) is integrable

The latter condition may be termed as sufficient but not a necessary one. It can be assumed safely that the existence of a physical meaning to a quantity qualifies it to possess a FOURIER transform.

The inverse FOURIER transform converts the function back to its own domain from the frequency representation. Mathematically it is stated as

$$g(x) = \int_{-\infty}^{\infty} G(f).e^{i2\pi fx}.df \qquad (4.1.4)$$

$$= \int_{-\infty}^{\infty} [G(f).df].e^{i2\pi fx} \qquad (4.1.4a)$$

According to LEE, 1960 (37), eq. (4.1.4a) points to the fact, that an aperiodic function can be synthesized by an infinite aggregate of sinusoids of all possible frequencies. That FOURIER analysis is applied to study the frequency spectrum of such function, has thus enough justification.

Eq. (4.1.4) and eq. (4.1.1) are thus different modes of representation of the same quantity. Thus g(x) and G(f) are known as a FOURIER transform pair and generally denoted by the symbol $\leftrightarrow$

$$g(x) \leftrightarrow G(f)$$

An example of such a pair is shown in fig. 4.1.1 the sinc function sin x/x, and the rectangular function. If the sinc function is represented in the function domain, then the rectangular function is its spectrum in the frequency domain and vice versa.

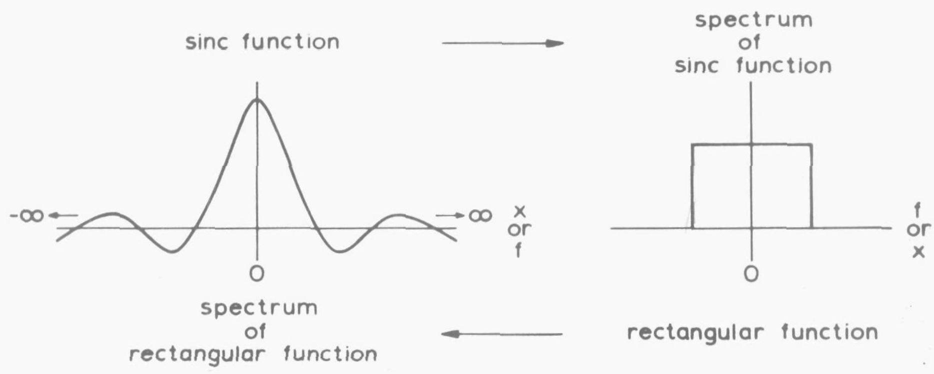

fig. 4.1.1 A FOURIER Transform pair

Two of the important properties of Fourier transform (2, 5) with which we will be concerned with, are

1) If the FOURIER transform of a function is known, then the FOURIER transforms of any of the derivatives of that function are also known; i.e. if

$$g(x) \leftrightarrow G(f)$$

then

$$\left(\frac{d}{dx}\right)^n g(x) \leftrightarrow (i2\pi f)^n . G(f) \qquad (4.1.5)$$

2) If

$$g_1(x) \leftrightarrow G_1(f) \text{ and } g_2(x) \leftrightarrow G_2(f)$$

and if c_1, c_2 are real constants,

then

$$\{c_1 . g_1(x) + c_2 . g_2(x)\} \leftrightarrow \{c_1 . G_1(f) + c_2 . G_2(f)\} \qquad (4.1.6)$$

Eq. (4.1.6) suggest the linearity of FOURIER transforms.

4.2 Linear Filters

(a) *Property of Linear systems*

A physical system is said to be linear, when an excitation g(x) applied to it and the corresponding response f(x) given by it, could be expressed by a linear equation. That is, a graph between these two quantities would be a straight line. This relationship is better understood by the following property of linear system:

If $f_1(x)$, $f_2(x)$ *and* $f_3(x)$ *are respectively the responses to excitations* $g_1(x)$, $g_2(x)$ *and* $g_3(x)$ *applied individually to the system, then* $\{f_1(x)+f_2(x)+f_3(x)\}$ *should be the response to a combined excitation* $\{g_1(x)+g_2(x)+g_3(x)\}$.

This is known as the *superposition* theorem and is inherent to linear systems. Another aspect of this theorem states:

If the excitation g(x) *is multiplied by a real constant* c, *then the response will also be multiplied by the same constant, for all values of* c *and* g(x).

A linear system is said to be x-invariant:

If the excitation is shifted by x_0*, where* x_0 *is a real constant, then the corresponding response will also be shifted by the same constant. That is* $f(x-x_0)$ *will be the response to the excitation* $g(x-x_0)$.

FOURIER analysis is a powerful tool in solving problems in systems in which linearity and invariance is met (5).

A linear system is termed a *filter* when the excitation and response to the system represent the input and output. However, there are several other ways of representing a filter (8), which will become apparent in the following section.

(b) *Applicability of electric filters to physical problems*

SWARTZ and SOKOLOFF, 1954 (65), have quoted PIETY (1942), in bringing out the fact, that the concept of electrical filter theory is not restricted only to *electric circuits*, but in fact is quite general and can be applied to all forms of physical problems that are linear in nature and even be extended to numerical or graphical data.

In electrical filters the input and output are voltages that vary with time, whereas in the problem we are confronted with, the single independent variable is distance. The properties discussed in part (a) of this section equally apply to both problems. However, the electric filters start to produce an output from $t = 0$, whereas geophysical filters depend on all available data.

A clear picture pointing to the difference between electric filter and those used for handling geophysical data has been brought about by TREITEL and ROBINSON, 1964 (57). They use a term called *advance* filter meaning that the filter has a finite response for $t<0$. They have quoted an example of filtering operation during recording of seismic signals in the field and have brought out the fact that the filter can not respond to energies that have not yet arrived. On the other hand if the seismic information is available on magnetic tape advance filters are possible, as all the data is at hand and we need not worry about the filter working on the excitation of an energy. Thus the field operation may be said to be working on *real* time and the other on *nominal* time (ROBINSON).

In the resistivity problem also we have all the data at our disposal and we can have responses from the filter at $x<0$. This is of course no limitation in the applicability of the knowledge of electric filters to physical problems. By removing the restriction imposed in electrical filters it adds 'versatility' to the filter by utilization of all available data [DEAN, 1958 (8)].

(c) *Pulse response of a linear filter*

A linear filter is defined by its response to an input of a *Dirac delta unit impulse function*, $\delta(x)$. This function is the limiting form of an even rectangular function where the height or amplitude tends to become infinite, as the base dx approaches zero. It is an integrable function such that

$$\int_{-\infty}^{\infty}\delta(x).dx = 1 \qquad (4.2.1)$$

Eq. (4.2.1) signifies that the total area of the function is unity. Thus graphically it is conventionally represented by a spike of unit height.

The response of a filter to an input of this spike function is known as the *unit impulse response* or simply the *pulse response* of the filter, $h(x)$. Its job is to weigh an input with its pulse response to produce an output. The output is thus expressed in terms of the applied input and the characterizing function of the filter. Fig. 4.2.1 shows the Dirac function and the pulse response of an 'arbitrary' filter box.

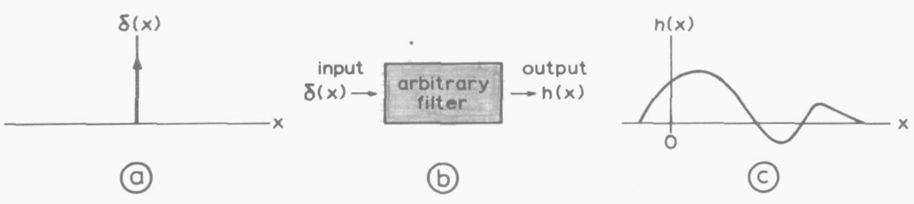

fig. 4.2.1 a. Dirac delta function
b. Action of an arbitrary filter
c. Unit impulse response

(d) *Representation of a filtering operation*

Mathematically the action of a linear filter can be represented by a *convolution* integral. The symbol * is used to signify convolution.

Let us assume that an input g(x) is being convolved in the filter with the pulse response of the filter, h(x). It will be stated as

$$f(x) = g(x)*h(x) \qquad \text{(in symbolic notation)}$$

$$= \int_{-\infty}^{\infty} g(\tau).h(x-\tau).d\tau \qquad (4.2.2)$$

The physical significance of the concept of the convolution is brought out in the German word for convolution, i.e. *Faltung*, which signifies a folding operation. The impulse function is displaced and then folded back and operated with the input to yield the output, f(x). This process is best illustrated graphically and can be found at several places (5, 37, 65). The value of the integral remains the same whichever of the two functions being convolved, is displaced and folded (37). Eq. (4.2.2) can be utilized to show that convolution is commutative.

In the frequency domain, convolution degenerates to simple algebraic multiplication such that eq. (4.2.2) takes the form

$$F(f) = G(f).H(f) \qquad (4.2.3)$$

where the FOURIER transforms, F(f), G(f) and H(f) convert the functions f(x), g(x) and h(x) respectively into the frequency domain. Eq (4.2.3) has tremendous advantages, as it gives a simple relation between the input and output in terms of the impulse response. It means that the output can be determined by simply multiplying the Fourier transform of the input by the Fourier transform of the impulse response, when it is known.

(e) *Filter characteristic*

From eq (4.2.3) we have

$$H(f) = \frac{F(f)}{G(f)} \qquad (4.2.3\ a)$$

H(f) is called the *filter characteristic* and is the frequency representation of the pulse response function. It is a complex quantity containing an amplitude spectrum and phase spectrum.

4.3 The Linear Filter analogy

The apparent resistivity and the resistivity transform are related to each other by

$$T(\lambda) = \int_0^{\infty} \rho_{aS}(s) . J_1(\lambda s) . \frac{ds}{s} \qquad (2.5.1)$$

We now introduce new variables in eq (2.5.1), defined by[1)]

$$\begin{aligned} x &= \ln s \\ y &= \ln (1/\lambda) = \ln u \end{aligned} \qquad \begin{aligned} s &= e^{x} \\ \lambda &= e^{-y} \end{aligned} \qquad (4.3.1)$$

where $u = 1/\lambda$ and has the physical dimension of distance.

Thus eq. (2.5.1) becomes

$$T(y) = \int_{-\infty}^{\infty} \rho_{aS}(x) . J_1[e^{-(y-x)}] . dx \qquad (4.3.2)$$

Eq. (4.3.2) is a convolution integral and suggests that the transformation process from the apparent resistivity function $\rho_{aS}(x)$, to the resistivity transform $T(y)$, defines the action of a simple linear filter, as such all characteristics of linear systems outlined in section 4.2 are applicable. Fig. 4.3.1 illustrates the linear filtering process.

$$\rho_a(x) \longrightarrow \boxed{\text{filter}} \longrightarrow T(y)$$

fig. 4.3.1 Shows that the conversion from the apparent resistivity to the resistivity transform as the action of a linear filter

----

1) note that $\log_e z = \ln z$ called natural logarithms

4.4 Frequency characteristic of the resistivity filter

The filter characteristic of the operation defined by eq. (4.3.2), can be determined with the help of eq. (4.2.3). It is the ratio of the Fourier transform of the resistivity transform by the Fourier transform of its corresponding resistivity function.

To determine the resistivity filter characteristic, a resistivity function is so chosen that its corresponding resistivity transform is known. Such a function is given below and has been taken from KOEFOED's collection of partial apparent resistivity functions(32, p. 24) and their associated kernels with the necessary change of variable as underlined by eq. (4.3.1) through eq. (2.2.3)

$$\left.\begin{aligned} \Delta\rho_{aS}(x) &= \frac{e^{3x}}{(1+e^{2x})^{5/2}} \\ \Delta T(y) &= \frac{1}{3.e^{y}\{e^{e^{-y}}\}} \end{aligned}\right\} \qquad (4.4.1)$$

The Fourier transforms were determined numerically and their ratio gave the resistivity filter characteristic (eq. (4.2.3)). This was later verified by repeating the same process on a second set of partial resistivity function and its corresponding resistivity transform

$$\left.\begin{aligned} \Delta\rho_{aS}(x) &= \frac{e^{3x}}{(1+e^{2x})^{7/2}} \\ \Delta T(y) &= \frac{e^{-y}+e^{-2y}}{15.e^{e^{-y}}} \end{aligned}\right\} \qquad (4.4.2)$$

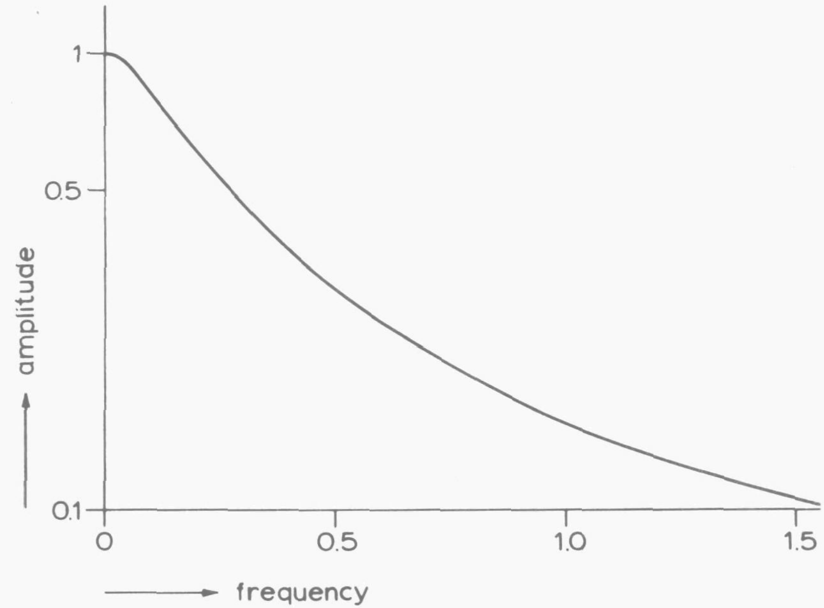

fig. 4.4.1 Amplitude FOURIER spectrum of the SCHLUMBERGER resistivity filter characteristic

The amplitude spectrum of the filter characteristic is shown in fig. 4.4.1. At zero frequency it has a magnitude equivalent to unity and decreases with increasing frequency to a low value which, however, is not zero.

4.5 Principle of the method proposed

In this thesis a method is proposed, based on sampling and filter theory, to obtain the resistivity transform from the apparent resistivity field curve.

The basic elements of sampling theory tell us that, if a function is sampled according to Nyquist rule (see chapter 5), then it is possible to recover the signal to any desired degree of accuracy. This is performed by replacing the sample values by interpolating functions of equivalent peak height and period determined by the sample rate. The sinc function shown in fig. 4.1.1 for example, is taken as the interpolating function. The property of sinc function is such that it is equal to unity at the sample point and zero at all other sample points. Addition of a finite number of sinc functions enables us to reconstruct the signal. Although in principle an infinite number of interpolation functions is required, but practically it suffices to use a finite number, at a loss of accuracy that can be controlled.

The apparent resistivity curve is sampled and replaced at the sample points by sinc functions. The resistivity transforms of each of these individual sinc functions are determined. And according to the superposition law of linear systems (see section 4.2) the sum of the transform of the partial functions gives us the total resistivity transform of the apparent resistivity curve.

The sinc function is a continuous curve such that its transform is also continuous. The addition process, however, is a laborious and timeconsuming one, so a simpler approach is given based on digital methods. The sinc response of the filter is determined and sampled in the function domain at the same rate as the apparent resistivity curve. This gives us the sampled digital operators. Different sets of filter coefficients need to be determined for the SCHLUMBERGER and WENNER arrangement.

The operators are required to be known once for all, such that the interpretation boils down in each field case, to run a weighted average of the sampled field apparent resistivity data with the operators. This is described by the following digitalized convolution process and can be applied both numerically or graphically

$$T_K = \sum_{j=-\infty}^{\infty} a_j . R_{K-j} \tag{4.5.1}$$

where

T_K = resistivity transform at sample point K

R_K = apparent resistivity value at sample point K

a_j = filter coefficients, number determined by length of filter to be used.

Eq. (4.5.1) yields the values of the resistivity transform at the sample points. The transform curve is obtained by joining the transform values at the sample points. The interpolation is quite reasonable if the points are not too far off from each other. It may be recalled that the apparent resistivity curve was also obtained in a similar manner by interpolation of the readings at various electrode distances as the electrodes were successively expanded. The basic problem is thus

1) to determine the sampling rate
2) to determine the filter operators.

In chapter 5 the problem of sampling is discussed, whereas in chapter 6 the filter operators are determined. Accuracy of the method and the time involved in the process will also be investigated.

CHAPTER 5

FIXATION OF THE SAMPLING INTERVAL

5.1 Introduction

Sampling is the art of representing a smooth continuous function by discontinuous function values at discrete points of the independent variable, which might be any physical quantity. The lay-out of the sample points defines the sampling pattern. Several variations used in practice have been outlined by MONROE (41). Here we shall be concerned only with equispaced data that calls for *periodic* sampling. The period at which the sample points appear is known as the *sampling interval* and its inverse gives us the *rate* of sampling.

The theory of equispaced data is much simpler to use. The resistivity observations in the field correspond to increasing electrode distances which are not linear. However, switching over to the logarithmic scale makes the data linear and amenable to sampling.

Sampling is applied mostly as a technique for easy and quick handling of a signal or function by using only a limited number of the data, as the basis of scientific work lies in simplification (ROBINSON, (58)). However, to use only specific values of a function, it should be ensured that these values are truly representative of the whole signal or function.

In our problem as enunciated in section 4.5, we have to replace the observed apparent resistivity curve by a number of sinc functions at the sampled points of the curve, Thus the initial task in the process is to determine the sampling interval with an eye that the sample values do truly represent the total field data.

5.2 SHANON's Sampling Theorem

The conditions under which a certain function g(x), can be sampled at all are

1) $g(x) \leftrightarrow G(f)$

2) $G(f) \simeq 0$, for $f > f_c$

where f_c is called the cut-off frequency.

The idea is that the art of applying sampling is filtering out the high frequency components of the function, provided the amplitude spectrum above f_c is practically zero. It signifies that sampling is applicable only to *band-limited* functions.

The choice of the proper sampling interval is vital in the recovery process of the signal from the sample values. SHANON's theorem guarantees that provided the sampling has been done according to the given condition, it is possible to recompute the function (if so desired) from the sample values only

$$0 \leq \Delta x \leq \frac{1}{2f_c} \tag{5.2.1}$$

where Δx is the sampling interval.

The largest permissable sampling interval is found from (5.2.1)

$$\left.\begin{aligned} \Delta x &= \frac{1}{2f_c} \\ \text{or} \quad f_c &= \frac{1}{2\Delta x} \end{aligned}\right\} \tag{5.2.2}$$

eq 5.2.2 is also known as the Nyquist rule. If the cut-off frequency is chosen too small (Δx large), such that the highfrequency components are not eliminated, then in the reconstruction process they manifest themselves into an effect called *aliasing* or *undersampling* (5, 55). Such a sampling is said to be *coarse*. (grof / ruw)

On the other hand if we apply a very fine sampling we do not lose any information about the function. But this means too many sampling intervals in a given range of the function which reduces the speed and efficiency of handling the data. Thus keeping a watch on the fact that the sampling interval be not greater than $\frac{1}{2}f_c$, we should try to fix it with the following points in consideration:

1) accuracy desired
2) speed and easiness in handling the sampled values
3) costs involved.

The third point may be lumped with the second for many purposes.

5.3 Reconstruction

A band-limited function sampled according to the condition stated by (5.2.1), can be completely recovered through the sample values.

The process of reconstruction of the function at intermediate points is effected by replacing the sample values by sinc functions of equivalent peak height and period determined by the sampling rate (fig. 5.3.1).

The sinc functions may be specified at as many points as desired. Addition of an infinite number of such functions truly redefines the original function. This is stated in the following equation, the proof of which can be found elsewhere (5, 55).

$$g_r(x) = \sum_{m=-\infty}^{\infty} g(m.\Delta x).\frac{\sin[\pi(x-m.\Delta x)/\Delta x]}{[\pi(x-m.\Delta x)/\Delta x]} \qquad (5.3.1)$$

where

$g_r(x)$ = reconstructed function

$g(m\Delta x)$= sample values of the original function at the sample points Δx, $2.\Delta x$, $3.\Delta x$ .... $m.\Delta x$.

$\frac{\sin[\pi(x-m.\Delta x)/\Delta x]}{[\pi(x-m.\Delta x)/\Delta x]}$ = so called 'sinc function' (WOODWARD, 1953), also known as interpolating function. It has the form of $\sin \nu/\nu$ and has the property:

sinc o = 1; sinc m = 0, where m = 1, 2, 3, ...

At the sample point it is equivalent to 1 and at all other sample points is equal to zero. Also

$\int_{-\infty}^{\infty} \sin\nu d\nu = 1$

The reconstruction is said to be complete only when

$$g_r(x)-g_o(x) = 0 \qquad (5.3.2)$$

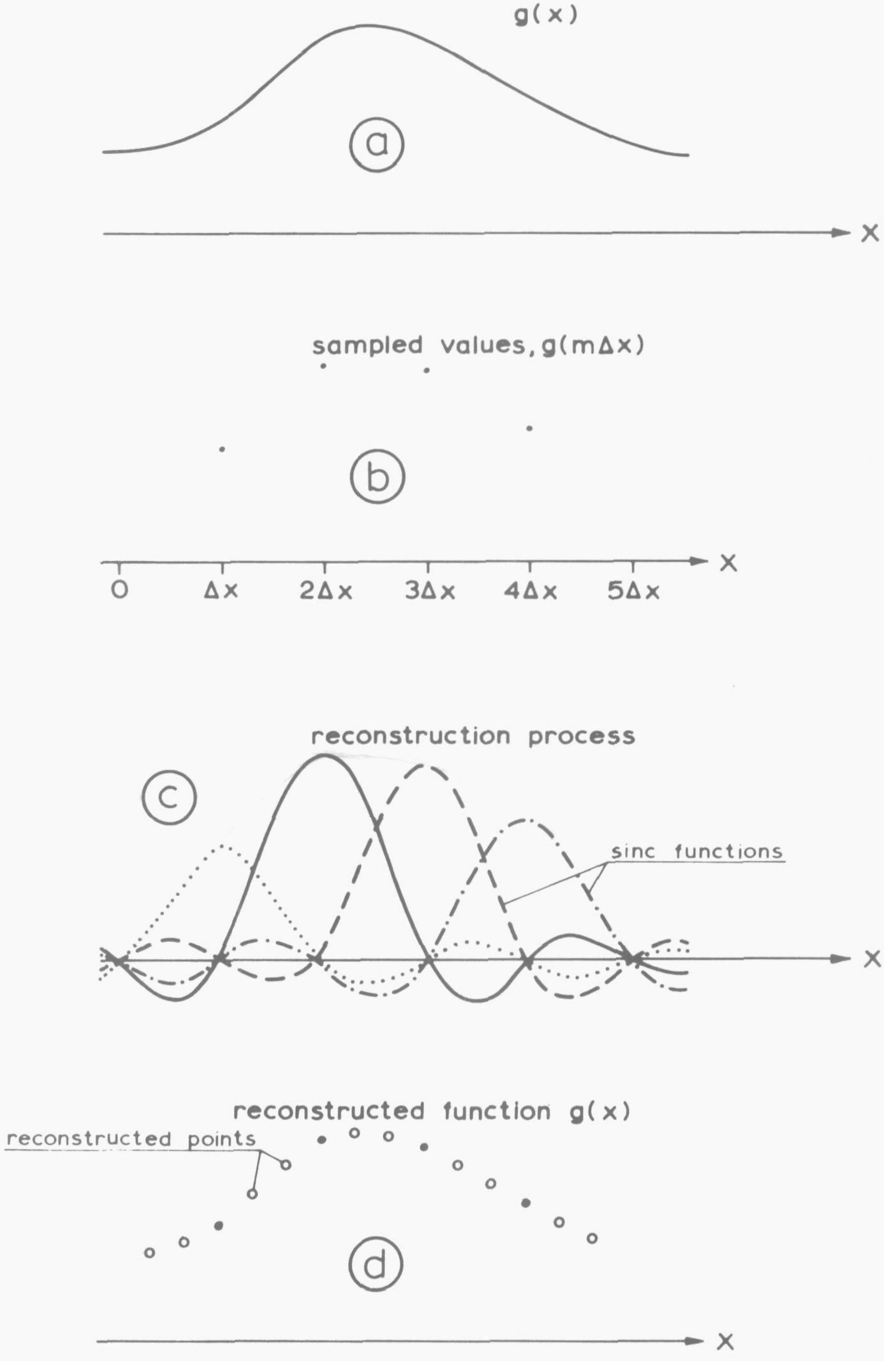

fig. 5.3.1 Sampling and Reconstruction

where

$g_o(x)$ = original function

5.4 Errors due to sampling

That eq (5.3.2) is never realized can be attributed to two main reasons:

a) that most functions are not by nature band-limited which brings about distortion in the reconstructed function, due to violation of conditions stated in section 5.2.

b) that in practice only a limited number of sinc functions corresponding to sample values within a finite range of the function are considered. We neglect the sample points outside this range, which in principle should extend up to infinite distances outside the range. The sinc function is one that approaches to zero only at infinite distances on either side. Thus there will be contributions from sinc functions situated at neglected sample values even far off from the range. Fortunately, however, the values of the sinc functions alternate in sign while their relative magnitudes go on decreasing the farther the sample point is from the range of our interest. Thus the combined effect of the neglected sample points may be quite small, and in any case the accuracy can be controlled.

These two errors manifest into a combined error such that we can state

$$\text{percentage error} = \frac{g_r(x)-g_0(x)}{g_0(x)} \times 100 \qquad (5.4.1)$$

This error has to be kept to a minimum, being guided by the accuracy with which sampling is to be applied.

5.5 Fourier Analysis of Apparent Resistivity curves

A frequency analysis is necessary to acquire a knowledge of the spectral behavior of apparent resistivity function. This should enable us to determine the cut-off frequency and hence the sampling interval.

Numerical evaluation of the Fourier transform of apparent resistivity is difficult because of the complicated nature of the expression of $\rho_{aS}(x)$, which has to be substituted for g(x) in eq (4.1.1). On the other hand the expressions for T(y) are rather simple to use (see section 2.3). The Fourier spectrum of apparent resistivity curves can be readily determined from the knowledge gained in section 4.3 and 4.4 from

$$G(f) = \frac{F(f)}{H(f)} \tag{4.2.3a}$$

where H(f) is the filter characteristic shown in fig (4.4.1) and

$$T(y) \leftrightarrow F(f) \text{ and } \rho_{aS}(x) \leftrightarrow G(f)$$

An initial difficulty in numerical integration of eq (4.1.1) for cases of T(y) in which the curve approximate to constant values, specially for ascending and descending type curves, were removed by taking the linearity property of Fourier transform into account (eq 4.1.6). The spectra were determined by parts and later summed up to give the total spectrum. Two methods utilized gave identical results:

1) In the first the T(y) curve was replaced by a convergent part and a part which approached to a constant value. The Fourier transform for the first part can easily be evaluated by applying numerical integration by using approximate integrals for eq (4.1.1). The latter part had the familiar form of a step function with amplitude corresponding to the asymptotic resistivity value. Although the integral of such a function diverges, the Fourier transform can still be determined by applying limiting processes (37). The spectrum of such a function is known.

2) Another method used to determine the Fourier transform was to replace the ascending or descending part of the T(y) curve by a slope

function having a comparable slope. It might be recalled that the block rectangular function having an amplitude (ζ) is the derivative of a slope function having a slope (ζ). Moreover the spectrum of a block function is known (fig. 4.1.1). Thus we have by the application of eq (4.1.5)

Fourier Transform of slope function

$$= \frac{\text{Fourier transform of block function}}{i2\pi f}$$

It is seen from the above relation that the spectrum has only an imaginary part. This is easily understood from the fact that it is derived from a symmetrical function which in general have no real components.

Cases examined

Resistivity distributions are numerous in nature but from the point of view of frequency behavior study, we could in general group them into ascending, descending and maximum or minimum bowl-shaped varieties. It is hoped that the study of these cases should yield sufficient information regarding the cut-off frequency to be used in resistivity sampling in general.

The list of cases including the mathematical expression used for the Fourier transform is given below. For the expression of T(y) to be used in place of g(x) in eq (4.1.1) we should refer back to section 2.3. Putting in the new variables defined by eq (4.3.1) into the expression of T(λ) for two and three layer cases give us the corresponding expressions for T(y). The case for the point pole has also been treated and the expression has been derived from the expression T(λ) for point pole given by KOEFOED (32). This case although not encountered in practical problems is, however, of basic fundamental importance in the theory of resistivity interpretation. The Fourier transform of G(f) is determined from F(f) by application of eq 4.2.3a. Taking $\rho_1 = 1$ and $u = e^y$ we have for

Point pole case

$$F(f) = \int_{-\infty}^{\infty} e^{-1/u} . e^{-i2\pi fy} . dy \qquad (5.5.1)$$

and
$|F(f)|$ appears in fig. 5.5.1 A

$|G(f)|$ appears in fig. 5.5.1 B

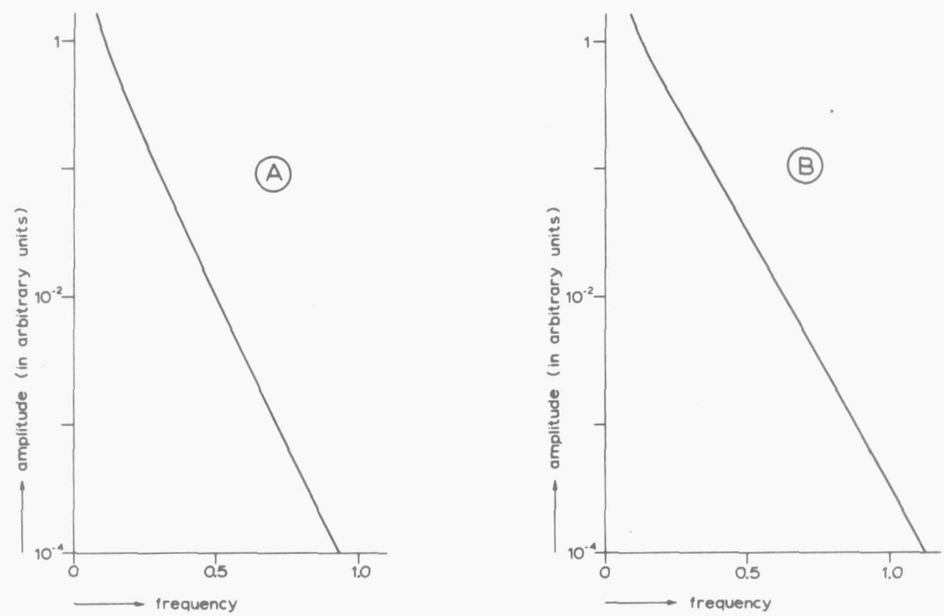

fig. 5.5.1 Amplitude FOURIER spectrum of (A) T(y) and (B) $\rho_{aS}(x)$ for point pole case

Two layer case

$$F(f) = \int_{-\infty}^{\infty} \frac{1+k_1 . e^{-2d_1/u}}{1-k_1 . e^{-2d_1/u}} . e^{-i2\pi fy} . dy \qquad (5.5.2)$$

with $d_1 = 1$ and $\rho_1 = 1$.

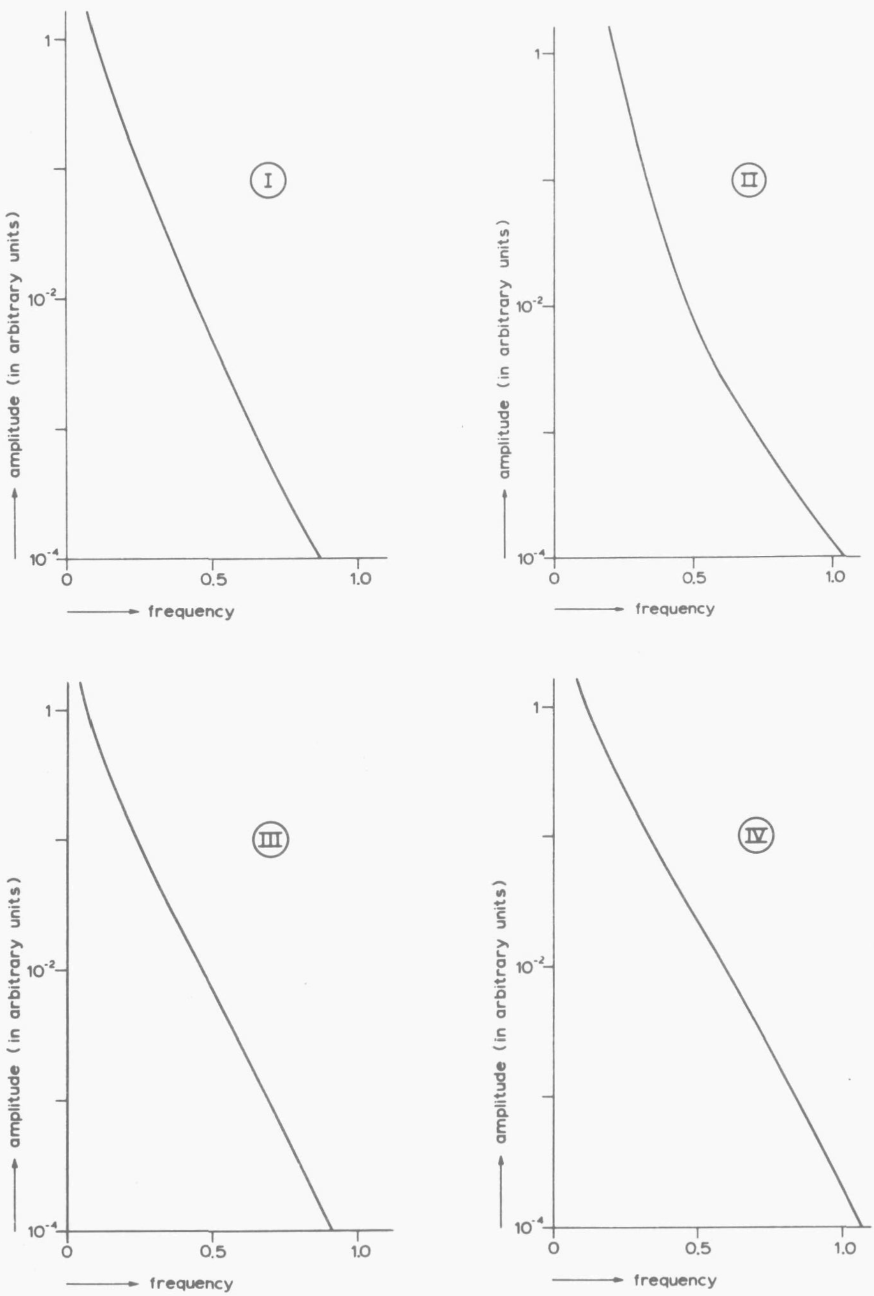

fig. 5.5.2.A Amplitude FOURIER spectrum of T(y) for two layer cases
(I) $k_1 = 0.3$ (II) $k_1 = 0.9$ (III) $k_1 = -0.3$ (IV) $k_1 = -0.9$

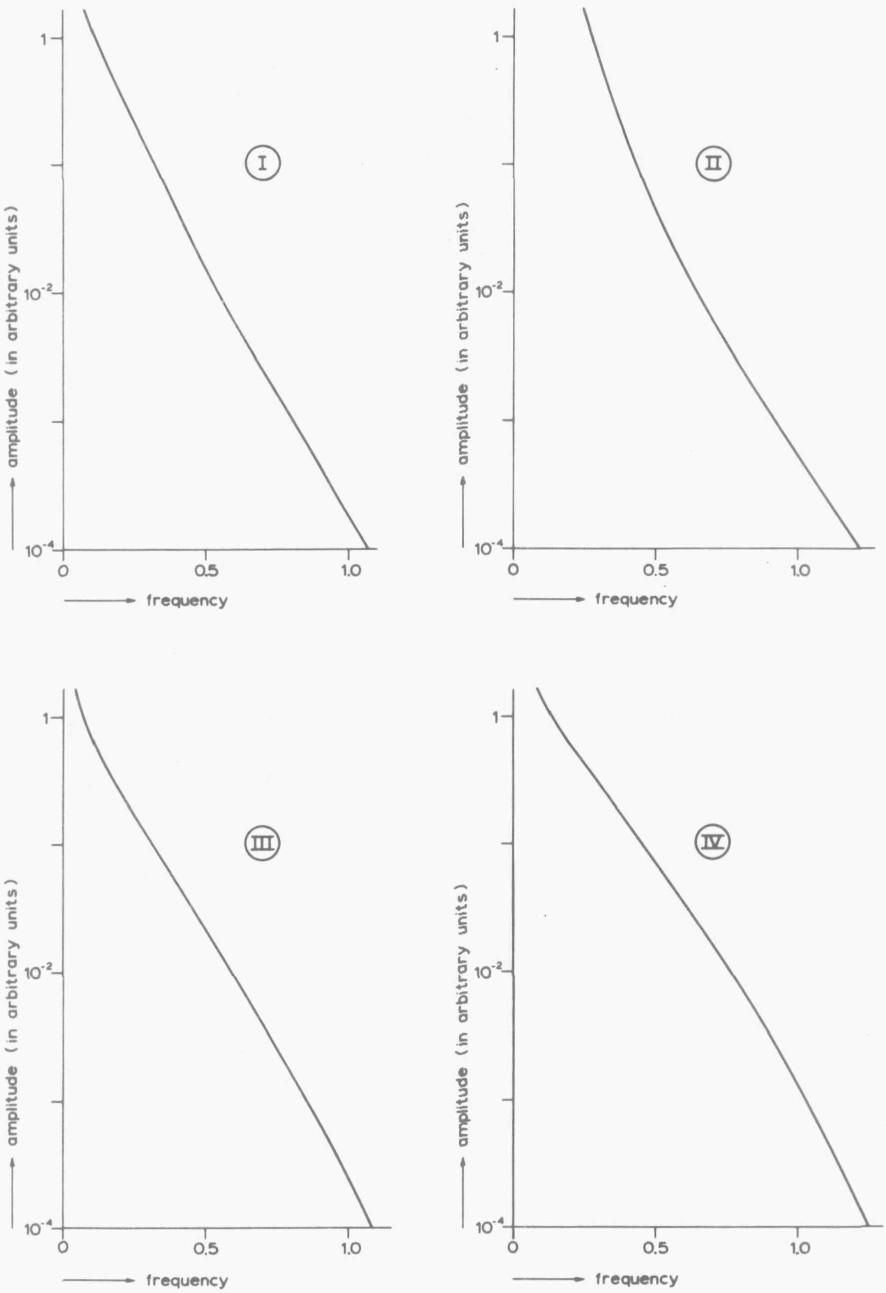

fig. 5.2.2.B Amplitude FOURIER spectrum of $\rho_{aS}(x)$ for two layer with
(I) $k_1 = 0.3$ (II) $k_1 = 0.9$ (III) $k_1 = -0.3$ (IV) $k_1 = -0.9$

and $\left.\begin{array}{l} |F(f)| \text{ is shown in fig. 5.5.2 A} \\ |G(f)| \text{ is shown in fig. 5.5.2 B} \end{array}\right]$

for

i) $k_1 = 0.3$ ii) $k_1 = 0.9$

iii) $k_1 = -0.3$ iv) $k_1 = -0.9$

<u>Three layer cases</u>

$$F(f) = \int_{-\infty}^{\infty} \frac{(1-k^2.e^{-2d_2/u})+k(e^{-2d_1/u}-e^{-2(d_1+d_2)/u})}{(1-k^2.e^{-2d_2/u})-k(e^{-2d_1/u}-e^{-2(d_1+d_2)/u})} . \quad e^{-i2\pi fy}.dy \tag{5.5.3}$$

with $d_1 = 1$; $\rho_1 = \rho_3 = 1$ *i.e.* $k = k_1 = -k_2$ and for varying thickness for the intermediate layer.

The amplitude spectra are shown in the following figures for

$$\left.\begin{array}{ll} |F(f)| & \left[\begin{array}{ll} \text{fig. 5.5.3 A (i)} & \text{with } d_2 = 2 \\ \text{fig. 5.5.3 A (ii)} & \text{with } d_2 = 3 \\ \text{fig. 5.5.3 A (iii)} & \text{with } d_2 = 5 \end{array}\right. \\ |G(f)| & \left[\begin{array}{ll} \text{fig. 5.5.3 B (i)} & \text{with } d_2 = 2 \\ \text{fig. 5.5.3 B (ii)} & \text{with } d_2 = 3 \\ \text{fig. 5.5.3 B (iii)} & \text{with } d_2 = 5 \end{array}\right. \end{array}\right] \quad \begin{array}{l} \text{for} \\ \text{a) } k = 0.3 \\ \text{b) } k = 0.8 \\ \text{c) } k = -0.3 \\ \text{d) } k = -0.8 \end{array}$$

Discussion on the amplitude Fourier spectrum of resistivity and transform curves

The use of the logarithmic scale facilitates the accommodation of the large drop in amplitude into a single diagram. The amplitude spectrum for two layer cases for low frequencies approach to infinity whereas for the three layer cases they have a 'singular' point with infinite value at zero frequency.

The amplitudes in general for all curves decrease with increasing frequency, being sharper for the three layer than the two layer cases. The decrease is less steep for the resistivity curves than the transform curves as is to be expected from the nature of the filter.

The pattern of decrease is quite encouraging from sampling view point. The amplitudes are quite small but do not completely become zero.

So a zero level has to be chosen below which the amplitudes can be considered negligible. However, there is left a considerable lot of discrepancy in the choice of this level *i.e.* in determining the cut-off frequency. Thus it was thought safer instead to assume a few sampling intervals corresponding to different cut-off frequencies (eq 5.2.2) and to see how well they reproduce a known function.

5.6 Determination of the sampling interval

Known two and three layer transforms were chosen for reconstruction. Three sampling intervals were tried out

a) $\Delta x_a = \ln(10)/4$

b) $\Delta x_b = \ln(10)/3$

c) $\Delta x_c = \ln(10)/2$

The two and three layer curves were first calculated using the expression for T(y) discussed in section 5.5 for varying values of the reflection coefficient. This gives us the original function. Next the curves were sampled according to the above intervals and the sampled values were used in eq (5.3.1) to construct the function at various intermediate points. The percentage error was then calculated in each case between the original and reconstructed function at various points by the help of eq (5.4.1). All the errors at these points will not be

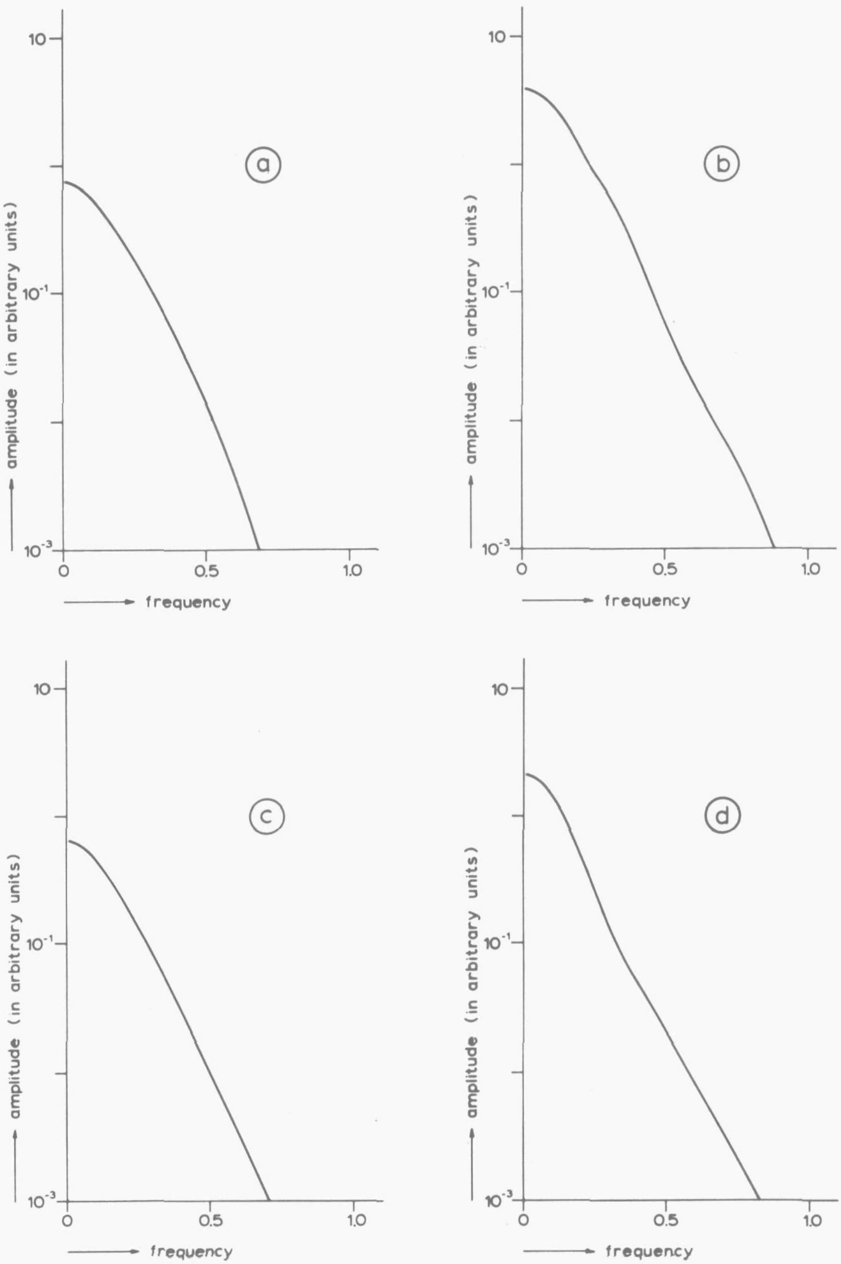

fig. 5.5.3. A (i) Amplitude FOURIER spectrum of T(y) for three layers with d_2 = 2 and (a) k = 0.3 (b) k = 0.8 (c) k = -0.3 (d) k = -0.8, where k = k_1 = $-k_2$

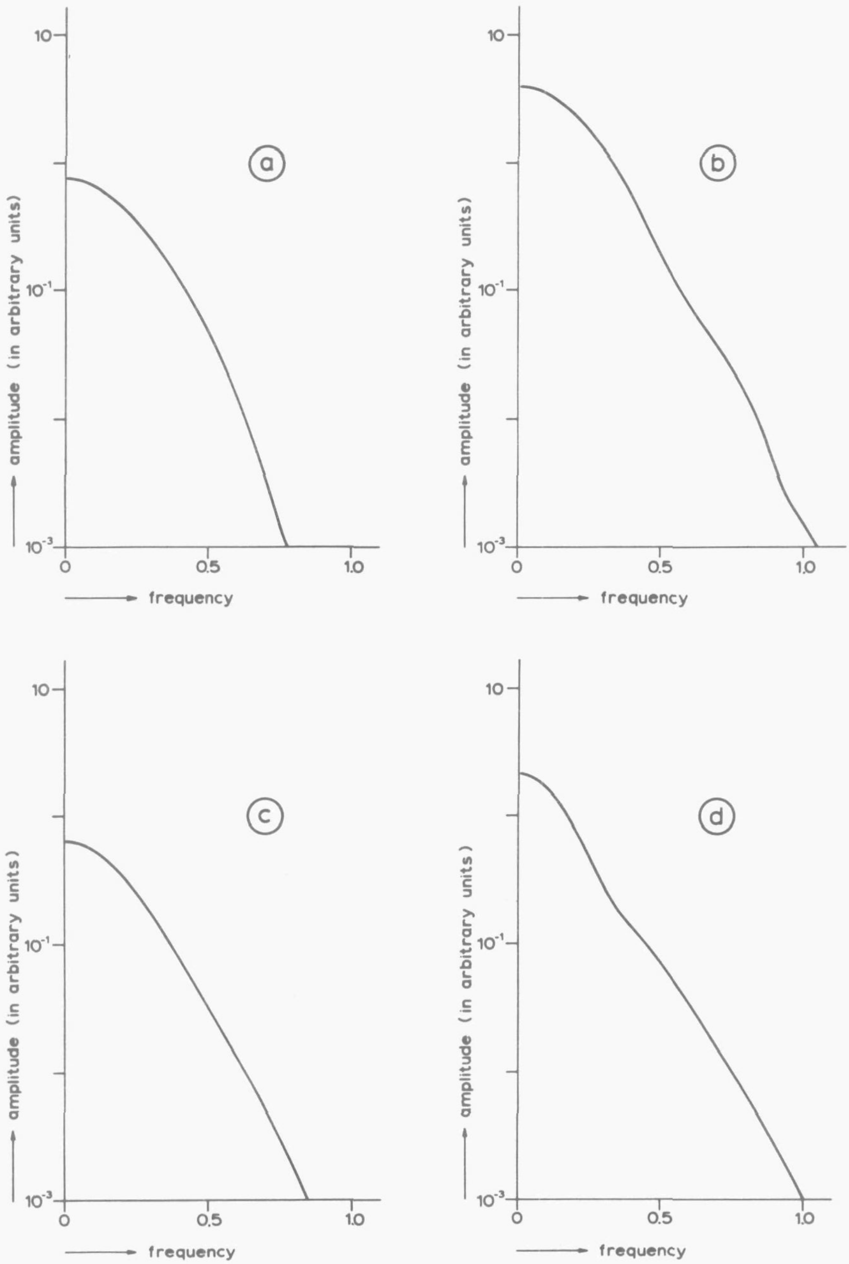

fig. 5.5.3. B (i) Amplitude FOURIER spectrum of $\rho_{aS}(x)$ for three layers with $d_2 = 2$ and (a) $k = 0.3$ (b) $k = 0.8$ (c) $k = -0.3$ (d) $k = -0.8$, where $k = k_1 = -k_2$

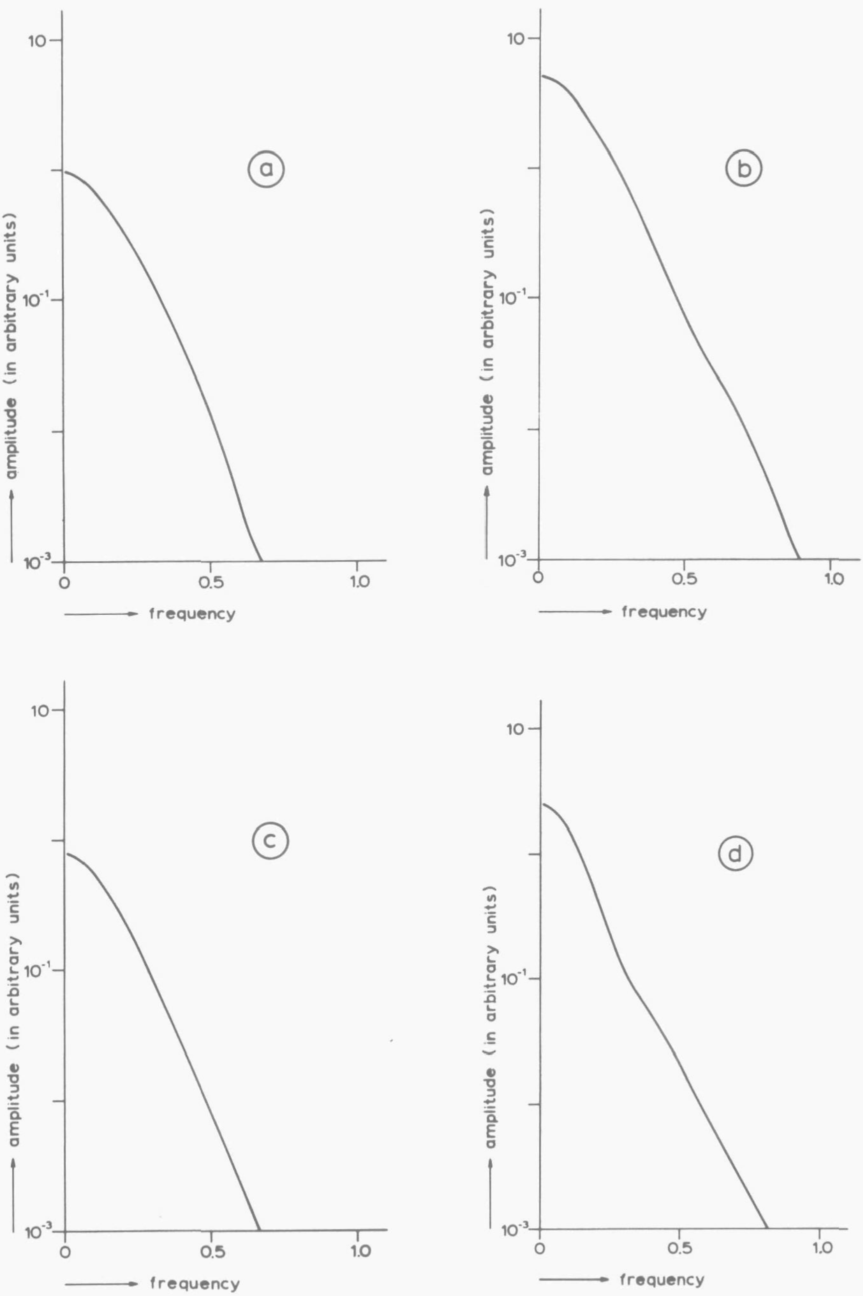

fig. 5.5.3. A (ii) Amplitude FOURIER spectrum of $T(y)$ for three layers with $d_2 = 3$ and (a) $k = 0.3$ (b) $k = 0.8$ (c) $k = -0.3$ (d) $k = -0.8$, where $k = k_1 = -k_2$

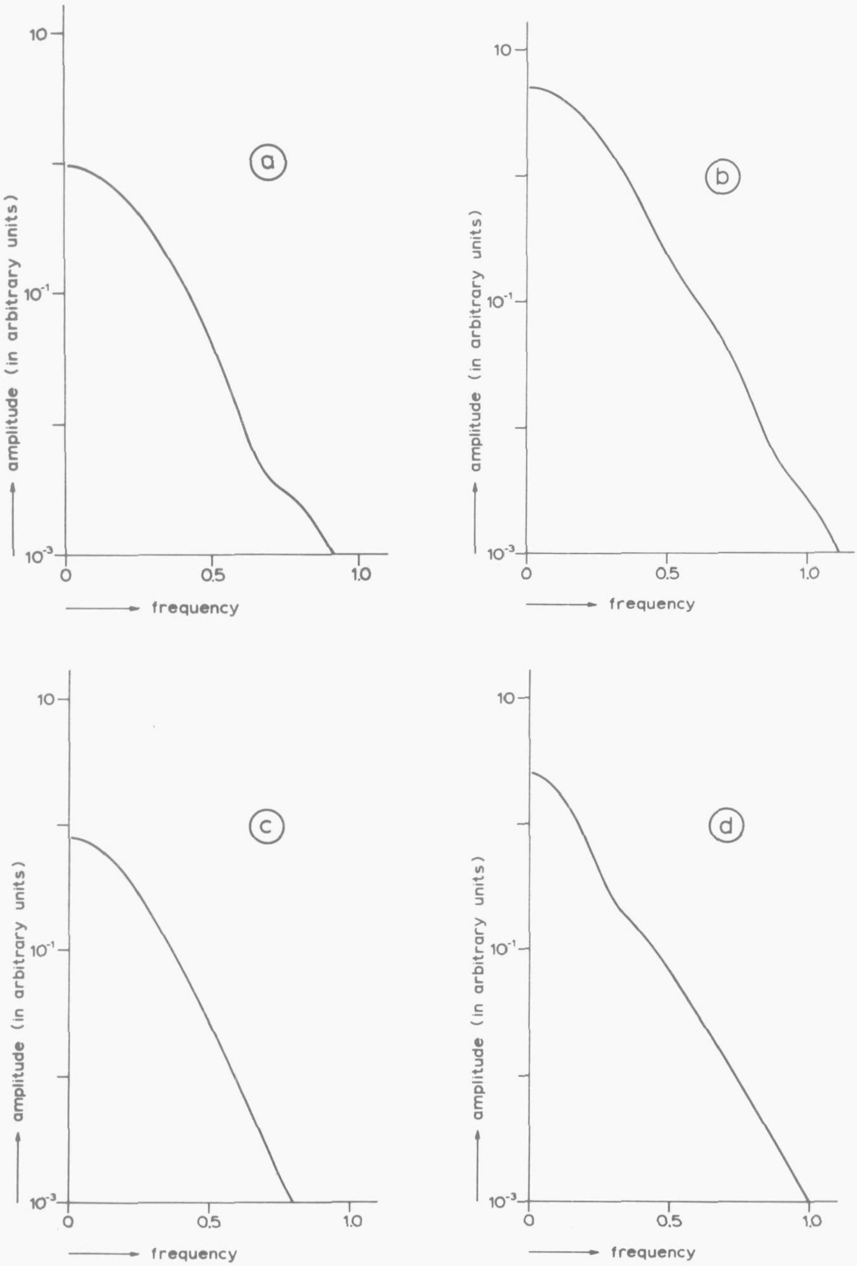

fig. 5.5.3. B (ii) Amplitude FOURIER spectrum of $\rho_{aS}(x)$ for three layers with $d_2 = 3$ and (a) $k = 0.3$ (b) $k = 0.8$ (c) $k = -0.3$ (d) $k = -0.8$, where $k = k_1 = -k_2$

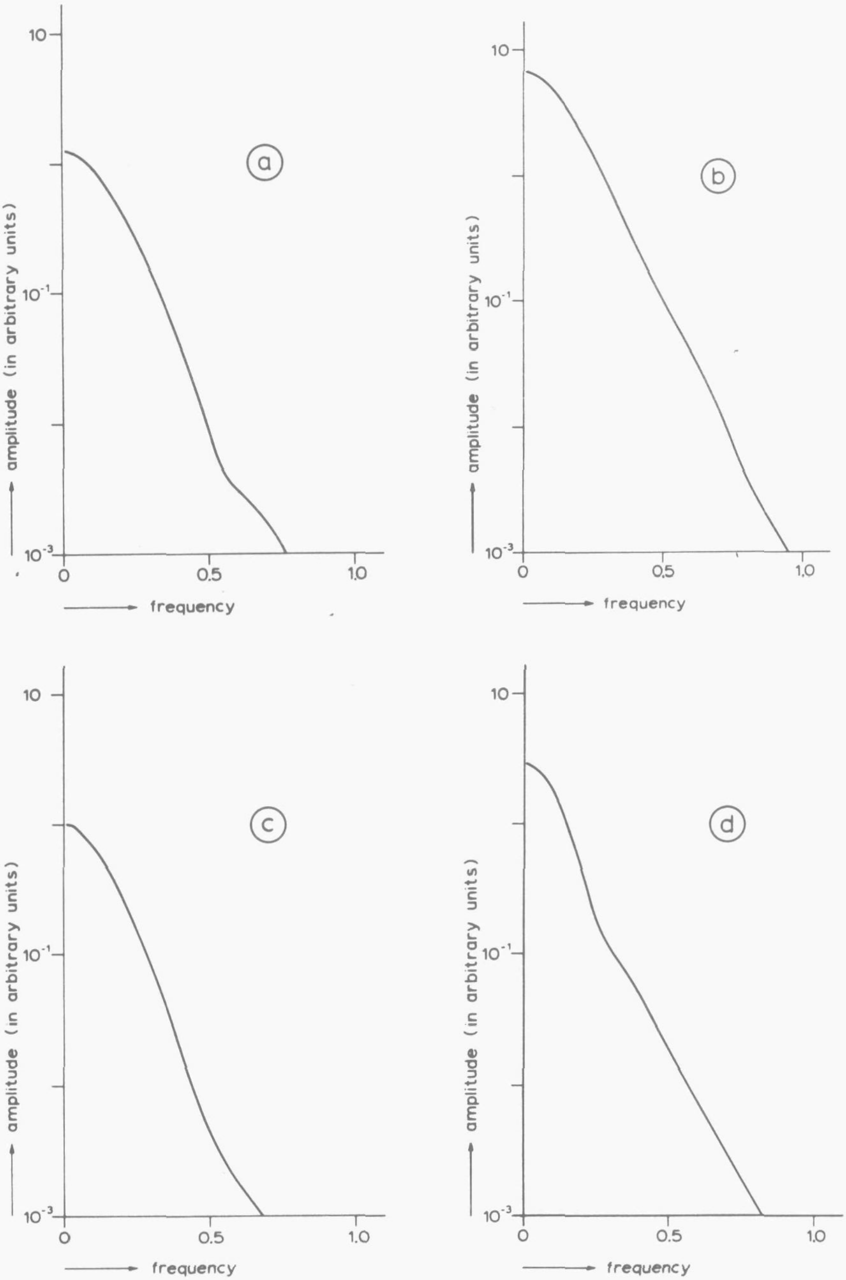

fig. 5.5.3. A (iii) Amplitude FOURIER spectrum of $T(y)$, for three layers with $d_2 = 5$ and (a) $k = 0.3$ (b) $k = 0.8$ (c) $k = -0.3$ (d) $k = -0.8$, where $k = k_1 = -k_2$

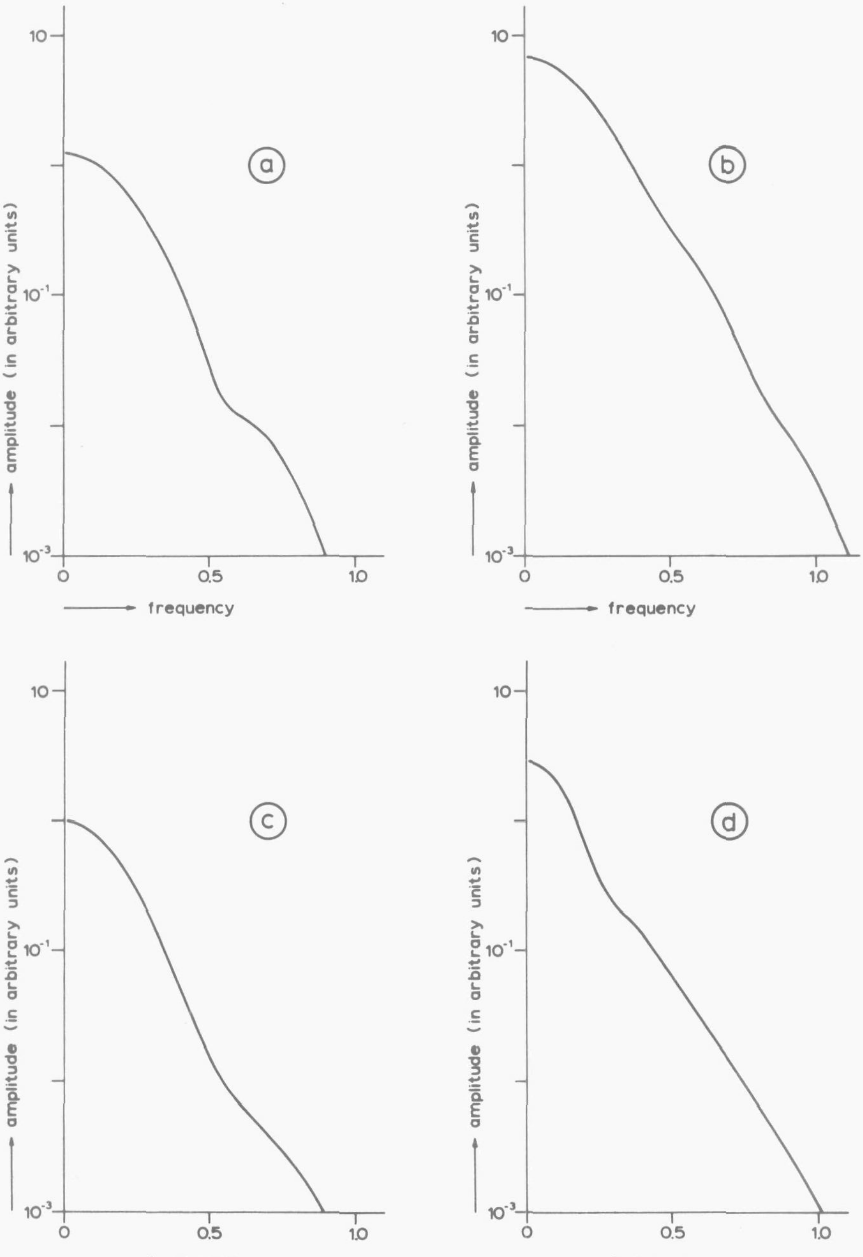

fig. 5.5.3. B (iii) Amplitude FOURIER spectrum of $\rho_{aS}(x)$ for three layers with $d_2 = 5$ and (a) $k = 0.3$ (b) $k = 0.8$ (c) $k = -0.3$ (d) $k = -0.8$, where $k = k_1 = -k_2$

Table 5.6.1. Showing the maximum percentage error between original and reconstructed two layer transform function for various values of the reflection coefficient, using different sampling intervals.

sampling → interval k_1 ↓	$\Delta x_a = \ln(10)/4$	$\Delta x_b = \ln(10)/3$	$\Delta x_c = \ln(10)/2$
0.3	$0.50.10^{-2}$	-0.04	-0.42
0.9	0.02	-0.11	-1.07
-0.3	$0.76.10^{-2}$	-0.07	0.57
-0.8	0.09	0.25	2.67
-0.9	0.19	0.64	6.24

Table 5.6.2. Showing the maximum percentage error between original and reconstructed three layer transform with $d_1 = 1$, $d_2 = 3$ and for various values of k where $k = k_1 = -k_2$, using different sampling intervals.

sampling → interval k ↓	$\Delta x_a = \ln(10)/4$	$\Delta x_b = \ln(10)/3$	$\Delta x_c = \ln(10)/2$
0.3	$0.85.10^{-2}$	0.06	0.89
0.9	0.06	0.68	5.59
-0.3	$-0.59.10^{-2}$	0.06	0.67
-0.8	-0.03	0.24	0.96
-0.9	-0.04	0.28	1.73

shown but only the maximum deviation is illustrated in table 5.6.1 and 5.6.2 to give an idea of what should be the correct interval to be used.

It is immediately clear that the sampling interval Δx_c does not recover the function and apparently does not satisfy the condition stated by eq 5.2.1, thus it is rejected. In principle both the sampling intervals Δx_a and Δx_b can be used, for they yield an accuracy which can be termed as quite high.

So our choice between these two intervals will thus naturally be guided by the speed of application. In this context let us consider a resistivity survey with a spread equivalent to 300 m. This is the most common length of survey used for ground water exploration, although it is conceded that there are exceptions controlled by geological conditions. Δx_a refers to 4 and Δx_b to 3 intervals in a factor 10 of a log-log scale on which resistivity curves are commonly plotted. This means we have 12 sample points while working with Δx_a and 10 sample points with Δx_b, where we desire to find the T(y) values from the $\rho_{aS}(x)$ values. This literally means that considerable speed is gained by working with an interval Δx_b without loss of accuracy from our point of view. This interval is thus recommended to sample resistivity curves, plotted on a log-log scale preferably on a 62.5 modulus.

CHAPTER 6

DETERMINATION OF THE SCHLUMBERGER FILTER COEFFICIENTS

6.1 Sinc response of the SCHLUMBERGER filter

After having determined the sampling interval the next important task is determining the response of the filter to an input of sinc function. The period of the sinc function is fixed by the sampling interval decided upon. According to the principle of the proposed method laid down in section 4.5 of Chapter 4, the digital operators will be given by the sample values of this response. A running weighted average of the resistivity sample values with the filter coefficients yield the transform values at the sample points.

The sinc response of the filter can be found out in two different manners which are given below:

a) *by convolution*

In the first procedure the sinc function, $\frac{\sin 2\pi f_c x}{2\pi f_c x}$ is treated as the input in lieau of $\rho_{aS}(x)$ in eq (4.3.2), such that the transform of the sinc function or simply the sinc response is given by

$$\text{sinc response} = \int_{-\infty}^{\infty} \frac{\sin\beta}{\beta} . J_1\{e^{-(y-x)}\}.dx \qquad (6.1.1)$$

$$\text{sinc response} = \text{sinc } \beta * h(x) \qquad (6.1.1a)$$

where

$\beta = 2\pi f_c x$

$h(x)$ = pulse response of the resistivity filter

The numerical integration of eq. 6.1.1 can be achieved either by ROMBERG's method or SIMPSON's method. However, due to rapid oscillations of the BESSEL function the computing time is enormous and also the accuracy with SIMPSON's method may be effected.

b) *operation in frequency domain*

An alternative procedure is to operate in the frequency domain, such that eq 6.1.1a becomes

$$B(f) = \text{spectrum of sinc function} \times H(f) \qquad (6.1.1b)$$

where

$H(f)$ = frequency characteristic of the resistivity filter shown in fig. 4.4.1

$B(f)$ = frequency representation of the sinc response.

The sinc response b, can be recovered from B(f) by applying the inverse Fourier transform given by eq (4.1.4). The sinc response of the filter is shown in fig. 6.1.1.

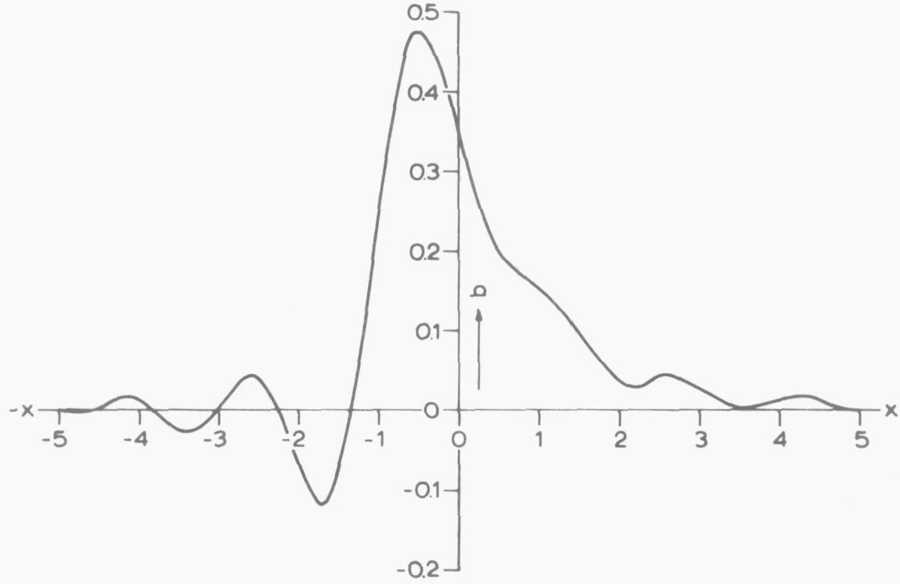

fig. 6.1.1 Sinc response of the SCHLUMBERGER filter

It has finite responses for both positive and negative values of the independent variable. The response oscillates, however, the magnitude diminishes rapidly with increasing value of the independent variable on either side. Moreover, the magnitude of the response is favourably placed with respect to the sampling interval (Δx = ln(10)/3≈0.77).

This is quite encouraging as for practical application only a finite interval of the response need be considered.

6.2 Filter coefficients

The response is sampled in the x-domain at the same interval as was used to sample the resistivity data i.e. $\Delta x = \ln(10)/3$. This is important if we wish to obtain the same form of sampled output as the input. If we now take the sampling interval Δx as our unit then the filter coefficients will be situated at the index values of the independent variable, -3, -2, -1, 0, 1, 2 and so on. Let us denote by a_j the filter coefficients. The arrow at a_0 indicates the centre of the filtering operation.

The twelve point filter [1] $[a_{-3}, a_{-2}, a_{-1}, a_0, a_1, a_2, a_3, a_4, a_5, a_6, a_7, a_8]$ is shown in table 6.2.1. We shall term this as the long filter, reasons for which will be given subsequently.

----

[1] In the terminology used in seismic data processing this would be referred to as a two sided filter with a memory function $(a_0 \ldots a_8)$ and an anticipation function $(a_{-3} \ldots a_{-1})$. However, as the purpose and principle involved in obtaining the operators are quite different we have avoided using these terms. It may suffice here to say that our purpose is to find the depths and resistivities and thus we need higher accuracies. For the same reason we chose the sinc function instead of Dirac function used in seismic data processing. The main object there is to enhance the resolution of adjacent traces and for that purpose they use filter coefficients to deconvolve the trace, i.e. the problem there is to determine such operators which when applied to the input would yield a DIRAC pulse (1,0,0,0....). These operators are thus known as inverse operators. The stability of such operators are increased by using a two sided filter (57).

Table 6.2.1. The long SCHLUMBERGER filter coefficients

a_j	values	a_j	values
a_{-3}	0.0060	a_3	0.0358
a_{-2}	-0.0783	a_4	0.0198
a_{-1}	0.3999	a_5	0.0067
a_0	0.3492	a_6	0.0051
a_1	0.1675	a_7	0.0007
a_2	0.0858	a_8	0.0018

6.3 Length of the filter

In digital operations the length of the filter refers to the number of coefficients defining the response. The following considerations govern the choice of the number of terms:

a) how far the response of the filter is represented by the coefficients chosen?

b) what is the accuracy obtained while working with the chosen coefficients?

c) what is the speed realized?

d) what is the nature of the input?

The twelve point filter choice was governed mainly only by the first consideration. We shall in this section analyze it in the light of the other three questions raised.

The speed and accuracy of working with the coefficients is partly dependent on the form of the input data. This question of accuracy does not arise on filters working on real time, as there are no coeffients for $t<0$. This signifies that the output let us say at $t = T'$, will depend on the input at $t = T'$ and also on the inputs prior to that, but not on future values of the input after the interval $t = T'$.

This will be understood completely from the knowledge how these digital operators function. We shall leave this to chapter 7 and only mention here that the operators are reversed about x or $t = 0$ and then applied on the input. Thus for filters, that have only responses for $t \geq 0$, there are no coefficients beyond the sample point $t = T'$. Also even for a two sided filter, there will be no dependence on future values of the input, if the input or function approach to zero on right side of the range up to where the output is desired.

However, the case involved in the resistivity problem is different. We know for certain that the ρ_a curve to the left approaches ρ_1 for small electrode spacing and to the resistivity of the substratum to the right for large electrode spacing and also that the filter has finite responses for $x<0$. We shall explain the implications by the help of an example:

Let us imagine that the curve obtained in the field is defined between 1 to 300 m of electrode spacings. We now desire to determine the transform within that range by the filter coefficients defined by Table 6.2.1. The real problem is at the two ends of the curve. We have said that the coefficients to operate have to be reversed about $x = 0$. This means to know the output at the right end of the curve, we still need three more sample values of the curve beyond 300 m, corresponding to the coefficients a_{-1}, a_{-2} and a_{-3}. That means the curve has to be extrapolated to the right up to three sample points. This operation here has an effect on the output if the extrapolation is not correct. Errors in extrapolation arise only when the asymptotic value of the curve has not been reached during the survey performed. On the other hand to the left of the curve we need maximum 8 extra sample points to yield the output from 1 to 300 m, corresponding to the filter coefficients a_1, a_2 ... a_8. However, the extrapolation to the left is no real problem as it refers to small spacings and the resistivity if it could have been measured would always be the resistivity of the top layer as current is confined only to the first layer for small spacings.

Thus it is desirable that the number of filter coefficients for $x<0$ be as less as possible, to cut down errors due to extrapolation.

The speed is governed by the total number of coefficients. A survey of table 6.2.1 reveals that the coefficients a_{-3}, a_7 and a_8 are sufficiently small such that the length of the filter could be cut down by accommodating the magnitudes corresponding to them into adjacent coefficients. This procedure gives rise to considerable gain in working speed but will certainly reduce the accuracy because of violation of the first condition mentioned before.

6.4 Comparison between the two sets of filter coefficients

We call the resulting filter coefficients the short filter which is shown in Table 6.4.1. In the next chapter we have investigated the

Table 6.4.1. The short SCHLUMBERGER filter coefficients

a_{-2}	a_{-1}	a_0	a_1	a_2	a_3	a_4	a_5	a_6
-0.0723	0.3999	0.3492	0.1675	0.0858	0.0358	0.0198	0.0067	0.0076

effect on the accuracy of the method due to shortening of the filter. A resistivity function was so chosen that its theoretical transform could be calculated mathematically. Next the transform was calculated from the sample resistivity values by the filter method using both the long and the short filter coefficients. The resulting transform was then compared with the theoretical one. The long filter yielded an accuracy of about $\frac{1}{4}\%$ and the short filter about 1.5% (see Fig. 7.6.1). This error also included errors brought about by sampling. The speed of application was much faster with the short filter.

Thus it is concluded that the short filter be used, as it yields an accuracy of obtaining the transform which is reasonably high besides imparting speed to the process.

CHAPTER 7

PRACTICAL PROCEDURE OF APPLICATION, SCOPE AND ACCURACY OF THE METHOD

7.1 Introduction

This chapter deals with the practical aspects of the problem including the method of application, accuracy and range of applicability.

The process of application and accuracy obtained then are treated in the light of actual techniques adopted in the field in procuring resistivity data. For this various alternative suggestions are given in the mode of interpretation to suit diversified needs.

7.2 The process of obtaining the resistivity transform from the sampled apparent resistivity field curve

a) *Numerical calculation by convolution*

The convolution of the apparent resistivity sample values with the filter coefficients yields the resistivity transform. Since we are here concerned with sampled data at discrete interval of the independent variable, the convolution integral for example eq 4.3.2 is now to be replaced by a summation. The statement of the digitalized convolution would thus be

$$T_m = \sum_{j=-2}^{6} a_j \cdot R_{m-j} \qquad \sum_{-1}^{2} \qquad (7.2.1)$$

Eq. 7.2.1 signifies that a running weighted average of the input resistivity sample data with the filter coefficients a_j (short filter, table 6.4.1) yields the transform value at the sample points $m\Delta x$. If Δx is taken as out unit then the input will be given by R_m where m is an integer. For example the transform value at sample point 3 becomes

$$T_3 = a_{-2}R_5 + a_{-1} \cdot R_4 + a_0R_3 + a_1R_2 + a_2R_1 + a_3R_0 + a_4R_{-1} + a_5R_{-2} + a_6R_{-3} \qquad (7.2.2)$$

For convention sake we assume that the resistivity curve is defined starting from sample point 0 to let us say sample point 4, remembering tnat each sample point is at equal spacing, of $\Delta x = \ln(10)/3$ = our unit, from the other. Then eq (7.2.2) suggests that R_5 and (R_{-3}, R_{-2}, R_{-1}) have to be obtained by extrapolating the field curve to the left to obtain (R_{-3}, R_{-2}, R_{-1}) and to the right to obtain R_5. This is necessary from the nature of resistivity curves (see section 6.3), if a correct estimate on the output is to be obtained between sample point 0 and 4.

For those who are not conversant with the working of digital operators we shall try to clarify the process by considering the action of an arbitrary four point filter (a_{-1}, a_0, a_1, a_2) on the resistivity input data (R_0, R_1, R_2, R_3). The first step in the process is to reverse the filter coefficients about x = 0, (a_2, a_1, a_0, a_{-1}) and then to operate on the input as follows (R_{-2}, R_{-1} and R_4 are extrapolated sample values):

<u>at sample point 0</u>

$$T_0 = a_2R_{-2}+a_1R_{-1}+a_0R_0+a_{-1}R_1$$

R_{-2},	R_{-1}	R_0	R_1	R_2	R_3	R_4
a_2	a_1	a_0	a_{-1}			

<u>at sample point 1</u>

$$T_1 = a_2R_{-1}+a_1R_0+a_0R_1+ a_{-1}R_2$$

R_{-2},	R_{-1}	R_0	R_1	R_2	R_3	R_4
	a_2	a_1	a_0	a_{-1}		

<u>at sample point 2</u>

$$T_2 = a_2R_0+a_1R_1+a_0R_2+ a_{-1}R_3$$

R_{-2},	R_{-1}	R_0	R_1	R_2	R_3	R_4
		a_2	a_1	a_0	a_{-1}	

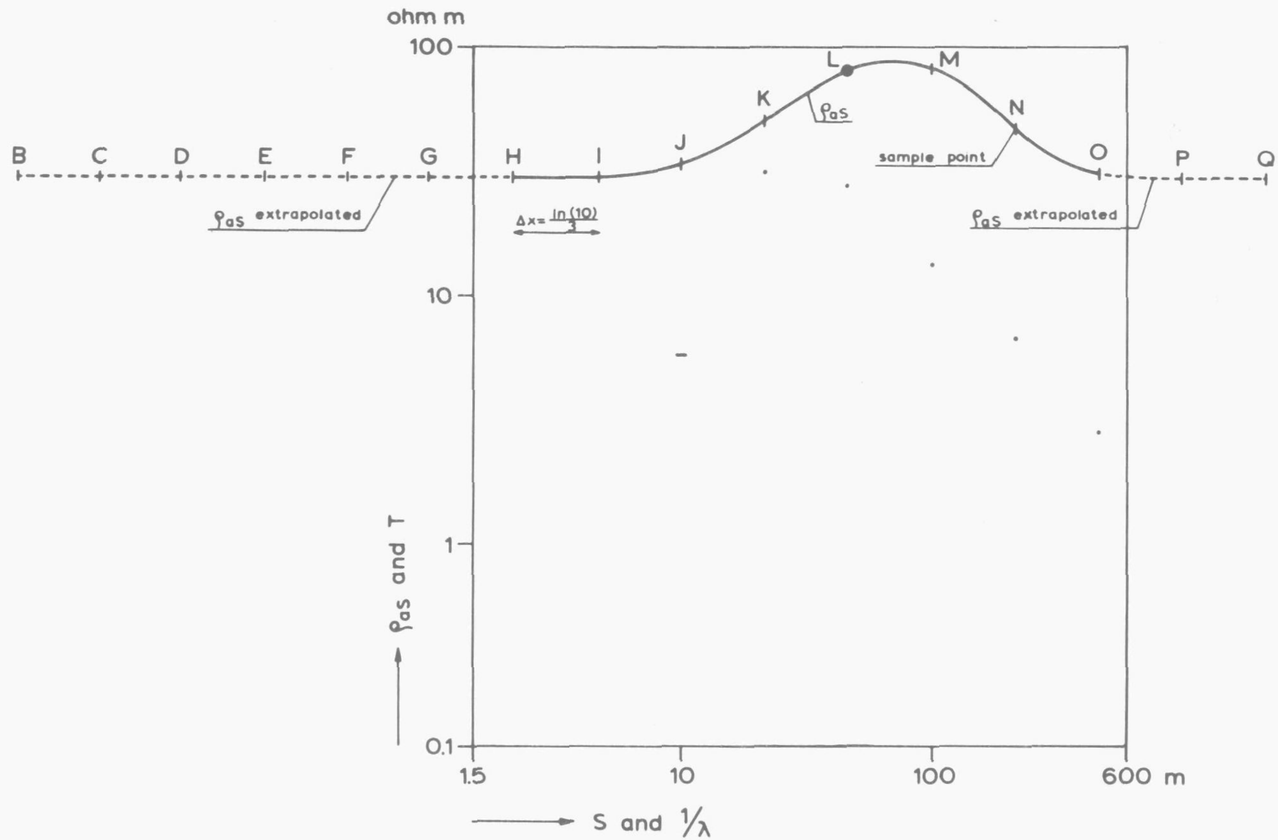

fig. 7.2.1 Illustration of the graphical process of application of the method

<u>at sample point 3</u>

$$T_3 = a_2R_1 + a_1R_2 + a_0R_3 + a_{-1}R_4$$

$$\begin{array}{lcccccl} R_{-2},\ R_{-1} & \boxed{R_0} & \boxed{R_1} & \boxed{R_2} & \boxed{R_3} & & R_4 \\ & & \boxed{a_2} & \boxed{a_1} & \boxed{\overset{\uparrow}{a_0}} & \boxed{a_{-1}} & \end{array}$$

The above procedure and the expression of the transform clearly demonstrate the dependence of the output on the extrapolated values.

b) *Graphical process by superposition*

An alternative method, that would yield identical results as shown above, is to superimpose the individual responses obtained after each input data has been operated upon by the filter coefficients (a_{-1}, a_0, a_1, a_2).

This can be accomplished either numerically or graphically. We shall confine ourselves to the graphical method because of its utility to the field geophysicists. We shall redirect our attention to the SCHLUMBERGER short filter coefficients shown in table 6.4.1 and discuss the practical method of application on a true apparent resistivity curve shown in Fig. 7.2.1

The procedure to be followed to obtain the transform curve is summarized in the following steps:

1) For convenience of application retrace the field apparent resistivity curve on the top right portion of a log-log transparent paper. For the modulus to be used there is no restriction, but a 62.5 modulus is recommended. A 83.3 modulus can also be used, although on this modulus the interpolation between the derived transform points is more difficult.

2) The sample values are marked on the observed curve by a dash. In Fig. 7.2.1 they are defined from sample point H to 0. Also mark six extrapolated points to the left of H and 2 to the right of 0, if you are using the short filter. The sample points should be at an equal spacing of $\Delta x = \ln(10)/3$ i.e. on your logscale there should be 3 intervals in a factor of 10.

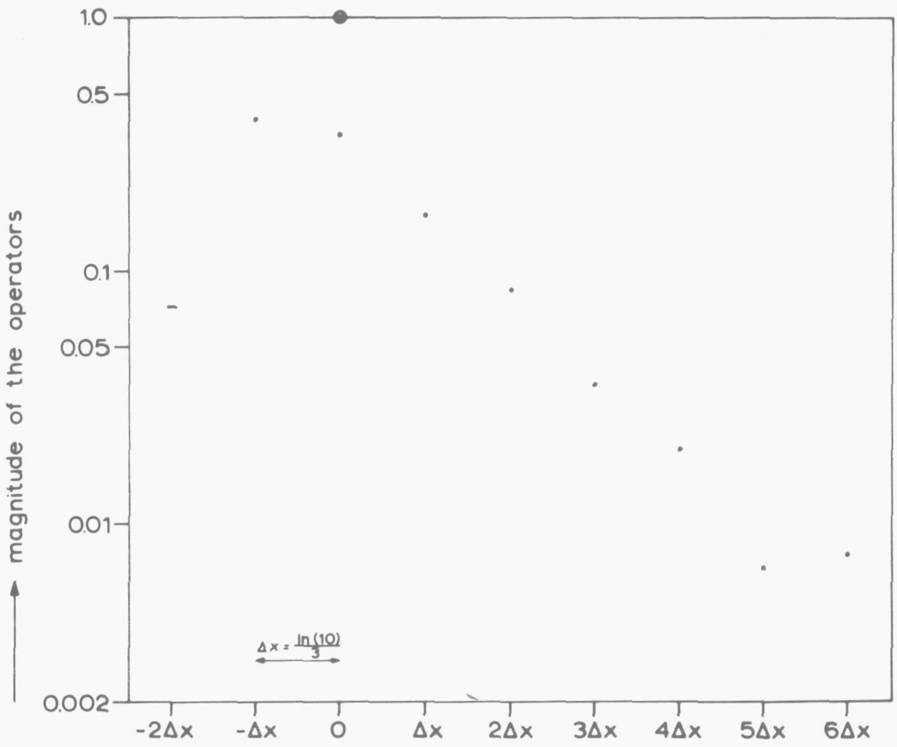

fig. 7.2.2 The SCHLUMBERGER short digital filter coefficients

3) Plot the filter coefficient on to another log-log paper of the same modulus with their proper magnitude and proper spacing i.e. the same spacing of $\Delta x = \ln(10)/3$. Put a cross at ordinate value of 1 and abscissa value of $x = 0$ i.e. directly above a_0. This is shown in fig. 7.2.2. Note that the filter coefficient a_{-2} has negative value and hence it is denoted by a dash sign to signify the fact that its contribution has to be subtracted from the rest.

4) The process of multiplication of the input with the filter operators is performed by first superimposing the resistivity chart upon the filter chart, then coinciding the sample value with the cross and tracing the filter points on to the resistivity chart. This is executed as follows:

a) Place the last extrapolated sample point to the left of the resistivity curve i.e. point B on to the cross and trace the filter points on to the resistivity chart. There is no need of tracing points that fall outside the range of the observed curve because the transform is need to be obtained only in this range.

b) Keeping the filter chart fixed, move the resistivity chart to the left over it in such a manner, that the second last of the extrapolated point i.e. C, is now at the cross. Trace the filter points on to the resistivity chart.

c) As a check, observe after performance of step (b) there should be two points below sample point H, and one below I. If this is not so, some errors have been committed regarding the number of extrapolated points in step 2 or in plotting the filter coefficients in step 3. Recheck these steps.

d) Perform the operation (b) at all other sample points from D to Q, by successively adjusting them to the cross and tracing the filter points on to the resistivity chart.

e) As another check, at least at each of the sample points in the middle range of the resistivity curve, there should be nine points corresponding to nine filter coefficients comprising the short filter, after the step (d) has been completed.

5) Now at each sample point from H to O, add the respective values of the points. Do not forget to subtract the value of the dash.

6) Plot the sum thus obtained at each sample point.

7) This gives us the transform value at each sample point corresponding to the sample resistivity value at that point.

8) By careful interpolation between the transform values draw the transform curve.

9) To determine the thickness and resistivities of the subsurface apply KOEFOED's method (33) to the transform curve so obtained.

Fig. 7.2.1 shows the operation at only one of the sample points viz. L.

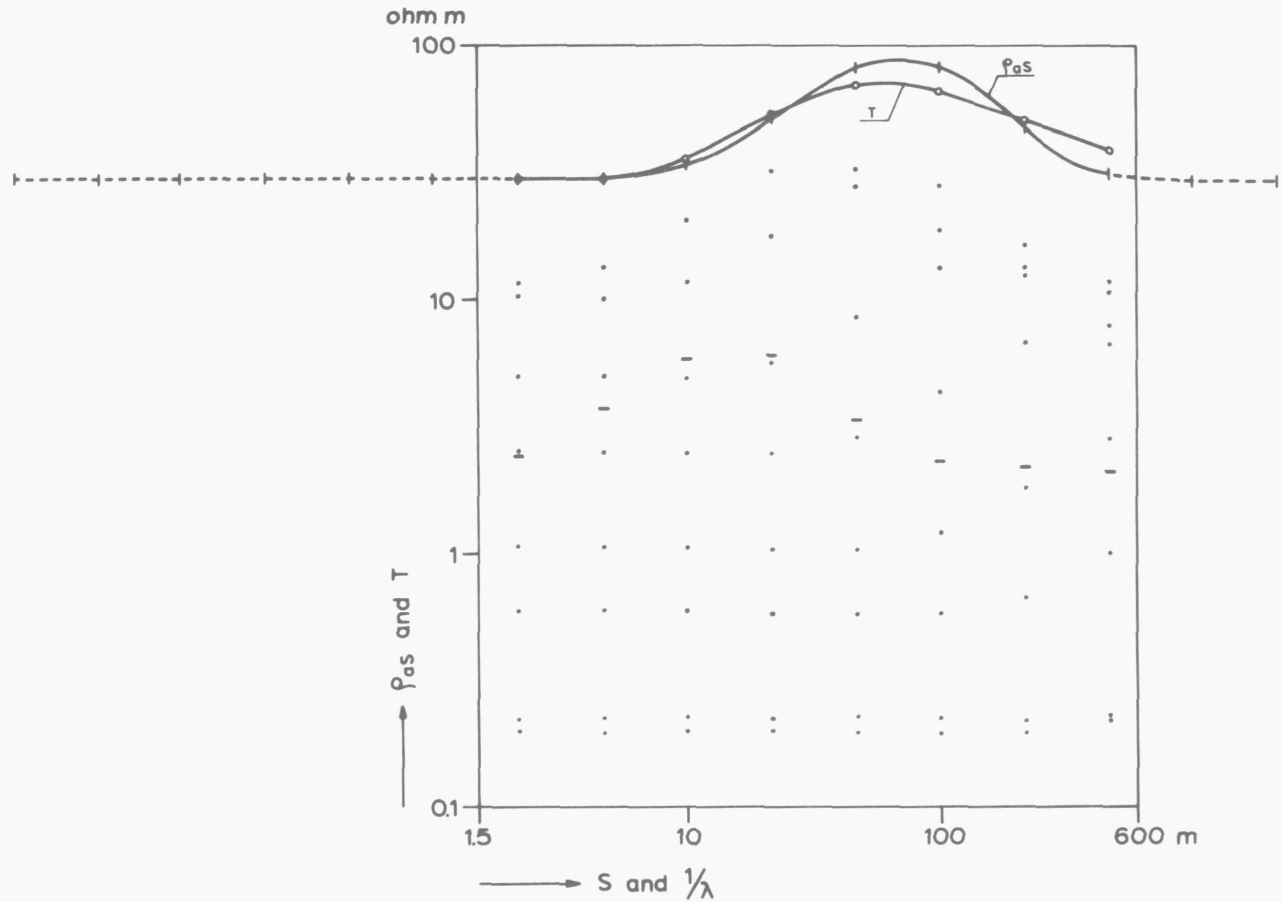

fig. 7.3.1 Derivation of the transform curve from the sample values of a three layer curve, with $\rho_1 = \rho_3$

7.3 On the applicability of the method

The question of applicability of the method will be treated in this section on the basis of a few examples worked out here, that will demonstrate the working of the method and the difficulties that may arise therefrom.

Fig. 7.3.1 to 7.3.4 show the application of the method in four diversified cases of layer distribution. The dashed points on the resistivity curve are the sample values, the circles are the transform values determined from them, by the filter method discussed in section 7.2.

First example

Fig. 7.3.1 shows the application of the method to a simple three layer case with $\rho_1 = \rho_3$. This curve could have been matched with the standard three layer curve out of the C.G.G. collection for example. Thus it is quite unlikely that the direct method would at all be applied for this case. However, no difficulty arises in determining the transform. As the curve approaches asymptotically to ρ_1 and the resistivity of the substratum to the left and right respectively, there is no ambiguity in the manner the curve has to be extrapolated on either side. So in problems irrespective of the number of layers involved, the method depends to some extent on the asymptotic behavior of the last portion of the curve.

Second example

Fig. 7.3.2 shows a curve which was still descending rapidly when the survey was abandoned with the result that the asymptotic part was not reached. This gives some uncertainty about extrapolation to the right. However, in this particular case, errors due to extrapolation would be considerably less because the magnitude of the extrapolated sample values is very low such that their effect on the output would be negligible anyway.

Sometimes working experience of the area and geological evidence furnish sufficient information about the range of resistivity values to

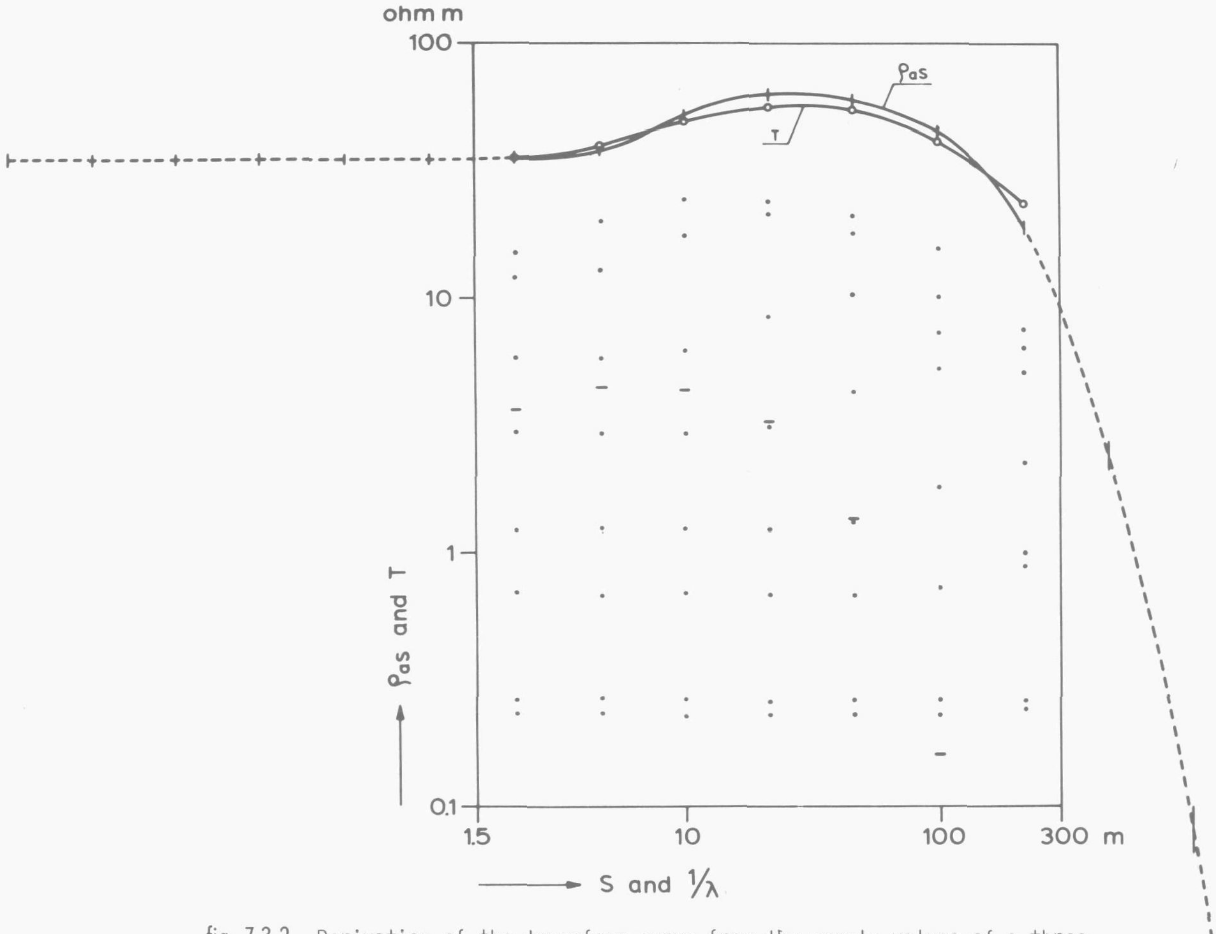

fig. 7.3.2 Derivation of the transform curve from the sample values of a three layer field curve obtained in the Western part of the Netherlands

be expected from the substratum. The same is true for this problem. The resistivity curve shown was obtained by the Geoelectrical Workgroup of the TNO, the Netherlands, during a project undertaken by them on behalf of Amsterdam Drinking Water Company, to delineate the fresh-saltwater boundary. The status of groundwater resources is quite delicate in the Netherlands (7a) because of the low elevation of the country and the continued upsurge of salt water caused by withdrawal of fresh water for drinking purpose and other hydrogeological aspects. For this reason it was desired to find the level of contamination of the fresh-water reservoirs. The curve refers in all probability to a three layer problem with a surficial clay layer. The knowledge of the resistivity of the formation carrying saline water gives sufficient ground for extrapolation, which is also the reason why unnecessary large lengths of surveys are avoided. In neighbouring dune areas a sandy surface layer of high resistivity may change the pattern of this curve to a descending step type pattern.

Third example

Fig. 7.3.3 refers to a three layer case with $\rho_1 = 1000$ ohm m, $\rho_2 = 50$ ohm m and $\rho_3 = 100$ ohm m and $d_1 = 10$ m and $d_2 = 30$ m.This curve shows a relatively large length of survey with the result that curve approaches to a value of 100 ohm m. Thus there is no difficulty in extrapolation, such that the transform could be obtained quite correctly.

Fourth example

This is a special problem undertaken to investigate into one of the limitations of direct methods in particular, and to resistivity interpretational methods in general. The statement of the problem is that, whether the use of the resistivity transform as the intermediatary step in interpretation increases or decreases the possibility of indentifying different layer stratification not quite apparent in the field curve, due to let us say limited length of survey. Fig. 7.3.4 shows such a dual curve taken from the private collection of the Rijkswaterstaat, The Hague. The parameters are defined as

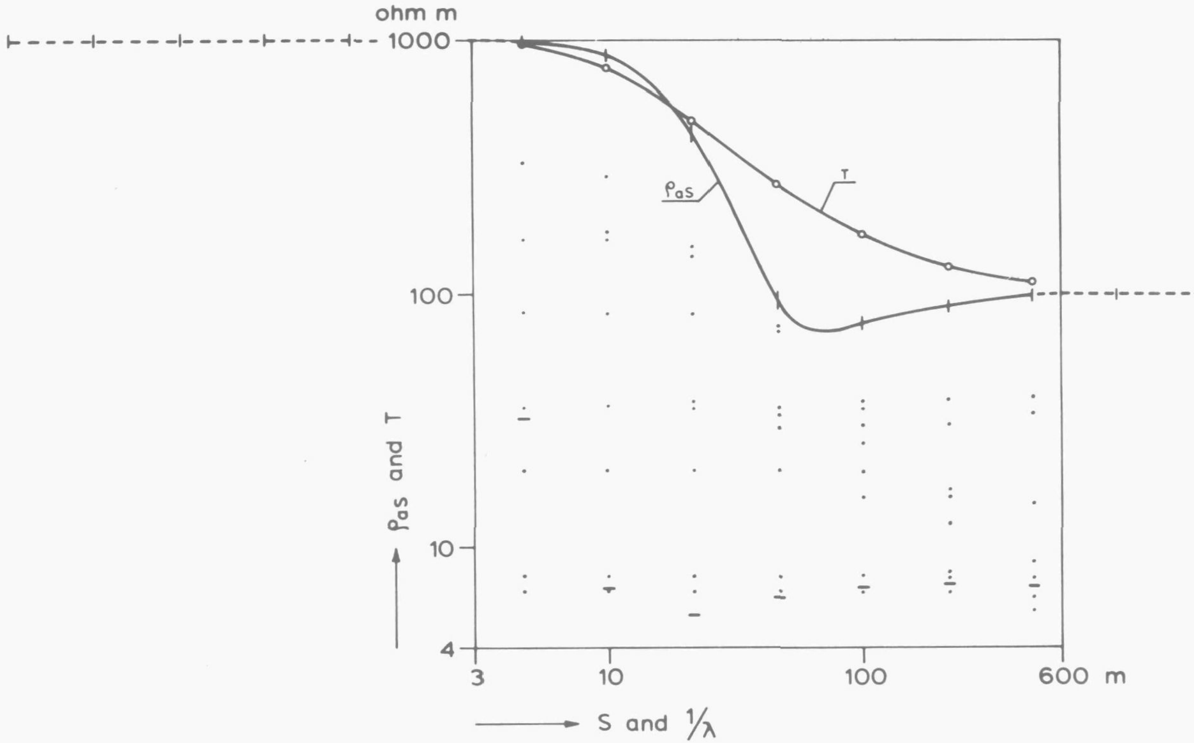

fig. 7.3.3 Derivation of the transform curve from the sample values of a three layer curve with $\rho_1 = 1000$ ohm m, $\rho_2 = 50$ ohm m and $\rho_3 = 100$ ohm m and $d_1 = 10$ m, $d_2 = 30$ m

curve I $\rho_1:\rho_2:\rho_3::1:0.0833:2$; $d_2/d_1 = 3$

curve II $\rho_1:\rho_2:\rho_3::1:0.0833:1$; $d_2/d_1 = 2.75$

The curves are in principle widely different concerning the asymptotic value of the last part of the curve. But for reason of short length of the survey only a small difference exists that gives no hint towards the actual value of the substratum. By the filter method thus there is considerable uncertainty in the manner of extrapolation. To be on the safe side we have extrapolated to only one sample point. This means the transform curve determined will have one sample length less than the resistivity curve.

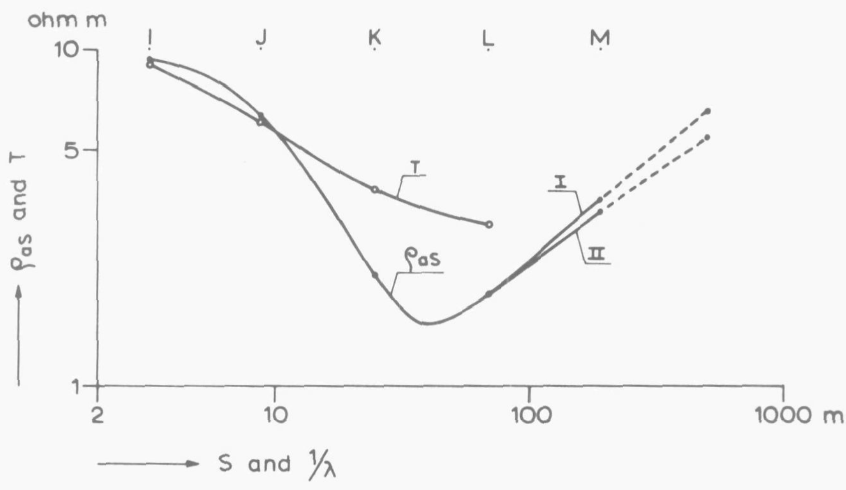

fig. 7.3.4 Ambiguity arising due to derivation of the transform curve for shorter lengths than the corresponding resistivity curves

The transform curves for both the cases shown in fig. 7.3.4 are almost identical. There were minute differences of the value at the extreme sample point of the transform curve which on the logarithmic scale do not show up. So we may conclude that although we are perhaps able to cut down errors due to extrapolation by extrapolating up to only one point, this process reduces the differences that were actually hinted by the resistivity curve.

On the other hand determining the transform up to the total range of the curve would preserve the difference but this requires very careful extrapolation up to two sample points to the right. This can be achieved in two manners

1) by taking large length of surveys

or

2) using two layer standard curves which are asymptotic to the last part of the curve. This can act as a guide to correct extrapolation.

In this manner we are able to remove some of the difficulties encountered with the problem of extrapolation in the filter method giving rise to ambiguity in the transform curve.

Concluding remarks: It is concluded that the method is applicable to any problem irrespective of the subsurface distribution. Only special care has to be taken in extrapolation when the survey is abandoned before the asymptotic value is reached, especially when the trend of the curve is towards high resistivity.

7.4 Speed of application

The speed of working with the short filter was examined both for numerical and graphical application. In the presence of a hand calculator, for a reasonable length of survey, the transform could be obtained in less than 10 minutes. Graphically it took about a quarter of an hour. We can set aside another quarter of an hour to obtain the layer distribution by KOEFOED's method. This means that the physical interpretation should not take more than half an hour.

This can be termed as considerably fast. At the moment there is no limit set to the question of what should be the proper investment time towards interpretation in comparison to the time required for obtaining the data. This point has been hinted to by KELLER (26) although he gives no figure for it. It is agreed that it is very much a personal factor and it depends on individual organizations and companies of what they consider as a reasonable investment of time. In that context perhaps the long filter coefficients may be used.

7.5 Utilization of all field information

There is no definite rule as to the ratio at which the electrodes be expanded. In the field every organization have their own method of working which also varies according to the problem, time and costs involved in that project. It is, however, observed that a ratio of about 1.4 to 1.8 is commonly used.

To compare the above quoted figures for the ratio of expansion of the electrode with the sampling interval used for interpretation, we shall convert them to the x scale by recalling that

$$ds = e^{dx} \text{ or } dx = \ln ds$$

such that

$$dx_1 = \ln 1.4 = 0.34$$

$$\text{and } dx_2 = \ln 1.8 = 0.59$$

This suggests that the interval at which the field resistivity data appears is closer than the sample resistivity values utilized for interpretation which is $\Delta x = \ln(10)/3 \simeq 0.77$. This means that in some type of field survey there are chances of loss of even half of the field information.

Although sampling does ensure us that in principle the whole data is represented adequately through the sample points, it may not be acceptable to various organizations to spend money and effort of collecting data and yet use only a part of them. There are two alternative suggestions to be made to this demand:

a) either to alter the field procedure used to suit the interpretation method

or

b) to use an alternative method of application in interpretation with the same field procedure.

The alternative suggestion is illustrated in fig. 7.5.1 and the steps followed are:

1) Sample the resistivity curve using a sampling interval of Δx = ln(10)/3. Let us say they are represented by the points.

2) Apply the filter method to these points to obtain the transform values corresponding to the sample points.

3) In between the first set of sample points mark a second set of sample points defined by the circles which themselves are at a spacing of Δx = ln(10)/3.

4) Again apply the filter method to this second series of sample points and obtain the transform values corresponding to this series.

5) Thus the transform values are defined at an interval of Δx= ln(10)/6, which means at an interval of 0.38.

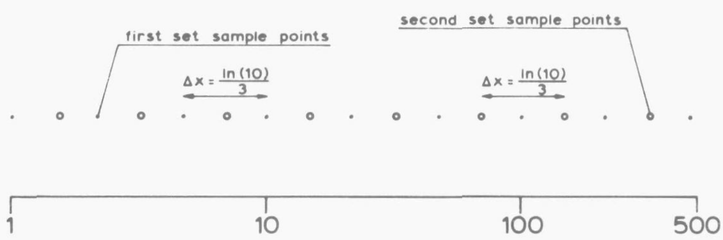

fig. 7.5.1 Alternative procedure for utilization of all field information. The filter method is first applied to the points and then repeated to the second set of sample points denoted by the circles with the results that the transform is yielded at a spacing of ln(10)/6

By this process the resistivity data will be utilized at an interval of 0.38 which compares very favourably with the procedures followed by different companies [dx = 0.34 to 0.59] such that there is no appreciable loss of field information. We stress that this additional procedure is recommended only to persons who feel like using all the data they have. This procedure is given with an eye to the fact that big organizations like Rijkswaterstaat (The Hague), the Niedersächsisches Landesamt für Bodenforschung at Hannover, etc., have to their disposal small office computers[1] such that they could afford to determine the transform at a spacing of $\Delta x = \ln(10)/6$. This by graphical application would mean a time of about 30 to 40 minutes. These suggestions are given and it is up to the interpreter to decide what are his needs. In principle the procedure suggested in section 7.2 is fast in application and considered sufficient in the light of the errors expected in other stages of the resistivity method.

7.6 Accuracy of the method

We shall try to test the accuracy by determining the transform of resistivity functions by the filter method and then comparing it with their theoretical transform evaluated mathematically. A set of partial resistivity functions are so selected that they have strong resemblance with actual resistivity curves. It is conceded therefore that the accuracy so determined may be slightly more favourable than for the resistivity curves. However, it is fruitless to test the accuracy of the method by comparing the transform thus obtained with the transform obtained by other methods, because this process points to combined inaccuracy of the two methods which is difficult to isolate. Errors by this method are twofold in nature (1) firstly because sampled data is used (2) and secondly because of the finite length chosen for the filter.

This is manifested into a combined error represented as

$$\text{percentage error} = \frac{T_{fil} - T_t}{T_t} \times 100 \qquad (7.6.0)$$

where

T_{fil} = transform of the resistivity function calculated by filter method

T_t = theoretical transform

----

[1] These small office computers are being employed more and more by developing as well as established prospecting organizations.

Fig. 7.6.1 to 7.6.4 show the results of the tests.

The points refer to the sample value of the resistivity function and the circles to their corresponding transform calculated by the filter method. The alternative procedure (section 7.5) was used to obtain the transform at a spacing of $\Delta x = \ln(10)/6$. The full drawn curve is a standard curve taken from the C.G.G. or MOONEY and ORELLENA collection to show the resemblance of the functions with resistivity curves. The lower part of the fig. gives an estimate of the percentage error through eq. 7.6.0. The following cases were tested

a) descending type (Fig. 7.6.1)

$$\left.\begin{aligned} \Delta\rho_{aS}(x) &= 1 + 8\,(1 + e^{x} + e^{2x}/2\,)/e^{e^{x}} \\ \Delta T(y) &= 1 + \frac{12}{(1 + e^{2y})^{1/2}} - \frac{4}{(1 + e^{2y})^{3/2}} \end{aligned}\right\} \qquad (7.6.1)$$

Both the long (Table 6.2.1) and the short (Table 6.4.1) filter were used.

b) ascending type (Fig. 7.6.2)

$$\left.\begin{aligned} \Delta\rho_{aS}(x) &= 10 - \frac{9(1+e^{x})}{e^{e^{x}}} \\ \Delta T(y)' &= 10 - \frac{9}{(1+e^{2y})^{1/2}} \end{aligned}\right\} \qquad (7.6.2)$$

only the short filter was used.

c) bowl shaped maximum type (Fig. 7.6.3)

$$\left.\begin{aligned} \Delta\rho_{aS}(x) &= \frac{1+e^{x}}{e^{e^{x}}} + \frac{(2.7\ e^{x})^{3}}{|1+(2.7\ e^{x})^{2}|^{3/2}} - 0.7 \\ \Delta T(y) &= \frac{1}{(1+e^{2y})^{1/2}} + e^{-\left(\frac{1}{2.7\ e^{y}}\right)} - 0.7 \end{aligned}\right\} \qquad (7.6.3)$$

only the short filter was used.

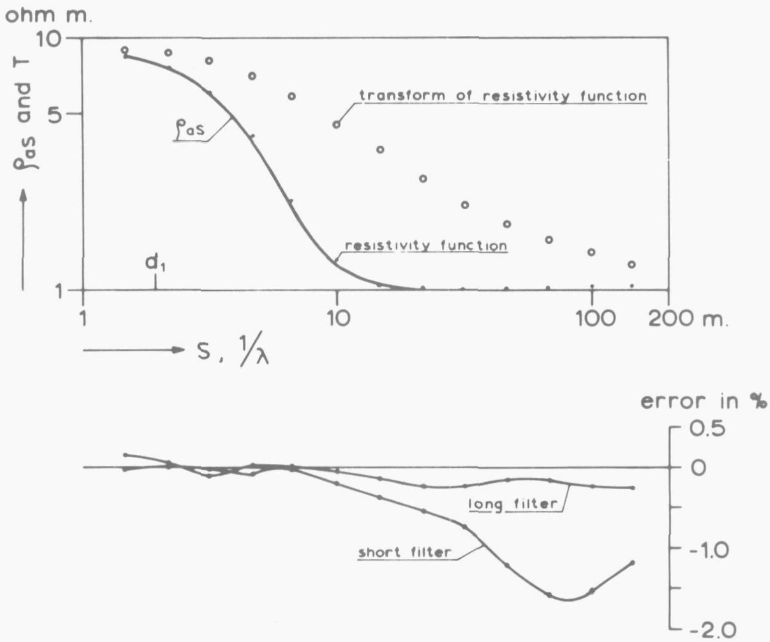

fig. 7.6.1 Upper part of the figure shows the transform derived from the sample values of a partial resistivity function by the filter method. A descending type two layer curve (C.G.G. collection) shows the similarity of the function used, with resistivity curves.
Lower part shows the percentage error between the derived and the theoretical transform using successively the long and short filter.

d) bowl shaped minimum type (Fig. 7.6.4)

$$\Delta\rho_{aS}(x) = \frac{e^{3x}}{(1+e^{2x})^{3/2}} + e^{-30.e^{x}} \{ 1 + 30.e^{x} + \frac{1}{2}(30.e^{x})^2 + \frac{1}{6}(30.e^{x})^3 + \frac{1}{24}(30.e^{x})^4 \} + 0.5$$

$$\Delta T(y) = e^{-e^{-y}} + \{ 8 + 28(30.e^{y})^2 + 35(30.e^{y})^4 + 20(30.e^{y})^6 \}/8.\{ 1 + (30.e^{y})^2 \}^{7/2} + 0.5$$

only the short filter is used. (7.6.4)

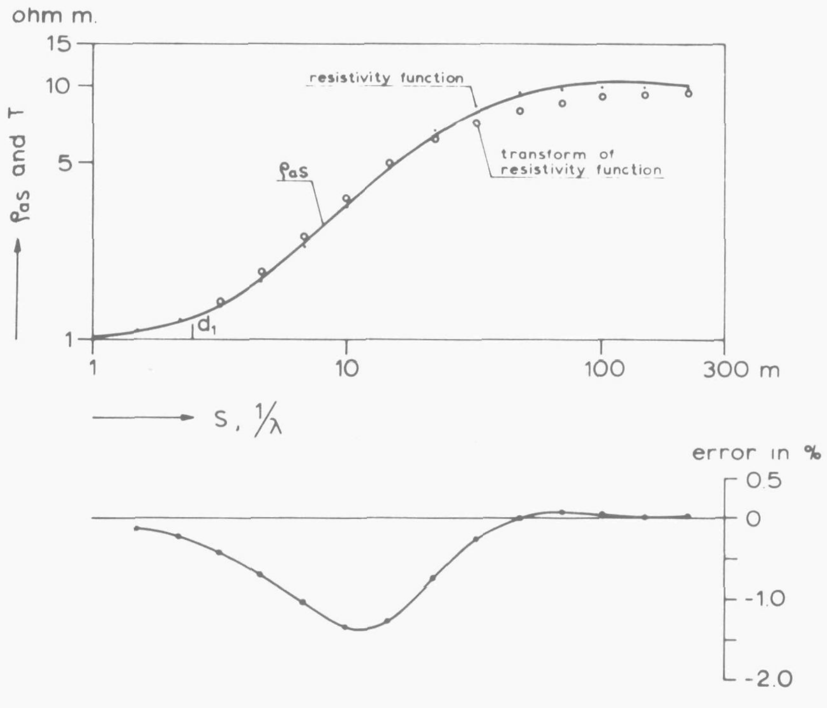

fig. 7.6.2 Upper part of the figure shows the transform derived from the sample values of a partial resistivity function (approximating to an ascending three layer curve taken from the MOONEY-ORELLANA collection) using the short filter. Lower part shows the percentage error between the derived and theoretical transform.

Discussion

The bottom part of Fig. 7.6.1 to 7.6.4 gives an estimate of the percentage error by using the filter method at each sample value where the transform was determined (upper diagrams).

The first remark at a glance of the error curve is that the error is less for bowlshaped curves than for ascending and descending type curves. It appear that the maximum discrepancy occurs during the part of ascent or descent.

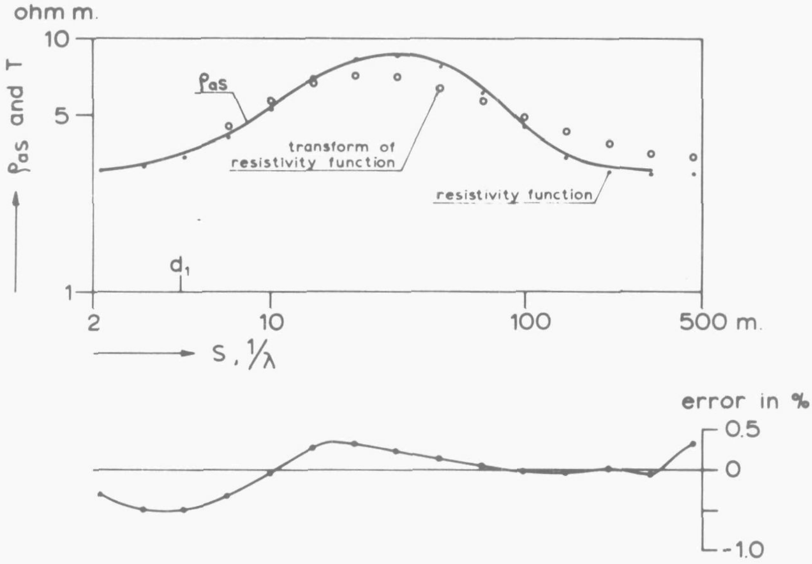

fig. 7.6.3 Upper part of the figure shows the transform derived from the sample values of a partial resistivity function that has the similarity with a three layer bowl shaped maximum type resistivity curve (C.G.G. collection). The short filter was used.
Lower part shows the percentage error between the derived and the theoretical transform.

Fig. 7.6.1 bottom part, shows the accuracy obtained in using both the long and short filter. It is apparent that the long filter is much more accurate but this may not appear necessary when we stop to think for a moment that our data itself does not possess that reliability. With the short filter, on the other hand the maximum percentages error for the cases discussed does not exceed 1.7. Accepting even a 2% error resulting from the transformation procedure of field resistivity curves, the accuracy of this procedure is still higher than the certainty of field data itself. This will be clear from the following consideration.

It has been pointed out by KELLER and FRISHKNECHT that with most inexpensive experiment used to obtain the resistivity data, an accuracy

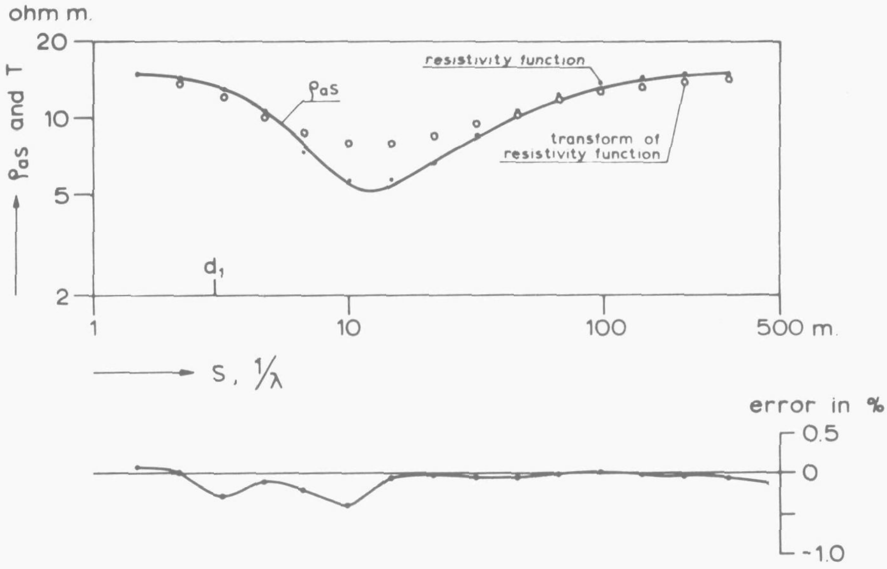

fig. 7.6.4 Upper part of the figure shows the transform derived from the sample values of a partial resistivity function that has the similarity with a three layer bowl-shaped minimum type curve (C.G.G. collection). The short filter was used. Lower part shows the percentage error between the derived and the theoretical transform.

of ± 5% can be expected to account for observational and instrumental errors. This can be cut down to ± 3% with refined field procedures and sensitive instruments capable to read up to one hundredth of a millivolt and even up to microvolt in some instances. Thus our value of accuracy is much within safe limits while using the short filter which further promises speed in application.

CHAPTER 8

APPLICATION OF THE LINEAR FILTER THEORY TO THE WENNER SYSTEM

8.1 Linearity of the WENNER system

It might be recalled that it was possible to apply the filter theory to the SCHLUMBERGER system on the ground that the process of conversion of the apparent resistivity to the resistivity transform was a linear one. This linearity was demonstrated on the basis of a convolution integral (eq 4.3.2) which was obtained after the introduction of the new variables x and y (eq. 4.3.1) in the explicit expression of the transform (eq. 2.5.1).

However, for the WENNER arrangement such a procedure is not possible. This is realized from the difficulty in obtaining an explicit expression for the resistivity transform of identical form as for the SCHLUMBERGER arrangement (eq. 2.5.1), by the application of HANKEL's inversion to

$$\rho_{aW} = a\int_0^\infty T(\lambda).\left[J_0(\lambda a)-J_0(\lambda.2a)\right].d\lambda \qquad (2.4.4)$$

PAUL, 1968 (53), has worked out an expression for $T(\lambda)$ by applying HANKEL's inversion, but unfortunately this is in the form of an infinite series and not suitable from the point of view of converting it into a convolution integral.

This, however, does not restrict the fact that the transformation in the WENNER system is also linear in nature. And as we have marked in chapter 4, there are several possibilities of demonstrating the linearity of a system viz. the superposition theorem. If we have two resistivity curves defined by

$$\left.\begin{aligned} &\rho_{aW_1} = a\int_0^\infty T_1(\lambda).\left[J_0(\lambda.a)-J_0(\lambda.2a)\right].d\lambda \\ \text{and}\quad & \\ &\rho_{aW_2} = a\int_0^\infty T_2(\lambda).\left[J_0(\lambda.a)-J_0(\lambda.2a)\right].d\lambda \end{aligned}\right\} \qquad (8.1.1)$$

we readily obtain

$$(\rho_{aW_1}+\rho_{aW_2}) = a\int_0^{\infty}\{T_1(\lambda)+T_2(\lambda)\}\left[J_0(\lambda.a)-J_0(\lambda.2a)\right].d\lambda \qquad (8.1.2)$$

Eq. 8.1.1 and 8.1.2 show that the linearity of the WENNER system goes without doubt. In fact the idea of KOEFOED (32) of approximating the WENNER apparent resistivity by partial resistivity functions and then obtaining the total kernel function as a sum of the corresponding kernel functions would not have been possible if the condition of linearity was not satisfied.

8.2 Principle of the WENNER method

The basic principle of obtaining the resistivity transform from the WENNER apparent resistivity remains exactly the same as stated in section 4.5 of chapter 4. That is the WENNER resistivity curve is sampled at a rate[1)] of Δx = ln(10)/3, and replaced by sinc functions. The digital approach, like the SCHLUMBERGER method, would be convolution of the resistivity sample values with the WENNER digital filter operators. These operators are the sampled values of the sinc response of the WENNER filter stated in the following equation

$$B_W(f) = \text{spectrum of sinc function} \times H_W(f) \qquad (8.2.1)$$

where

$B_W(f)$ = FOURIER spectrum of WENNER sinc response

$H_W(f)$ = Frequency characteristic of WENNER resistivity filter.

----

1) The expression for the transform for the WENNER and SCHLUMBERGER curves are the same,thus the FOURIER spectrum shown in Fig. 5.5.1A to Fig. 5.5.3A is also valid for the WENNER case. For the FOURIER spectrum of the WENNER resistivity we have to divide it by the Frequency characteristic of the WENNER filter. This gives us sufficient ground to use the same cut-off frequency and hence the same sampling interval.

It goes without saying that eq. (8.2.1) will be valid only for linear systems. The difference between the sinc response of the WENNER and the SCHLUMBERGER case is brought about by the fact that the two curves and consequently their filter characteristics are different.

8.3 Frequency characteristic of the WENNER filter

A knowledge of $H_W(f)$ is all that is needed to be determined in the process of obtaining the sinc response. The frequency characteristic, $H_W(f)$ is defined as

$$H_W(f) = \frac{F(f)}{G_W(f)} \tag{8.3.1}$$

where

$$F(f) \leftrightarrow T(y) \text{ and } G_W(f) \leftrightarrow \rho_{aW}(x)$$

It has been shown by DEPPERMAN, 1961 (9) and others that the WENNER curve can be approximately obtained from the SCHLUMBERGER curve by shifting the latter to the left by a factor 0.7. For the purpose of evaluating eq. (8.3.1) we shall try to obtain the expression for the partial WENNER resistivity function from the SCHLUMBERGER partial resistivity functions used in section 4.4, by the application of the following relationship (32)

$$\Delta\rho_{aW} = 2a\int_a^{2a} \frac{\Delta\rho_{aS}}{s} .ds \tag{8.3.2}$$

we thus obtain, for the two cases stated in section 4.4

$$\left.\begin{aligned} \Delta\rho_{aW}(x) &= \frac{2}{3}\left[\frac{e^x}{(1+e^{2x})^{3/2}} - \frac{e^x}{(1+4.e^{2x})^{3/2}}\right] \\ \Delta T(y) &= \frac{1}{3.e^y.e^{e^{-y}}} \end{aligned}\right\} \tag{8.3.3}$$

and

$$\left.\begin{aligned} \Delta\rho_{aW}(x) &= \frac{2}{5}\left[\frac{e^x}{(1+e^{2x})^{5/2}} - \frac{e^x}{(1+4.e^{2x})^{5/2}}\right] \\ \Delta T(y) &= \frac{(e^{-y} + e^{-2y})}{15.e^{e^{-y}}} \end{aligned}\right\} \qquad (8.3.4)$$

The expressions given in 8.3.3 and 8.3.4 were separately used to determine $H_W(f)$ which is shown in fig. 8.3.1. The nature at higher frequencies is particularly different from that obtained for the SCHLUMBERGER filter (fig. 4.4.1). The FOURIER spectrum of sinc response of the filter, however, utilizes the filter characteristic up to the cut-off frequency because of the nature of the spectrum of the sinc function (eq. 8.2.1 and fig. 4.1.1), or in other words

$$B_W(f) = 0 \text{ for } f > f_c$$

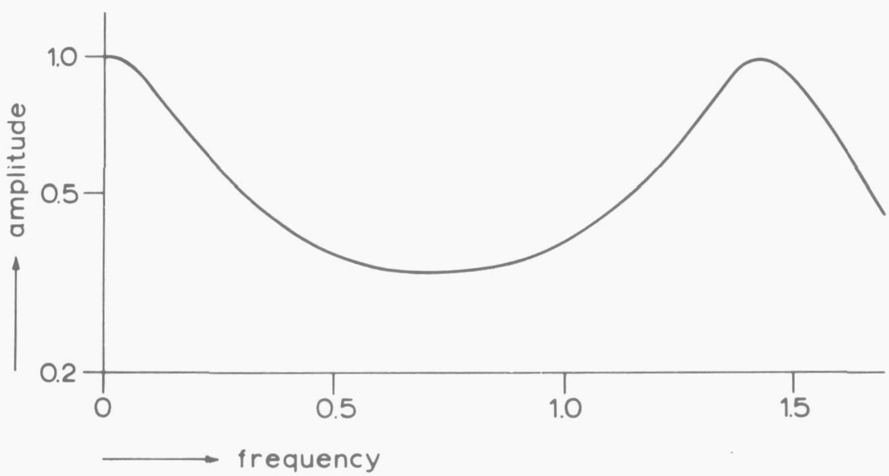

fig. 8.3.1 Amplitude FOURIER spectrum of the filter characteristics for the WENNER system

8.4 Sinc response of the WENNER filter

The sinc response obtained after the application of the Inverse FOURIER transform of $B_W(f)$ is shown in fig. 8.4.1. The striking feature

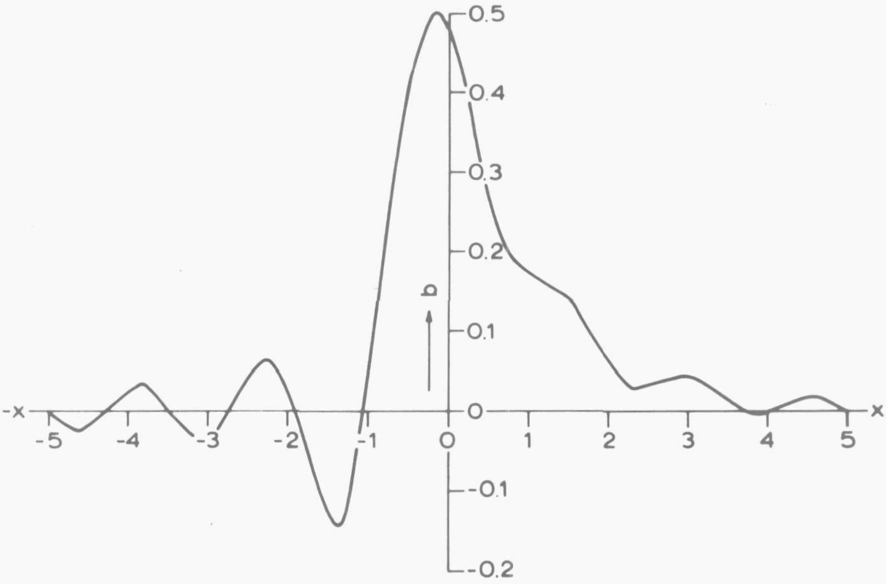

fig. 8.4.1 Sinc response of the WENNER filter

in contrast to the SCHLUMBERGER one (fig. 4.4.1) is that the sample points (at a spacing of $\Delta x = \ln(10)/3 \simeq 0.77$) are not favourably placed.

By this we mean that particularly to the left side, that is for responses for $x < 0$, they occupy the crest and trough of the response which should make the length of the filter quite long. This has partial disadvantages from the digital filtering point of view. To avoid this situation we have applied a shift of $\ln(1.616) = 0.48$ to the left between $x = 0$ and the first filter coefficient which we now give the nomenclature a_0. All other filter coefficients are marked with respect to a_0 at the same constant spacing of $\ln(10)/3$.

8.5 The WENNER digital filter coefficients

The coefficients obtained by the above process are shown in table 8.5.1. The difference with the SCHLUMBERGER coefficients is that the nomenclature is slightly different i.e. the suffix 0 in the filter

Table 8.5.1 The WENNER digital filter coefficients

a_{-2}	a_{-1}	a_0	a_1	a_2	a_3	a_4	a_5	a_6
0.0212	-0.1199	0.4226	0.3553	0.1664	0.0873	0.0345	0.0208	0.0118

coefficient does not refer to the abscissa value of x = 0 but now refers to a point shifted ln(1.616) to the left. The implication is that the output will also be shifted with respect to the input by the same factor.

8.6 Operation with the filter coefficients

a) *Numerical calculation by convolution*

The process of operation numerically can be kept the same as stated through eqs (7.2.1) and (7.2.2) for the SCHLUMBERGER case, if we keep in mind that the output let us say T_3 corresponding to the resistivity sample value R_3 refers to a point shifted to the left of R_3 by ln(1.616). This is true for each transform value. This thus implies that the transform curve obtained will be defined to a shorter length to the right by a factor ln(1.616) and extended to the left by the same factor.

b) *Graphical process*

The delay in the output can be easily taken into consideration in the graphical method. This can be accomplished as follows:

1) Plot the filter coefficient shown in table 8.5.1, such that a_0 is at the abscissa value of $\Delta x = -\ln(1.616) = -0.48$. The cross is placed at x = 0 and ordinate value of 1. All other filter coefficients are plotted with their appropriate value with equal spacing of ln(10)/3. with respect to a_0. This is shown in fig. 8.6.1.

2) the method of application is now exactly the same as stated in section 7.2(b) of chapter 7. The sampled resistivity values are brought in turn to the cross starting from the extreme left i.e. the sixth

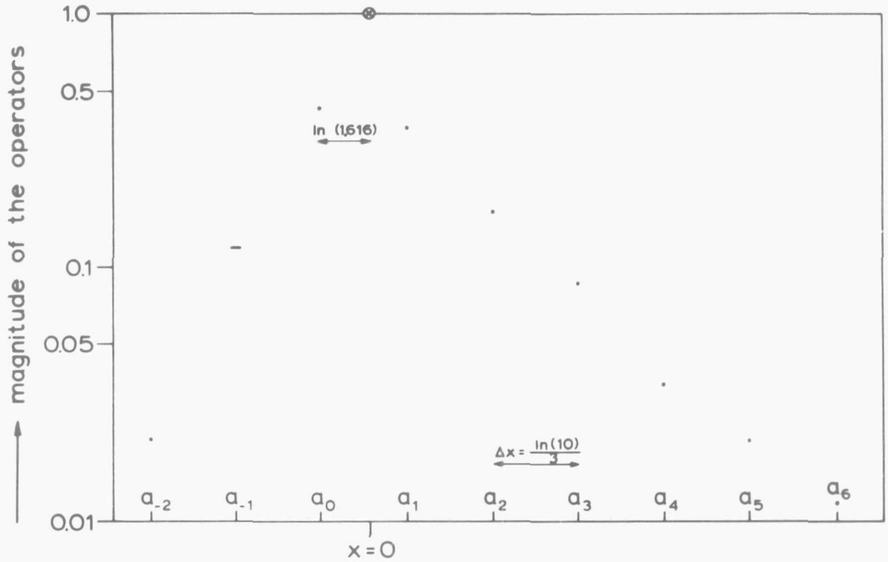

fig. 8.6.1 The WENNER digital filter coefficients

extrapolated point to the second extrapolated point to the right of the curve. The filter points are successively traced on to the resistivity chart.

3) The difference with the SCHLUMBERGER situation is that as a consequence of the above procedure, the transform value obtained by addition of points and substraction of the dashes, is automatically shifted with respect to the sample resistivity values to which they refer by the same constant shift, ln(1.616).

8.7 Examples

The working of the graphical process is demonstrated through two examples which are so chosen that they give also an indication about the limitations of the WENNER method that might arise.

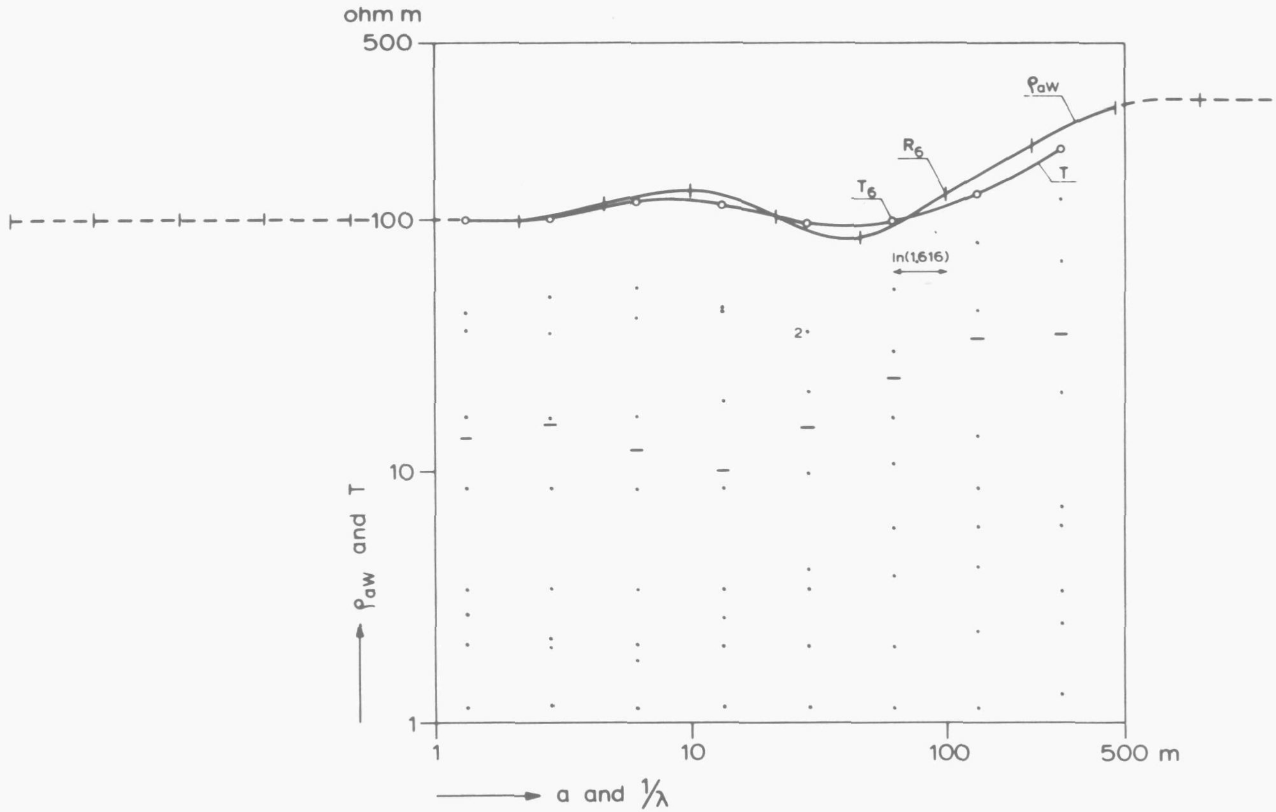

fig. 8.7.1 Derivation of the transform from the sample values of a four layer WENNER apparent resistivity curve with ρ_1 = 100 ohm m, ρ_2 = 300 ohm m, ρ_3 = 33.3 ohm m, ρ_4 = 300 ohm m and d_1 = 5 m, d_2 = 5m and d_3 = 20 m. The derived transform T_6 is shifted to the left by a factor ln(1.616) w.r.t. the sample resistivity value R_6.

a) First example

Fig. 8.7.1 shows the derivation of the transform from the four layer WENNER apparent resistivity curve with ρ_1 = 100 ohm m, ρ_2 = 300 ohm m, ρ_3 = 33.3 ohm m and ρ_4 = 300 ohm m and d_1 = 5 m, d_2 = 5 m and d_3 = 20 m.The transform curve is shown drawn through the circles and is derived for a shorter length to the right side.

The rising nature of the curve presents the same difficulties as with the SCHLUMBERGER method, as regards extrapolation. Moreover, as the transform curve is known for a shorter length it might be advisable to take larger spreads for the WENNER method or to carefully extrapolate further on to the right so as to compensate partly for the shortening effect of the transform.

b) Second example

Fig. 8.7.2 shows the application to a four layer case taken from the album of MOONEY and ORELLENA (44) with, let us assume, ρ_1 = 1000 ohm m, ρ_2 = 400 ohm m, ρ_3 = 200 ohm m and ρ_4 = 100 ohm m, d_1 = 10 m, d_2 = 30 m, d_3 = 10 m. For resistivity curves such as these, there arises no difficulty in extrapolation, such that the transform curve could be known by virtue of extrapolation of the resistivity curve to a longer length than the actual survey. This, however, should not be confused with the fact that even in this case the transform curve will be shorter than the resistivity curve chosen to be interpreted by a factor ln(1.616).

8.8 Concluding remarks

The above two examples give some idea of the applicability of the WENNER method. As regards other aspects of working procedure including speed of application they remain essentially the same as stated for the SCHLUMBERGER arrangement. Regarding the question of utilization of all field information, the author has the impression that for the WENNER arrangement the spacing between consecutive electrodes (a) is doubled as the electrodes are expanded. This means that the interval

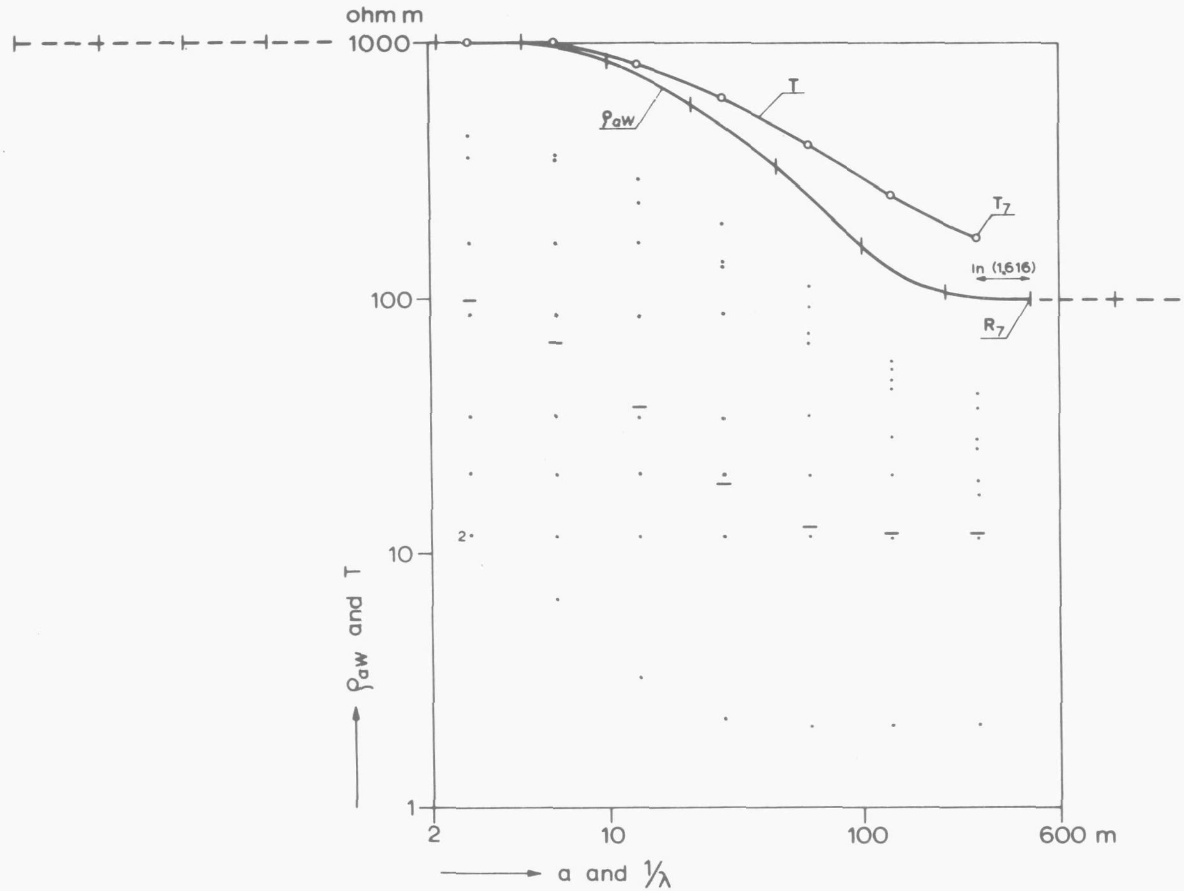

fig. 8.7.2 Derivation of the transform from the sample values of a four layer WENNER apparent resistivity curve with ρ_1 = 1000 ohm m, ρ_2 = 400 ohm m, ρ_3 = 200 ohm m, ρ_4 = 100 ohm m and with d_1 = 10 m, d_2 = 30 m, d_3 = 10 m. T_7 is shifted to the left by a factor ln(1.616) w.r.t. the sample resistivity value R_7.

at which the data appears on the x-scale is 0.69 which is just a bit closer than the interval 0.77 used for interpretation. Thus the conclusion is that little field information is lost in using this sampling procedure of interpretation. However, if the ratio used to expand the electrodes is by some chance less, the alternative procedure suggested for the SCHLUMBERGER case can be applied for using all information. It is to be expected that the filter method for the WENNER would also yield an accuracy in the neighbourhood of that obtained for the SCHLUMBERGER case.

CHAPTER 9

THE INVERSE PROBLEM

9.1 Introduction

This part of the thesis does not concern the direct method of interpretation. On the contrary, it involves an indirect problem viz, the computation of apparent resistivity curves from sampled values of the transform curves. The main idea is that transform curves are simpler to compute than resistivity curves such that the filter theory can be applied to derive the latter from the former.

9.2 Frequency characteristic of the Inverse filter

The process of transformation of $\rho_{aS}(x)$ to $T(y)$ was defined through the convolution integral given by eq. 4.3.2 whose frequency domain representation is given in the form

$$F(f) = G(f) \;.\; H(f) \tag{4.2.3}$$

where as usual we have

$$F(f) \leftrightarrow T(y); \; G(f) \leftrightarrow \rho_{aS}(x)$$

and H(f) as the resistivity frequency characteristic of the SCHLUMBERGER filter.

Rewriting we have

$$G(f) = F(f) \;.\; \frac{1}{H(f)}$$

or

$$G(f) = F(f).Q(f)$$

$$Q(f) = \frac{G(f)}{F(f)} \tag{9.2.1}$$

Q(f) is the frequency characteristic of the Inverse SCHLUMBERGER filter and can be determined through the sets of equation given in section 4.4 for $\rho_{aS}(x)$ and T(y).

9.3 The Inverse SCHLUMBERGER Digital filter coefficients

The sinc response of the inverse filter is given in the frequency domain as

$$I(f) = \text{FOURIER spectrum of sinc function} \times Q(f) \qquad (9.3.1)$$

The sinc response can thus be derived from I(f) by applying the inverse FOURIER transform. The nature of the response was such that it was necessary to shift the coefficient a_0 to the left of $x = 0$ by a small factor of ln(1.05) i.e. by 5%. The other filter coefficients are at equal spacing of $\ln(10)/3 \simeq 0.77$. The coefficients of the inverse filter are shown in table 9.3.1.

Table 9.3.1 The Inverse SCHLUMBERGER filter coefficients

a_{-3}	a_{-2}	a_{-1}	a_0	a_1	a_2	a_3	a_4	a_5
0.0225	-0.0499	0.1064	0.1854	1.9720	-1.5716	0.4018	-0.0814	0.0148

9.4 Operation with the filter coefficients

The filter coefficients shown in table 9.3.1 operate with the sampled values of the transform, sampled at an interval of 0.77 to yield the resistivity values which, however, now refer to an abscissa point which is to the left of the transform sample point by a factor of ln(1.05). The shift of the output w.r.t the input is similar to the WENNER method but, however, the shifts have different magnitudes and also the meaning of the input and output are reversed.

The numerical process of operation is the same as mentioned in earlier chapters defined through eq. 7.2.1 and 7.2.2 but we should remember that 'R' and 'T' change positions and also the resistivity values obtained are to be shifted to the left by ln(1.05).

In the graphical process the shift is taken into account by plotting a_0 to the left of $x = 0$ by ln(1.05) and all the other coefficients with

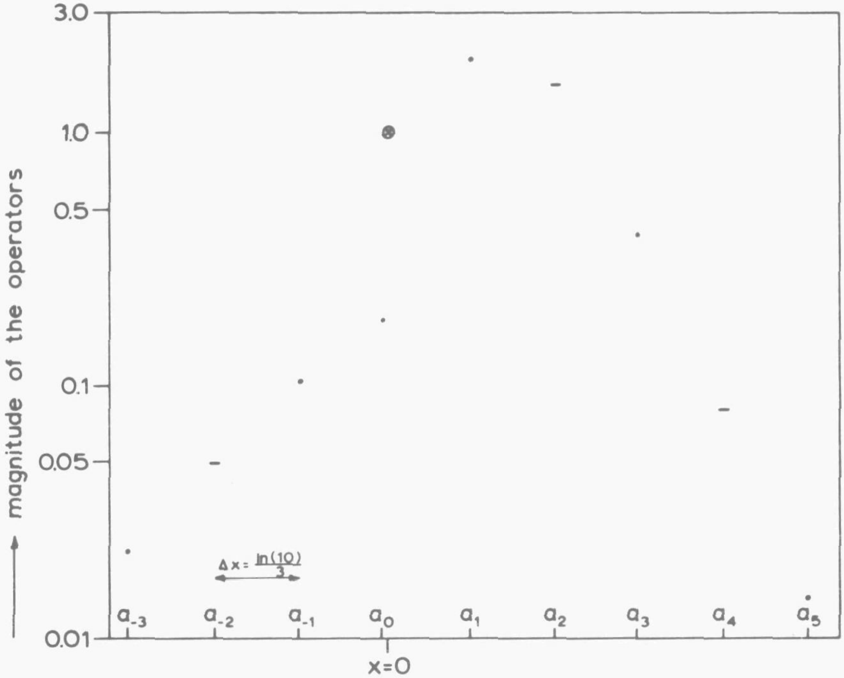

fig. 9.4.1 The SCHLUMBERGER inverse filter coefficients

respect to a_0. The cross as usual is placed at ordinate 1 and at x = 0. This is illustrated in fig. 9.4.1.

The application of the graphical process is the same as mentioned in chapter 8 except that instead of the 'resistivity' chart we refer now to the 'transform' chart. The steps are the same i.e. the transform curve[1] is sampled at an interval of ln(10)/3. Then the transform chart is superposed on the filter chart with the fifth extrapolated point[2] to

----

[1] The easiest manner to obtain the transform curve is to replace in equation 2.3.1 and 2.3.2 λ by $1/u$ and to plot T(u) against u on log-log scale. Sampled values of this curve at an interval of ln(10)/3 gives T(y) which now can be utilized for operation.

[2] Five extrapolated points are necessary to the left and three to the right to correspond to the nature of the coefficients in table 9.3.1.

the left on the cross and as usual the steps mentioned earlier in chapter 7 and 8 are followed up to the point when the third extrapolated point is on the cross. The points are added and subtracted from the dashes and the resultant value is plotted. The resistivity values so obtained are automatically shifted to the left by the factor ln(1.05). Interpolation amongst the resistivity values so obtained yields the apparent resistivity curve for the earth model for which the transform curve was calculated by the help of expressions given in section 2.3.

9.5 Discussion

While suggesting this simple procedure of computing apparent resistivity curves, the author is not completely aware of its subsequent utility in the field of resistivity interpretation but the study was guided at least by the following considerations:

1) It is often desirable to know the shape of the apparent resistivity curve that will be produced by a certain subsurface distribution in connection with the question of detectability of a layer in that subsurface.

2) It might be desirable as a check on the parameters obtained by direct methods, to reconstruct the apparent resistivity curve.

3) This computational procedure may find some applications when indirect interpretation is used. The easy manner of computation of theoretical curves may be of decided advantage of field parties who need to compute their field curves.

4) It can also be used in wide scale computation of apparent resistivity curves using computers. This procedure is to be preferred over direct numerical integration in computing resistivity curves as this process would save much computational time. (It is well known that due to rapid oscillation of BESSEL function, numerical computation of apparent resistivity curves is not only time consuming but also inaccurate) This is of particular importance to institutes and organizations who have only a limited computer time allocated to them.

Accuracy

The method was applied on the sampled values of a transform function whose corresponding true resistivity partial function was known. This resistivity function had close similarity with 2 layer descending type apparent resistivity curve. Errors between true and calculated resistivity values at the sample points by the filter method were found to be within 1 percent.

CHAPTER 10

SUMMARY AND CONCLUSIONS

Geoelectrical depth sounding resistivity methods have wide applications in diversified fields notably of which is in the sphere of hydrology in connection with ground water exploration for drinking and agricultural purposes. The field data obtained in the form of an apparent resistivity curve (ρ_a), is interpreted in terms of basic theory and the results are then correlated with available geohydrological information to arrive at a realistic picture of the subsurface structure. The first step is thus termed as physical interpretation and the subsequent procedure as geological interpretation.

The foundations of physical interpretation are laid down in the STEFANESCO expression for the potential due to a point source of current on the surface of a horizontally stratified earth. The integrand of this expression, which is the product of a BESSEL function and the *kernel* function, is of vital importance in theoretical interpretation mainly because of the fact that the latter function is dependent exclusively on the subsurface layer parameters, i.e. on the thicknesses and resistivities of the enclosed layers.

Procedures in interpretation are termed as *direct* or *indirect* depending upon the manner the information about the subsurface is derived from the field data. In indirect methods the field curve is compared with a set of precalculated master curves (6, 44) for known geological conditions of the earth. A match of the curves is interpreted as a match of the parameters. This method is simple and fast in application but invariably the method fails because a fit cannot be obtained with the collection at hand.

Direct methods on the other hand depend on the determination of the kernel function as an intermediate step in the process of deriving the layer parameters from field measurements. The status of direct methods today, as established through the work of LANGER, 1933 (35),

SLICHTER, 1933(64), PEKERIS, 1940 (54), KOEFOED, 1965-70 (29, 30, 31, 32, 33), and others (3, 71) is that although there exists an extremely practical method of obtaining the layer distribution from the kernel function (33), there is no fast and simple method to carry out the first step, namely the evaluation of the kernel function from field resistivity observations.

Thus the principal aim of this thesis is to present such a method. The knowledge of sampling and filter theory is applied in deriving a function called the *resistivity transform* function T (33), related to the kernel, from the apparent resistivity curve. The layer parameters could then be obtained from the T curve by the method cited above.

It has been shown that the conversion from the apparent resistivity to the transform is a linear one such that the principle of linear filtering could be applied.

The resistivity field curve is sampled at an interval of $\Delta x = \ln(10)/3$ i.e. 3 intervals in a factor of 10 of log paper used, being guided in the process by the fundamentals of sampling as laid down in SHANON's theorem. The sampled values are then replaced by functions of the form sin x/x called *sinc* functions. The resistivity transform of each of these sinc functions can be obtained separately and because the property of linearity holds good, the sum of these transforms gives us the total transform of the whole apparent resistivity curve.

For simplification in application the digital approach is followed. This involves determining the sinc response of the filter, sampled values of which give us the digital operators. A running weighted average of the filter operators with the input i.e. the resistivity sample values yield the output i.e. the transform values. Interpolation among the derived transform values gives us the transform curve T.

The process of application can be performed numerically or graphically. Two sets of filter coefficients, the long filter with 12 points and the short filter with 9 points are given for the SCHLUMBERGER case. Approximately a quarter of an hour is required in obtaining the T curve while working with the short filter, but the accuracy of about 2% obtained with it is less than with the long filter, which naturally takes more time. The WENNER filter has 9 points and time required for operation is the same as for the SCHLUMBERGER filter. An alternative procedure is given that enables us to obtain the transform at closer spacing of $\ln(10)/6 \approx 0.38$, with the result that most of the field observational data is utilized in the interpretation. Chapter 7 deals with the process of application with the SCHLUMBERGER method while Chapter 8 deals with the operation with the filter coefficient for the WENNER method.

In Chapter 9 an indirect procedure is treated, namely the computation of apparent resistivity curves from sample values of the transform curve. This has been given with the sole idea that transform expressions are simpler to compute than apparent resistivity expressions. Thus the ρ_{aS} curve could be obtained from the T curve by the application of the inverse filter operators given.

The numerical calculations reported in thesis during the development of the method have been carried out in the electronic computer (No. TR 4; Algol 60) of the Wiskundige Dienst (Mathematical Centre) of the Technological University at Delft.

The conclusions reached as a result of the present work can be summarized as:

1) The method suggested is simple in application. The graphical process is particularly suited to the field geophysicist, whereas the numerical one could be applied conveniently when calculators are available.

2) The method is applicable for both the SCHLUMBERGER and WENNER form of field procedure.

3) There is no limitation in what form the apparent resistivity field data is given; in the graphical process any form of logarithmic paper may be used, if care is taken that the resistivity chart and filter coefficients are plotted on identical modulus.

4) The transform can be obtained in less than a quarter of an hour using the 9 point filter which implies that in conjunction with KOEFOED's

method of deriving the layer distribution (33) from it, the whole physical interpretation should not take more than half an hour. This gives a new meaning to direct methods of interpretation.

5) The accuracy of about 2% can be termed as sufficiently reasonable. The use of the long filter can better this accuracy but is doubted how far that will be necessary when we stop to think for a moment that the accuracy of the field data itself is nowhere better than 3%.

6) The alternative procedure suggested adds considerable flexibility to the method by being adaptable to diversified needs.

7) The transform can be obtained for any type of layer distribution, but the question whether small layer differences will acutally show up in the transform curve depends mostly on the question whether such differences have actually been measured in the field.

8) The difficulty in extrapolation, especially in cases where the asymptotic part of the curve has not been reached, can be removed either taking long spreads or using standard curves asymptotic to last measured segment of the apparent resistivity curve, to aid careful extrapolation.

9) The use of the resistivity transform instead of the kernel has at least two distinct advantages:

a) there is no loss of information during the process of conversion of ρ_a to T, which is of prime importance to a method that utilizes an intermediate step in obtaining the layer distribution from the field data

b) the property that for small and large values of l/λ, the T curve follows the ρ_a curve is a sufficient check to errors committed during the derivation of the T curve, at least at the two ends.

10) Likewise there are additional checks in the middle part of the operation.

11) Direct methods have at least one distinct advantage over indirect methods in that the splitting of the interpretation into two steps gives sufficient scope to take into consideration the implications of the equivalence problem (34, 39). It has been shown that the transform is an unambiguous representation of the ρ_a curve. As such it is neces-

sary to change the second part of the interpretation as drillhole and other data become available from time to time. Moreover, the T function gives a clearer insight into the equivalence phenomena than is apparent from the resistivity curves (KOEFOED, 1970, 33a). Standard curves given in the above mentioned paper facilitate the study of equivalent cases.

Hence the conclusion is justified that the application of the filter theory has been able to give rise to a new method of obtaining the kernel that has not only the ease and speed of application, but at the same time is accurate.

CHAPTER 10A

SAMENVATTING EN CONCLUSIES

Geoelektrische weerstandsmethoden worden uitgebreid toegepast op uiteenlopende terreinen, met name in de hydrologie waar ze gebruikt worden voor de grondwaterexploratie in verband met de watervoorziening.

Uit de veldwaarnemingen, in de vorm van een *schijnbare weerstandskromme*, wordt in de eerste fase (de fysische interpretatie) een weerstandsprofiel van de ondergrond berekend. In de tweede fase (de geologische interpretatie) wordt dit weerstandsprofiel gecorreleerd met de uit de boringen bekende geologische gegevens.

De fysische interpretatie berust op de formule van STEFANESCO voor de potentiaal in een gelaagde ondergrond veroorzaakt door een puntelektrode aan het aardopppervlak. De integrand van deze uitdrukking is het produkt van een Besselfunktie van de nulde orde en de *kernfunctie*. De kernfunktie bevat gegevens over de dikten en weerstanden van de lagen in de ondergrond.

De methoden in de fysische interpretatie worden direkt of indirekt genoemd, afhankelijk van de manier waarop de interpretatie omtrent de ondergrond wordt afgeleid uit de veldwaarnemingen.

Bij de indirekte methode wordt de veldkromme vergeleken met een reeks bekende standaardkrommen (berekend voor theoretische weerstandsprofielen). Door het samenvallen van de veldkromme met één van de standaardkrommen zijn de weerstanden en dikten van de lagen bekend. Deze methode is eenvoudig en snel van toepassing. Maar vaak komen de veldkrommen niet overeen met de beschikbare verzameling (6, 44) omdat het aantal mogelijke weerstandsprofielen zeer groot is[1] vergeleken met de voorbeelden, waarvoor de standaardkrommen beschikbaar zijn, of kunnen worden samengesteld.

----

[1] het aantal neemt toe, naarmate het aantal lagen in de ondergrond vermeerdert

De huidige stand van zaken bij de direkte methode is het resultaat van het werk van SLICHTER, 1933 (64), PEKERIS, 1940 (54), KOEFOED, 1968 (32), en anderen. De direkte methode berust op de bepaling van de kernfunktie in de integraal van STEFANESCO om rechtstreeks het weerstandsprofiel uit de veldwaarnemingen te verkrijgen. Dit wordt gedaan in twee stappen, n.l.:

1) de kernfunktie wordt bepaald uit de schijnbare weerstandskrommen

2) de dikten en de weerstanden van de verschillende lagen worden daarna bepaald uit de kernfunktie.

Voor de tweede stap bestaat er reeds een nauwkeurige methode, niet echter voor de eerste stap. Dit proefschrift wil een eenvoudige methode geven om deze eerste stap uit te voeren.

De kennis van de "sampling" en "filter"theorie is gebruikt om uit de schijnbare weerstandskromme een funktie, genaamd *weerstandstransformatie* af te leiden, die samenhangt met de kernfunctie. De conversie van de schijnbare weerstandskromme naar de weerstandstransformatie wordt hierbij opgevat als de werking van een lineair filter. De schijnbare weerstandskromme wordt gesampled op intervallen ter grootte van 1/3 deel van de logarithmische eenheid $\Delta x = \ln(10)/3$ van het logarithmische papier waarop de schijnbare weerstandskromme is uitgezet.

De keuze van de grootte van de intervallen berust op de principes van sampling volgens SHANON. De samplewaarden worden vervolgens vervangen door sincfunkties met piekhoogten ter grootte van de samplewaarden en periodes bepaald door het sample-interval. Als de aanname van een lineair filter juist is, dan kan de transformatiefunktie worden verkregen door sommering van de transformaties van de verschillende sincfunkties.

De vereenvoudigde digitale benadering is nu het bepalen van de sincresponsie van het filter en het samplen van deze responsie met dezelfde intervallen als bij de schijnbare weerstandskromme. Dit geeft de zogenaamde filter operatoren. Door convolutie van de filteroperatoren met de gesampelde schijnbare weerstandswaarden is de weerstandstransformatie op de gesampelde punten bekend. Door interpolatie wordt "weerstandstransformatie" verkregen. Het beschreven proces kan numeriek of grafisch worden uitgevoerd. Voor de SCHLUMBERGER methode is dit gedaan in hoofdstuk 7, en voor de WENNER methode in hoofdstuk 8.

De nauwkeurigheid van de afleiding van de transformatie blijkt in het geval van de SCHLUMBERGER methode, bij het gebruik van een kortfilter met 9 coëfficiënten, 2% te zijn. De tijd benodigd voor de grafische procedure is minder dan een kwartier. Grotere nauwkeurigheid, tot ¼% kan worden verkregen door het gebruik van een twaalfpuntsfilter, maar dit zal het proces zeker vertragen.

Met het oog op het gebruik van alle beschikbare informatie uit het veld wordt een alternatieve procedure gegeven die de waarden van de "weerstandstransformatie" geeft met intervallen ter grootte van 1/6 van de logarithmische eenheid ($\Delta x = \ln(10)/6$).

Er wordt ook een hoofdstuk gewijd aan het inverse probleem, n.l. de berekening van de schijnbare weerstandskromme uit de weerstandstransformatie kromme. Hiervoor zijn de filteroperatoren gegeven in het geval van de SCHLUMBERGER methode. Dit is gedaan omdat de weergave d.m.v. weerstandstransformatie gemakkelijker is te hanteren dan de weergave d.m.v. schijnbare weerstand. Dit is van belang in de indirekte methode om de schijnbare weerstandskromme te kennen in het geval dat de ondergrond bekend is.

Op grond van het verrichte onderzoek kunnen we tot het volgende concluderen:

1) De beschreven methode voorziet in een snelle en eenvoudige bepaling van de kernfunctie uit de veldwaarnemingen. Daarmee is het belangrijkste bezwaar tegen het gebruik van de direkte methode ondervangen.

2) De methode is te gebruiken voor zowel de SCHLUMBERGER als de WENNER-opstelling.

3) Er worden geen beperkingen gesteld aan de vorm, waarin de veldwaarnemingen beschikbaar zijn. Voor het grafische proces mag elk soort logarithmisch papier gebruikt worden, mits de schijnbare weerstandskromme en de filtercoëfficienten op papier met dezelfde modulus worden uiteengezet.

4) De weerstandstransformatie kan in een kwartier berekend worden. Dit betekent dat met het gebruik van KOEFOED's methode (33), ter verkrijging van een weerstandsprofiel, de gehele fysische interpretatie in een half uur uitgevoerd kan worden. Deze snelheid geeft een nieuwe betekenis aan de toepassingen in het veld van de direkte interpretatiemethode.

5) De nauwkeurigheid van ±2%, verkregen ondanks het gebruik van een kortfilter, is voldoende in vergelijking met de fouten gemaakt in andere gedeelten van de interpretatie en de onnauwkeurigheid van ±3% in de veldwaarnemingen.

6) De beschreven alternatieve procedure en het eventuele gebruik van een langfilter waarborgen een aanzienlijke flexibiliteit in de vorm van de toepassing om zo aan verschillende wensen te voldoen.

7) Het gebruik van de "weerstandstransformatie" i.p.v. de kernfunktie heeft zeker twee duidelijke voordelen:

a) Er is geen verlies aan informatie bij de konversie van schijnbare weerstandskrommen naar de weerstandstransformatie. Dit is zeer belangrijk voor een proces dat een tussenstap vormt in een methode voor het verkrijgen van een lagen-verdeling uit de veldwaarnemingen.

b) De eigenschap dat de "weerstandstransformatie" kromme voor zowel kleine als grote abciswaarden nadert tot bekende waarden geeft tezamen met andere eigenschappen een mogelijkheid tot controle op fouten gemaakt tijdens het converteren.

8) In de weerstandsmethoden is het mogelijk dat verschillende situaties in de ondergrond dezelfde schijnbare weerstandskromme geven. Dit probleem (het equivalentieprobleem ,34) geeft moeilijkheden bij de interpretatie in de indirekte methode. Maar bij de direkte methode is deze moeilijkheid gedeeltelijk ondervangen door het gebruik van de weerstandstransformatie. In dit geval hoeft alleen de tweede stap n.l. de berekening van het weerstandsprofiel uit de weerstandstransformatie veranderd te worden, indien er nieuwe gegevens beschikbaar komen over de geologie van de ondergrond.

Door het voorgaande is de conclusie gerechtvaardigd dat de toepassing van de filtertheorie het mogelijk heeft gemaakt om een nieuwe methode te ontwikkelen voor het bepalen van de kernfunktie uit veldwaarnemingen, die behalve eenvoudig en snel, ook nauwkeurig is.

References

1. ALFANO, L., 1960, The influence of surface formations on the apparent resistivity values in electrical prospecting, GP[1], vol. 8, p. 576-606.
2. ANDERS, E.B., et al., 1964, Digital Filters, National Aeronautical Space Administration, CR - 136.
3. BELLUIGI, A., 1957, Asymptotische Formeln zur Bestimmung des von einer oder von mehreren Elektroden in geschichteten Boden hervorgerufenen Potentials, ZG, vol. 23, p. 135-168 and 182-196.
4. BHATTACHARYA, P.K. and PATRA, H.P., 1968, Direct Current geoelectrical sounding, Elsevier, Amsterdam.
5. BRACEWELL, R., 1955, The Fourier transform and its applications, McGraw Hill.

----

[1] The abbreviations used refer to the following journals:

AMGP : *Geophysical Prospecting*, transactions of the American Institute of Mining and Metallurgical Engineers

BG : *Gerlands Beiträge zur Geophysik*, Leipzig, E.Germany

GE : *Geophysics*, official journal of the Society of Exploration Geophysicists, Tulsa, Oklahoma, USA

GEO : *Geoexploration*, Elsevier, Amsterdam, The Netherlands

GP : *Geophysical Prospecting*, official journal of the European Association of Exploration Geophysicists, The Hague, The Netherlands

IEEE : Transactions of the Institute of Electrical and Electronics Engineers Incorporated (USA)
Vol. GE: Volume on Geoscience electronics
Vol. AP: Volume on Antennas and Propogation

J.G.R. : *Journal of Geophysical Research*, journal of American Geophysical Union, Washington

Ph : *Physics*, A journal of General and Applied Physics, published by American Institute of Physics Inc.

ZG : *Zeitschrift für Geophysik*, Physica-Verlag, Würzburg, W.Germany

6. Compagnie Générale de Géophysique, 1963, Master curves for electrical Sounding, 2nd revised edition, E.A.E.G., The Hague.

7. DAM, J.C. van, 1964, A simple method for the calculation of standardgraphs to be used in geoelectrical prospecting, Ph.D. thesis at Delft Technological University. Uitgeverij Waltman, Delft. (see also GP, vol. 15, p. 57-70, 1967)

7(a). DAM, J.C. van,and MEULENKAMP, J.J., 1967, Some results of the Geo-electrical Resistivity Method in Ground Water Investigations in the Netherlands, GP, vol. 15, p. 92-115.

8, DEAN, W.C., 1958, Frequency analysis for gravity and magnetic interpretation, GE, vol. 23, p. 97-128.

9. DEPPERMANN, K., 1954, Die Abhängigkeit des Scheinbaren Widerständes vom Sondenabstand bei der Vierpunkt Methode, GP, vol. 2, p. 262-273.

10. DEPPERMANN, K., 1961, (abstract), On the calculation of electrical resistivity curves, Early papers and history of E.A.E.G. Leiden.

11. EBERT, A., 1943, Grundlagen zur Auswerkung geoelektrischer Tiefenmessungen, BZ, vol. 10, p. 1-17.

12. EHRENBURG, D.O., and WATSON, R.J., 1932, Mathematical theory of electrical flow in stratified media with horizontal, homogeneous isotropic layers, AMGP, p. 423-442 (see also AMGP, 1934, WATSON's Paper, p. 201-236)

13. ERDELYI, A., 1954, Tables of Integral transforms, McGraw Hill.

14. FLATHE, H., 1955, A practical method of calculating geoelectrical model graphs for horizontally stratified media, GP, vol. 3, p. 268-294.

15. FLATHE, H., 1955, Possibilities and limitations in applying geoelectrical methods to Hydrogeological problems in the coastal areas of North-West Germany, GP, vol. 3, p. 95-110.

16. GARNAR, L., 1968, Application of the function sin x/x to the solutions of 2-D geophysical problems, GEO, vol. 6, p. 33-53.

17. GLOGOVSKY, V.M., and KATS, S.A., 1960, Computation of Theoretical Resistivity Curves with a high-resistance Bed in the section, Industrial and Exploratory Geophysical Prospecting, Consultant Bureau, New York.

18. GRANT, F.S. and WEST, G.F., 1965, Interpretational theory in applied Geophysics, McGraw Hill.

19. HOEVEN, F.G. van der, 1964, Interpretation of geoelectrical resistivity curves, Ph.D. thesis at Delft Technological University, Uitgeverij Waltman, Delft.

20. HUMMEL, J.N., 1932, A theoretical study of apparent resistivity in the surface potential methods, AMGP, p. 392-422. (see also ZG, 1929, p. 89-104 and 228-238, Hummel's paper: Der Scheinbare spezifische Widerstand)

21. KALENOV, E.N., 1957, Interpretation of electrical sounding curves, (in Russian), Gostoptekizdat, Moscow.

22. KELLER, G.V., 1963, Electrical properties in the deep crust, IEEE, Vol. AP - 11, p. 344-357.

23. KELLER, G.V., et al., Geological Survey Investigations of the electrical properties of the crust and upper mantle, GE, vol. 31, p. 1078-1087.

24. KELLER, G.V. and ANDERSON, L.A., 1966, Experimental deep resistivity probes in the Central and Eastern U.S., GE, vol. 31, p. 1105-1122.

25. KELLER, G.V. and FRISCHKNECHT, F.C., 1966, Electrical methods in Geophysical Prospecting, Pergamon Press, New York.

26. KELLER, G.V., 1968, Discussion on "An inverse slope method of determing absolute resistivity" by Sanker Narayan, P.V. and Ramanujachary, K.R., GE, vol. 33, p. 843-845.

27. KOEFOED, O., 1955, Resistivity curves for a conducting layer of finite thickness embedded in an otherwise homogeneous and less conducting earth, GP, vol. 3, p. 258-267.

28. KOEFOED, O., 1960, A generalized Cagniard graph for the interpretation of geoelectrical sounding data, GP, vol. 8, p. 259-269.

29. KOEFOED, O., 1965, A semidirect method of interpreting resistivity observations, GP., vol. 13, p. 259-282.

30. KOEFOED, O., 1965, Direct methods of interpreting resistivity observations, GP, vol. 13, p. 569-591.

31. KOEFOED, O., 1966, The direct interpretation of resistivity observations made with a Wenner electrode configuration, GP, vol. 14, p. 71-79.

32. KOEFOED, O., 1968, The application of the kernel function in interpreting geoelectrical measurements, Geoexploration monographs, series 1 nr. 2, Gebrüder Borntraeger, Stuttgart.

33. KOEFOED, O., 1969, A fast method for determining the layer distribution from the raised kernel function in geoelectrical sounding (in press).

33(a). KOEFOED, O., 1970, An analysis of equivalence in resistivity sounding, GP, vol. 17, p. 327-335.

34. KUNETZ, G., 1966, Principles of direct current resistivity prospecting, Geoexploration monographs series 1 nr. 1, Gebrüder Borntraeger, Stuttgart.

35. LANGER, R.E., 1933, An inverse problem in differential equations, American Mathematical Society Bull., vol. 39, p. 814-820. (see also same journal vol. 42, pp. 747-754)

36. LASFARGUES, P., 1957, Prospection electrique par courants continus, carte de potentiel, résistivité, polarisation spontanée, polarisation induite, Mason and Cie, Paris.

37. LEE, Y.W., 1960, Statistical theory of communication, John Wiley, New York.

38. MAILLET, R. and DOLL, H.G., 1932, Sur un théorème relatif aux mileux electriquement anisotropes, et ses applications à la prospection électrique en courant continu, BG, vol. 3, p. 109-124.

39. MAILLET, R., 1947, The fundamental equations of electrical prospecting, GE, vol. 12, p. 529-556.

40. MEYERHOFF, H.J., 1968, Realization of sharp cut-off frequency characteristic on Digital Computers, GP, vol. 16, p. 208-220.

41. MONROE, A.J., 1962, Digital processes for sampled data systems, John Wiley, New York.

42. MOONEY, H.M., and WETZEL, W.W., 1956, The potentials about a Point Electrode and Apparent Resistivity curves for a two-, three-, and four-layered Earth, The University of Minnesota Press, Minneapolis.

43. MOONEY, H.M., et al., 1966, A resistivity computational method for layered earth models, GE, vol. 31, p. 192-203.

44. MOONEY, H.M. and ORELLENA, E., 1966, Master tables and curves for vertical electrical sounding over layered structures, Interciencia, Madrid.

45. MUSKAT, M., 1933, Potential distribution about an electrode on the surface of the earth, Ph, vol. 4, p. 129-147.

46. NABHIGHIAN, M.N., 1966, The application of finite forward differences in resistivity computations over layered earth, GE, vol. 31, p. 971-980.

47. NOSTRAND, R.G. van, and COOK, K.L., 1966, Interpretation of resistivity data, Geological Survey Professional paper 499, U.S. Dept. of Interior, Washington.

48. ONODERA, S., 1960, The Kernel Function in multiple layer resistivity problem, JGR, vol. 65, p. 3787-3794.

49. ONODERA, S., 1963, Numerical analysis of relative resistivity for horizontally layered earth, GE, vol. 28, p. 222-231.

50. PAPOULIS, A., 1965, The Fourier Integral and its applications, Mc Graw Hill, New York.

51. PARASNIS, D.S., 1962, Principles of Applied Geophysics, Metheun, London.

52. PARASNIS, D.S., 1966, Mining Geophysics, Elsevier, Amsterdam.

53. PAUL, M.K., 1968, A note on Direct Interpretation of Resistivity profiles for Wenner electrode configuration, GP, vol. 16, p. 159-162.

54. PEKERIS, C.L., 1940, Direct method of interpretation in resistivity prospecting, GE, vol. 5, p. 31-42.

55. PICKLES, ERIC, 1967, Lecture notes on the basic mathematics of digital processing of seismic data, a G.S.I. Inc. (USA) publication.

56. ROBINSON, E.A. and TREITEL, S., 1964, Principles of digital filters, GE, vol. 29, p. 395-404.

57. ROBINSON, E.A. and TREITEL, S., 1964, The stability of digital filters, IEEE, Vol. GE 2, p. 6-18.

58. ROBINSON, E.A., 1967, Statistical Communication and Detection, Charles Griffin and Co., Ltd.

59. ROMAN, I., 1934, Some Interpretations of Earth-resistivity data, AMGP, p. 183-197.

60. ROMAN, I., 1959, An Image analysis of multiplelayer resistivity problems, GE, vol. 24, p. 485-509.

61. ROMAN, I., 1963, The kernel function in the surface potential for a horizontally stratified earth, GE, vol. 28, p. 232-249.

62. SCHLUMBERGER, C. and M., 1932, Electrical studies of the earth's crust at great depths, AMGP, p. 134-140.

63. SCHLUMBERGER, C., et al., 1934, Some observations concerning electrical measurement in anisotropic media and their interpretation, AMGP, p. 159-182.

64. SLICHTER, L.B., 1933, The interpretation of resistivity prospecting method for horizontal structures, Ph, vol. 4, p. 307-322.

65. SOKOLOFF, V.M. and SWARTZ, C.A., 1954, Filtering associated with selective sampling of Geophysical data, GE, vol. 19, p. 402-419.

66. SOROKIN, L.W., 1953, Lehrbuch der Geophysikalischen Methoden zur Erkundung von Erdölvorkommen, Veb Verlag Technik Berlin (translated from Russian).

67. STEFANESCO,S.S., et al., 1930, Sur la distribution électrique potentielle autour d'une prise de terre ponctuelle dans un terrain à couches horizontales homogènes et isotropes, Journal Physique et Radium, séries 7, p. 132-141.

68. STEVENSON, A.F., 1934, On the theoretical determination of earth resistance from surface potential measurement, Ph, vol. 5, p. 114-124.

69. TAGG, G.F., 1934, Interpretation of Resistivity Measurements, AMGP, p. 135-147.

70. United Geophysical Corp., 1966, A pictorial digital atlas.

71. VOZOFF, K., 1960, Numerical Resistivity analysis- horizontal layering, GE, vol. 23, p. 536-556.

72. WATSON, G.N., 1966, A treatise on the theory of Bessel functions, Cambridge Univ. Press.

73. WETZEL, W.M. and McMURRAY, H.V., 1937, A set of curves to assist in the interpretation of the three layer resistivity problem, GE, vol. 2, p. 329-341.

74. WIENER, N., 1949, Extrapolation, Interpolation and smoothing of stationary time series, John Wiley, New York.

75. ZHODY, A.R., 1965, The auxiliary point method of electrical sounding interpretation and its relationship to the Dar-Zarrouk parameters, GE, vol. 30, p. 644-660.

76. ZHODY, A.R., et al., 1969, Application of deep electrical soundings for groundwater exploration in Hawaii, GE, vol. 34, p. 584-600.

77. ZYL, J.S.V. van, 1968, A deep Schlumberger sounding to investigate the electrical structure of the crust and upper mantle in South Africa, GE, vol. 34, p. 450-462.

78. Z.KRULC and MLADENOVIC, M., 1969, The application of geoelectrical methods to ground-water exploration of unconsolidated formations in semi-arid areas, GEO, vol. 7, no. 2, p. 83-96.

Stellingen

22.4.'70
Delft

D.P. Ghosh

1. There is in India complete lack of communication between Institutes and Universities imparting geophysical education to students and organizations employing these students.

2. The idea of indicating the south magnetic pole of the earth situated in the Northern Hemisphere as the north magnetic pole, to tally with the geographic nomenclature, is contrary to the convention used in magnetism based on the physical behavior of a magnet and is thus misleading.

3. The assumption of KAILA et al. that the value obtained from a single seismic survey, carried out at a location situated at the far end of the Himalaya foothill region, is representative of the average sedimentary layer velocity throughout the extensive foothill area and the vast Indogangetic plains, for the purpose of regional crustal structure determination is unjustified.

   "Crustal structure in Himalayan foothills area of North India".
   - KAILA et al. Bulletin of the Seismological Society of America, 1968, p. 597 - 612.

4. The third example given by HUMMEL to illustrate his method of combining layers in a resistivity profile, in an attempt to reduce complicated multilayer problems to simpler cases, is wrong and misleading. Krichoff's law of resistances in parallel on which the reduction is based is applicable to the problem only when the substratum is resistive compared to the overlying layers.

   "Apparent resistivity in surface potential methods" - HUMMEL, Geophysical Prospecting, 1932, AIME, Fig. 9, p. 421.

5. Closer cooperation is necessary amongst its various units, if earth science has to serve the cause for betterment of mankind.

6. The illustrations given by JAKOSKY and DOBRIN to demonstrate the self polarization phenomenon of sulphide ore bodies are ambiguous and are due to the inability from the part of the authors to bring out clearly the distinction between ionic and electronic nature of conduction of electricity, inside and outside the ore body.

   "Exploration Geophysics" - JAKOSKY, Trija publishing co., 1950, Fig. 266, p. 445.
   "Geophysical Prospecting" - DOBRIN, McGraw - Hill, 1960, Fig. 17 - 1, p. 343.

7. The question of contraction or on the contrary expansion of the earth still remains unsolved, mostly due to the failure on the part of either school of workers to substantiate their theories with concrete proofs.

8. A new exploration outlook is necessary to prospect for extensive low grade sedimentary ore deposits.

9. The usual treatment of the magnetic effect of ore bodies and geological structures, arising due to the induction of the earth's magnetic field, is far from being complete as the relevant boundary conditions are not considered.

10. The generalized statement appearing in geophysical literature, that the depth of current penetration is one third the current electrode spacing in resistivity measurements, without consideration of the electric state of the earth is wrong.

11. That the total mass of a causitive body can be determined uniquely, is a definite pluspoint to the suitability of gravity methods towards mineral exploration (in concern with the calculation of the total tonnage of the ore body) in spite of the ambiguity of gravity interpretation.

12. If a healthier outlook of the Indian society is desired there is immediate and urgent necessity that the dowry system of marriage be abolished.

13. Women of today want to emancipate without losing the privileges they enjoyed being the weaker of the two sexes.